Nr. 76 Mitteilungen
der Versuchsanstalt für Wasserbau,
Hydrologie und Glaziologie

an der Eidgenössischen Technischen Hochschule Zürich
Herausgegeben von Prof. Dr. D. Vischer

A model for TOPOGRAPHIC ROSSBY WAVES in channels and lakes

Thomas Stocker
Kolumban Hutter

Zürich, 1985

PREFACE

Temperature measurements that were perfomed in Lakes of Zurich and Lugano in the late seventies disclose long periodic oscillations whose structure suggests that they may be interpretable as second class eigenmodes of the respective basins. Verification by numerical solution of the topographic wave equation for these realistic basins is so far lacking, one reason being that FD and FE solutions exhibit a multitude of modes with varied structures in narrow frequency bands which make physical interpretation very difficult.

The aim of this study is to transform the topographic wave equation by the Principle of Weighted Residuals into a simpler operator equation, which for a large class of basin geometries can be studied qualitatively and thus provides physical insight into the secrets of the behavior of second class motions in closed basins. The method may be termed "channel method" and furnishes the topographic analogon of the Chrystal and Defant equations that were deduced more than 60 years ago (and have been extended by us) to explain the gravitational seiches in long lakes.

As the reader can judge himself, a further step towards understanding topographic waves in enclosed basins has been done, however many new questions have arisen that now await their proper answer.

K. Hutter

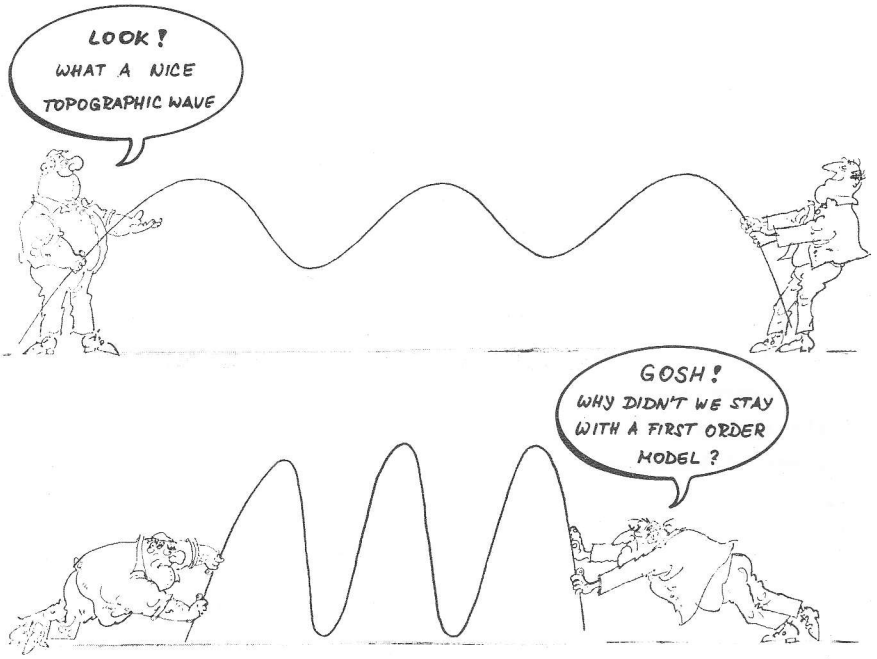
LOOK !
WHAT A NICE
TOPOGRAPHIC WAVE
GOSH !
WHY DIDN'T WE STAY
WITH A FIRST ORDER
MODEL ?

Contents

ABSTRACT

The topographic Rossby wave problem for a rotating elongated domain is approximately solved. To this end the two-layer shallow water equations, appropriate for a lowest order baroclinic model, are scaled and approximately reduced to a system of equations which govern topographic waves and their coupling. It is shown that in the limit of a small upper layer depth compared to the lower layer thickness, the conservation equation of barotropic potential vorticity still applies and that the internal baroclinic part of the motion is forced by the barotropic mass transport stream function.

The conservation of potential vorticity, which can be formulated as a two-dimensional boundary value problem in a natural coordinate system, is reduced to a set of coupled one-dimensional differential equations. This is achieved with the help of the method of Weighted Residuals: The mass transport stream function is expanded along the narrow side of the domain into a linear combination of prescribed basis functions. After a weighted integration over this transverse direction the problem reduces to a set of coupled two-point boundary value equations for the coefficient functions of the linear expansion of the stream function, which are functions of a single space coordinate and of time only. Depending on the number of terms carried through in the shape function expansion different orders of approximation are obtained. In view of the linearity this system admits solutions which have a wavelike structure both in space and time, such that the emerging system is purely algebraic.

This algebraic system of equations is used to analyze infinite straight channels with variable topography in the transverse direction. The dispersion relation of topographic wave motion is obtained and scrutinized for various profiles and several orders of expansion. It is shown that increasing the order of expansion leads to convergence of solutions, but low

order models are demonstrated to be sufficiently reliable in extracting the physically relevant properties.

By a linear superposition of channel solutions topographic wave motion in rectangular basins are analyzed using the width to length ratio (aspect ratio) as a characteristic parameter. It is shown that small aspect ratio basin solutions exhibit a rich modal structure and, therefore, differ substantially from those of known exact solutions. By contrast, lowest order expansion models for large aspect ratios show similiarities with known exact basin solutions, but their higher order models deviate, such that convergence properties are poor.

It is argued that these odd features of the large aspect ratio case can be understood in terms of the inappropriateness of the bathymetry approximations. Improvements of the model are discussed and one version is outlined, but explicit results for this extended case are left for further investigation.

ZUSAMMENFASSUNG

Das Problem topographischer Rossby-Wellen in langen rotierenden Gebieten wird näherungsweise gelöst, indem die Zweischicht-Flachwasser-Gleichungen -geeignet zur Beschreibung von baroklinen Bewegungen erster Ordnung - skaliert und nach gewissen Näherungen reduziert werden zu einem System von Gleichungen, die topographische Wellen und ihre Kopplung beschreiben. Es wird gezeigt, dass für Fälle, wo die obere Wasserschicht viel dünner ist als die darunterliegende, die Erhaltung der barotropen potentiellen Vorticity immer noch gültig ist. Der innere barokline Anteil der Bewegung wird dann durch die barotrope Stromfunktion gesteuert.

Die Erhaltung der potentiellen Vorticity, die als zweidimensionales Randwertproblem in einem natürlichen Koordinatensystem formuliert werden kann, wird auf ein System gekoppelter eindimensionaler Differentialgleichungen reduziert. Dies geschieht mit Hilfe der Methode der gewichteten Residuen: Die Stromfunktion wird längs der Schmalseite des Gebietes in eine Linearkombination von vorgeschriebenen Basisfunktionen entwikkelt. Nach einer gewichteten Integration über diese Richtung wird das Problem zu einem System von gekoppelten Zweipunkt Randwertgleichungen in den Koeffizientenfunktionen dieser linearen Entwicklung; diese hängen nun nur von einer Raumvariable und der Zeit ab. Je nach Anzahl Summanden dieser Entwiklung erhält man verschiedene Ordnungen der Näherungen. Da das Problem linear ist, erhält man daraus ein rein algebraisches System, wenn angenommen wird, dass die Lösungen in Ort und Zeit Wellenform besitzen.

Mit Hilfe dieses algebraischen Gleichungssystems werden unendlich lange, gerade Kanäle mit verschiedenen Querschnittprofilen untersucht. Die dadurch berechnete Dispersionsrelation topographischer Wellen wird für verschiedene Profile und Ordnungen der Näherung geprüft und es wird gezeigt, dass eine Erhöhung der Ordnung zu konvergierenden Lösungen führt. Schon

Modelle niedrigster Ordnung beschreiben die Bewegung zuverlässig und schälen die physikalischen Eigenschaften dieses Wellentypus heraus.

Durch eine Linearkombination von Kanallösungen können topographische Wellen in Rechteckbecken beschrieben werden. Das Verhältnis Breite zu Länge (Formparameter) erweist sich als charakteristische Grösse. Becken mit kleinem Formparameter besitzen eine komplizierte Wellenstruktur und unterscheiden sich deshalb wesentlich von bekannten exakten Lösungen. Demgegenüber zeigen Becken mit grossem Formparameter in Modellen niedrigster Ordnung klare Aehnlichkeit in der Wellenstruktur mit den exakten Lösungen. Allerdings verschwindet diese Aehnlichkeit in Modellen höherer Ordnung; die Konvergenzeigenschaften sind mager.

Dies kann damit zusammenhängen, dass im Fall der kleinen Formparameter die Beckentopographie ungenügend modelliert wurde. Verschiedene Verbesserungsvorschläge werden gegeben, deren explizite Resultate jedoch weiteren Untersuchungen überlassen sind.

RESUME

Le problème des ondes topographiques de Rossby pour un domaine allongé en rotation est résolu approximativement. Pour ce faire, l'équation pour eau peu profonde à deux couches, appropriée pour décrire des mouvements baroclines du premier ordre, est étalonnée et approximativement réduite à un système d'équations qui gouvernent les ondes topographiques et leurs noeuds. Il est montré que pour le cas où la couche d'eau supérieure est beaucoup plus mince que l'inférieure, l'équation de conservation du vortex barotropique potentiel est toujours valable et que la composante baroclinique interne de la vitesse est gouvernée par la fonction de courant barotropique.

La conservation du vortex barotropique potentiel, qui peut être formulée comme un problème à deux dimensions de valeurs au bord dans un système de coordonnées naturelles, est réduite à un système couplé d'équations différentielles à une dimension. On applique pour cela la méthode des résidus pondérés: la fonction de courant est développée linéairement dans une base donnée le long du petit côté du domaine. Après une intégration pondérée sur la direction transversale, le problème se réduit à un système couplé d'équations à valeurs au bord sur un intervalle pour les fonctions-coefficients du développement ci-dessus; celles-ci ne dépendent maintenant plus que d'une variable spatiale et du temps. Selon le nombre de termes du développement, on obtient divers ordres d'approximations. Le problème étant linéaire, on peu se ramener à un système algébrique linéaire sous l'hypothèse que la solution, dans l'espace et le temps, a une forme d'onde.

A l'aide de ces équations algébriques, on étudie des canaux de longueur infinie avec divers profils en travers. La relation de dispersion des ondes topographiques ainsi calculée est testée pour différent profiles et ordres d'approximations et il est montré qu'une augmentation de l'ordre mène a

des solutions convergentes. Mais déjà des modèles de petit ordre décrivent le mouvement d'une manière satisfaisante et mettent les caractéristiques physiques de ce type d'onde en évidence.

Les ondes topographiques dans un bassin rectangulaire peuvent être décrites par une combinaison linéaire des solutions pour canaux. Le rapport largeur sur longueur (paramètre de forme) se rélève être une grandeur caractéristique. Les bassins à petit paramètre de forme ont une structure d'onde complexe et divergent passablement de la solution exacte connue. Par contre, les bassins à grand paramètre de forme montrent dans des modèles de petit ordre une similitude évidente avec la solution exacte. Cette similitude disparait pourtant dans des modèles d'ordre d'approximation supérieur; les propriétés de convergence sont pauvres.

Ceci peut être dû au fait que la topographie des bassins à petit paramètre de forme a mal été modèlisée. Des propositions d'améliorations sont faites, leur résultat explicite étant laissé à des études ultérieures.

(traduction par Bernard Ott)

VARIABLES

α	Horizontal slope of the thalweg line in a Cartesian system, matrix index
B	Lake width
B^+	Lake boundary +n-direction
B^-	Lake boundary -n-direction
$\mathbb{B}$	Differential boundary operator
β	Matrix index, derivative of the Coriolis parameter
$\underline{C}, C_{\beta\alpha}$	Dispersion relation matrix (elements) for an infinite channel
$\mathbb{C}$	Complex field
$\tilde{\mathbb{C}}$	Complex field without $\mathbb{R}$ and $\mathbb{J}$
c	Exponential thalweg constant
c^I, c^{II}, c^{III}	Exponential thalweg constant for three subsequent lake domains
$\underline{c}, c_\alpha$	Kernel vector (components) of $\underline{C}$
$c_{\alpha\gamma}$	Kernel matrix elements to a given ω
$c^I_{\alpha\gamma}, c^{II}_{\alpha\gamma}, c^{III}_{\alpha\gamma}$	Kernel matrix elements to a given ω for three subsequent lake domains
γ	Matrix index
D_1	Constant epilimnion depth
D_2	Maximum cross section hypolimnion depth
$\underline{D}, D_{\alpha\gamma}$	Lake boundary condition matrix (elements)
$\mathbb{D}$	Differential topographic wave operator
$\mathcal{D}$	Lake domain
$\partial\mathcal{D}$	Lake boundary
$\underline{d}, d_\gamma$	Kernel vector (components) of $\underline{D}$
$d^I_\gamma, d^{II}_\gamma, d^{III}_\gamma$	Kernel vector components of $\underline{D}$ for three subsequent lake domains

$\underline{E}, E_{\alpha\gamma}$	Lake boundary and matching condition matrix (elements)
$\underline{e}, e_\gamma$	Kernel vector (components) of $\underline{E}$
ε	Side wall parameter
η	Elliptical coordinate
f	Coriolis parameter, $f = 1.033 \cdot 10^{-4} s^{-1}$, time scaling
g	Gravitational constant, $g = 9.81\ m\ s^{-2}$
$\underline{g}$	Vector of gravitational acceleration
g'	Density-reduced gravity
$\underline{g}_s, \underline{g}_n, \underline{g}_z$	Basis vectors of the natural coordinate system
H	Total depth of the lake
H_0	Topography depth
H_1	Basin depth
H_2	Basin depth, hypolimnion depth
h	Scaled basin topography, cross sectional depth
h'	Non-dimensional depth
h_0	Thalweg depth
$h_0^I, h_0^{II}, h_0^{III}$	Thalweg depth for three subsequent lake domains
h_1	Cross sectional depth
I_i	Integral function
i	Imaginary unity, $i^2 = -1$
J	Orthogonal metric in the natural coordinate system
J_1, J_2, J_3	Orthogonal metric in a general coordinate system
$\mathbb{J}$	Imaginary field
K	Curvature
$\underline{K}^{ij}, K^{ij}_{\beta\alpha}$	Constant matrix (element) components of $\underline{\mathbb{M}}$
k	Direction perpendicular to the boundary, wave number in the s-direction or x-direction
k_γ	Wavenumbers to a given ω

$k_\gamma^I, k_\gamma^{II}, k_\gamma^{III}$	Wavenumbers to a given ω for three subsequent lake domains
$\underline{\hat{k}}$	Unit vector perpendicular to the boundary
L	Length scale, length of the lake
L	Wave operator
ℓ	Direction along the boundary, wavenumber in the y-direction
$\underline{\hat{\ell}}$	Unit vector along the boundary
$\underline{d\ell}$	arcelement vector
M	Order of the approximation of the weighting function
$\underline{M}^{ij}, M_{\beta\alpha}^{ij}$	Matrix (element) components of $\underline{\mathbb{M}}$
$\underline{\mathbb{M}}, \mathbb{M}_{\beta\alpha}$	Differential matrix operator (elements)
$\underline{\tilde{\mathbb{M}}}$	Scaled differential matrix operator
m_1, m_2	Mass
N	Order of the approximation of the stream function, order of the model
n	Natural coordinate
$\hat{n}$	Unit vector in n-direction
$\Omega, \Omega_1, \Omega_2$	Angular velocity
$\underline{\Omega}$	Vector of angular velocity of earth rotation
$\omega, \omega_1, \ldots, \omega_4$	(dimensionless) frequency of wave motion
ω_z	Vertical component of relative vorticity
P_α	Basis function of the stream function
$P_\alpha^+ \; P_\alpha^-$	Symmetric and skew-symmetric part of P_α
p	Pressure
$\delta\phi_{\mathcal{D}}, \delta\phi_{\mathcal{D}}^\beta$	Weighting function (component) defined in $\mathcal{D}$
$\delta\phi_{\partial\mathcal{D}}, \delta\phi_{\partial\mathcal{D}}^\beta$	Weighting function (component) defined on $\partial\mathcal{D}$
ϕ	Cylindric coordinate

ψ	Barotropic or mass transport stream function
$\underline{\psi}, \psi^{\alpha}$	Vector (components) of the stream function
$\psi^{I\alpha}, \psi^{II\alpha}, \psi^{III\alpha}$	Stream function components for three subsequent lake domains
ψ_+, ψ_-	Symmetric and skew-symmetric part of the stream function
ψ_0	Scale of the stream function
ψ'	Nondimensional stream function
$\psi^I, \psi^{II}, \psi^{III}$	Stream function for three subsequent lake domains
$\underline{\psi}_+, \psi_+^{\alpha}$	Vector and components of the symmetric part of the stream function
$\underline{\psi}_-, \psi_-^{\alpha}$	Vector and components of the skew-symmetric part of the stream function
Q_{β}	Basis function of the weighting function
Q_{β}^+, Q_{β}^-	Symmetric and skew-symmetric part of Q_{β}
q	Topography parameter
R	Radius of curvature
R_i	Internal Rossby radius
$\mathbb{R}$	Real field
r	Cylindric coordinate, aspect ratio
r_1, r_2	Radius
$\underline{r}$	Position vector
ρ	Density
ρ_1	Epilimnion density
ρ_2	Hypolimnion density
S	Stratification parameter
s	Natural coordinate
s_1, s_2	Location of thalweg intersection
T	Temperature
$T, T_1, \ldots, T_4$	Periods of topographic wave motion

t	Time
t'	Nondimensional time
$\underline{\tau}$	Wind stress vector
τ_x, τ_y	Wind stress components in a Cartesian coordinate system
τ_s, τ_n	Wind stress components in a natural coordinate system
$\underline{\tau}'$	Dimensionless wind stress vector
τ_0	Wind stress scale
$\underline{u}$	Velocity vector
u, v	Velocity components in x,y-direction, respectively
$\underline{u}_1, u_1, v_1$	Velocity vector and components in the epilimnion
$\underline{u}_2, u_2, v_2$	Velocity vector and components in the hypolimnion
$\underline{u}^{bt}$	Barotropic part of the velocity field
v, v_1, v_2	see u
W_β	Components of the wind stress
x, y, z	Cartesian coordinates
x', y', z'	Nondimensional Cartesian coordinates
$\tilde{x}, \tilde{y}$	Cartesian thalweg parameter representation
x_1, x_2, x_3	Coordinates in a general coordinate system
ξ	Elliptic coordinate
y	see x
z	see x
$\hat{\underline{z}}$	Vertical unit vector
ζ, ζ_2	Elevation of the thermocline
ζ_1	Surface elevation
∇	Horizontal Nabla operator

1. INTRODUCTION

This report is concerned with an approximate solution technique of topographic Rossby waves in channels and enclosed water basins. This particular wave phenomenon will in this first section, be embedded in the context of geophysical fluid dynamics.

1.1 Waves in waters

Before discussing the variety of wave types which may arise in waters such as the open ocean, channels, lakes, etc., we shall not try to define the physical meaning of the notion "wave" but rather quote a beautiful statement of Einstein, that expresses the essentials of what is meant by waves more accurately than we could have done.

> "Irgend ein Klatsch, der, sagen wir, in Washington aufgebracht wird, gelangt sehr rasch nach New York, wenn auch nicht eine einzige von den an der Weitergabe beteiligten Personen tatsächlich von der einen Stadt in die andere reist. Wir haben es vielmehr gewissermassen mit zwei ganz verschiedenen Bewegungen zu tun, der des Gerüchtes selbst, das von Washington nach New York dringt, und der jener Personen, die das Gerücht verbreiten."

Among the great variety of types of waves which occur in nature we are interested here in water waves. To no surprise, waves in waters themselves exhibit a multitude of different types. In natural waters, which are always stratified, i.e. the density is a function of space and time $\rho = \rho(\underline{r},t)$, to each wave type there exists an internal and an external form. Internal wave motions are primarily felt within the medium leaving the water surface almost at rest and occur only in stratified waters. By contrast, what we see when standing at a lake shore or at the beach is all external wave patterns, motions which perturb the surface of the water.

There are basically two qualities which govern wave motion in waters. On the one hand, these are the mechanical, chemical

and electromagnetic properties of water, on the other hand there are the specific qualities of the "container" which is occupied by the medium. For instance, acoustic waves are due to the mechanical properties, namely the compressibility of water and are not influenced or modified by the "state" of the container. What we mean by this is, that the dispersion relation of acoustic waves is not modified when the container is rotating or has a complicated topography. Another example of waves governed by the property of the water would be the electromagnetic waves, light, of which the dispersion relation remains unaffected by a possible rotation of the container.

Seiche motions are governed by the shape of the container, i.e. the position of the boundaries determines both, frequency and wavelength (in a closed basin) of the seiche. Kelvin and Poincaré waves owe their existence to the rotation of the container and the Coriolis force which can be felt in such a noninertial frame. Topographic waves, finally, are governed mainly by the container, in that they require for their occurrence a container with nontrivial topography and rotation. Both qualities are natural features of lake basins, in that they exhibit a topography on the rotating earth.

It is interesting to notice that the larger the "scale" of the driving mechanism of the wave is the lower will, in general, be its frequency. Whereas a typical acoustic wave has a frequency of 10^2 s^{-1}, external seiches have about 10^{-3} s^{-1} and internal (topographic) waves in a lake even 10^{-5} s^{-1}. This is also a sign for the fact that waves in waters occupy a broad frequency spectrum which spans over more than 10 log cycles.

This brief survey, however, does not suffice to understand and explain fluid wave motion. A step towards this is provided by considering the set of equations which governs any fluid motion and is obtained by applying the laws of

- conservation of momentum,
- conservation of mass,
- conservation of energy.

These three fundamental laws and the equation of state lead to the set of equations, quoting Pedlosky (1979),

$$\begin{aligned} \frac{\partial \underline{u}}{\partial t} + (\underline{u}\,\mathrm{grad})\,\underline{u} + 2\underline{\Omega}\times\underline{u} &= \underline{g} - \underline{\Omega}\times(\underline{\Omega}\times\underline{r}) - \frac{1}{\rho}\,\mathrm{grad}\,p, \\ \frac{\partial \rho}{\partial t} + \mathrm{div}(\rho\,\underline{u}) &= 0, \\ \rho &= \rho(p,T), \\ \frac{\partial \rho}{\partial t} + (\underline{u}\,\mathrm{grad})\,\rho &= 0, \end{aligned} \qquad (1.1)$$

in which the chemical and viscous aspects of the problem have been ignored. The system (1.1) describes adiabatic fluid motion in a system subject to steady rotation; in other words, (1.1) contains all aspects of geophysical fluid dynamics. Mathematically, (1.1) consists of five non-linear partial differential equation with associated boundary conditions (depending on the specific problem) and an equation of state. These six equations determine the six unknown fields

$\underline{u}(\underline{r},t)$	the velocity field (3 dimensions),
$\rho(\underline{r},t)$	the density field,
$p(\underline{r},t)$	the pressure field,
$T(\underline{r},t)$	the temperature field,

which are all functions of space and time. The given fields are

$\underline{\Omega}(\underline{r})$	the angular velocity,
$\underline{g}(\underline{r})$	the gravity field,

and, furthermore the boundary conditions which are imposed on (1.1). These represent constraints on the motion, in that, for instance, boundary conditions select *eigenfrequencies*, seiches and other wave types in closed basins. Also, equations (1.1) pertain to a broad spectrum of wave motion: acoustic waves, capillary waves, inertial waves, gravity waves or seiches, Kelvin waves, Poincaré waves, shelf waves, topographic waves, etc. Not only water motion on the earth but equally atmospheric motion can be explained with (1.1). These are buoyancy waves, Föhn waves, frontal motions, Rossby waves, etc.

In parallel with the generality of equations (1.1) goes the difficulty to solve them. A general solution of (1.1), which would embrace all aspects of fluid motion in a given configuration (e.g. channel, lake basin, atmosphere, etc.) is not yet found and is not worth searching for. The only way out of this dilemma is to introduce more or less reasonable neglections and approximations which (i) simplify the system (1.1), (ii) filter out all those effects which are not of interest but (iii) retain the characteristics of the motion of interest. This approximation procedure has cast light in various different domains of the spectrum. These, however, lie apart and form distinct regimes with distinct behaviour. Connections to other mechanisms or other regimes can sometimes be obtained by adopting perturbation analysis.

1.2 Topographic Rossby waves

The subject of this work is to investigate a specific wave type of geophysical fluid dynamics. Here we try to explain the mechanisms of topographic waves by means of a mechanical analogy. The mechanism of topographic wave motion is the conservation of angular momentum. This is represented by the conservation equation

$$\frac{d}{dt}\left(\frac{\omega_z+f}{H}\right) = 0, \qquad (1.2)$$

where ω_z is the vertical component of relative vorticity, f the Coriolis parameter, H the basin depth and $\frac{d}{dt}$ the derivative with respect to time following the fluid motion. A simple derivation of (1.2) is given in Appendix D using a mechanical rigid body analogy. Equation (1.2) represents the conservation of barotropic potential vorticity on which Ball (1965) based his studies of topographic waves. The simple derivation in Appendix D demonstrates that the restoring mechanism of second class wave motion (topographic Rossby waves) consists in the conservation law of angular momentum. Equation (1.2) shows, that an increase of f in a container of constant depth requires a decrease of relative vorticity. This is the situation

where planetary Rossby waves in the atmosphere or ocean are observed. The mentioned container represents the atmosphere and an increasing f corresponds to a south-north motion (β-effect). On the other hand, an increase of the basin depth, e.g. in a lake, forces a corresponding increase of relative vorticity. This is the case for topographic wave motion. In a large ocean basin or in an atmosphere with strong orography both effects may work and then lead, in an ocean, to shelf waves. In this report, however, f will be assumed to remain constant, which is sufficiently obeyed for small lakes (north-south scale smaller than 100 km) distant from the equator.

There are two necessary conditions for the occurrence of topographic waves: a rotating "container" and a container-depth with topography variations. Unless both conditions are fulfilled, topographic or second class wave motion is not possible, as demonstrated in Appendix A.

1.3 Present works and experimental evidence

The study of second class waves in fluids -motions which are due to the rotation of the "container" - started a long time after that of first class motion which is due to gravity. The first trace of reference is probably the work of Poincaré (1910). He demonstrated the existence of long periodic oscillations in a rotating circular basin with a parabolic depth profile. A first explicit solution was given years later by Lamb (1932), again for the same configuration. Subsequently, after a long pause, Ball (1965) revived the issue with an exact solution for an elliptic basin with parabolic profile. This model allowed an examination of the effect of the basin shape on the eigenperiods of topographic wave motion through the excentricity of the ellipse. Saylor et al. (1980) presented for the first time observations *and* deduced a refined theoretical model. Instead of selecting different basin shapes, as Ball (1965) did, they investigated circular basins with radial profiles parameterized by a power law, which here will be applied

with changes, as well. Gratton (1983) presented a study of topographic waves in straight channels. He found that the baroclinic feed-back to the barotropic motion is small for stratified lakes which have a small ratio of epilimnion to hypolimnion depth. We analyze the same situation and this is why barotropic calculations are justified.

A further step in the field of theoretical approach was made by Mysak (1983, 1984) when he investigated topographic wave motion in elliptic basins using an elliptic coordinate system. To obtain a differential equation with constant coefficients he introduced a piecewise exponential depth profile akin to calculations performed for shelf waves (LeBlond & Mysak, 1978).

Csanady (1976), applying precursors of Hamblin (1972) and Simons (1975) explained observations of coastal motion in Lake Ontario by second class waves. Saylor et al. (1980) interpreted observed long-periodic oscillations (in the order of days) in Lake Michigan as topographic waves.

Recently, thermocline oscillations in the Swiss Lakes of Lugano and Zürich were interpreted as topographic wave motion. This is a surprise for such small scale lakes but the observed periods could not be explained by an internal seiche mode (first class waves), as the periods lie significantly above those of the fundamental internal seiches. Spectras of the temperature data indicate for Lake of Lugano a significant peak at about 70-80 h, see Mysak et al. (1983, 1984) and measurements of phase differences between spectra of isotherm depth pairs show a counterclockwise rotation around the basin which is also reminiscent of topographic waves.

It was only recently, that the data of the 1978 campaign of Lake of Zürich were explored with respect to long periodic wave motion. Temperature measurements and the isotherm depth spectras indicate a clear signal at 100-110 h which, again, can not be explained by an internal seiche motion. The fact that phase differences of isotherm depth pairs show anticlock-

wise motion around the basin can again be taken as a sign that the associated motion is probably a topographic Rossby wave (K. Hutter, personal communication). In short, experimental evidence for topographic waves is striking but theoretical models -even as approximations - are largely lacking.

1.4 Aim of this work

Up to now there exists a rather limited quantity of exact solutions of the topographic wave problems. Analytical procedures are found only for very special basin shapes and topographies, such as the parabolic circles or ellipses of Lamb (1932) and Ball (1965) or the elliptic basin with exponential depth profile, Mysak (1983, 1984). All these models could describe the periods of observed wave motion provided that a set of parameters was well chosen. It turned out, however, that the configurations, determined by the fitted parameters, did not show much similarity with the natural basins or profiles. For instance, in order to explain a topographic mode in Lake of Lugano Mysak et al. (1984) were forced to choose a basin shape which was much fatter and did not resemble the shape of Lake of Lugano. They were not able to obtain the required value of the period when selecting realistic length to width ratios. Therefore, at the moment there is certainly a lack of adequate theoretical models which could satisfactorily explain topographic waves in *realistic* basins.

By contrast, Finite Difference and Finite Element techniques are effective tools in explaining wave motions under very specific aspects. However, they are not likely to enlarge our knowledge from a *physical* point of view. Furthermore, they require immense computational effort for a problem which, in its basics, still lacks a thorough understanding. Questions concerning the spectrum and the modal structure or behaviour in curved and more complicated basins are still unanswered.

This is why this report proposes a method that treats the

problem from another point of view. It is not tried to find more exact solutions or other numerical techniques. We rather simplify the problem by making assumptions which are apt to the specific problem of second class waves. We attempt to show a way which can combine the preciseness of an exact model with the facility of the basin modelling supplied by a FD- or FE-method. A test of such a model is likely to bring about also the important properties of e.g. a lake basin under the aspect of long-periodic wave motion. Furthermore, we hope to obtain an answer about the quality and strength of such a method and a hint towards specific improvements of assumptions, which are invoked in the course of developments.

2. BASIC EQUATIONS

In this section we shall list those equations, that will eventually be used in our further developments. No details will be given as the essentials were already presented by Mysak (1984).

2.1 Two layer model

Vertical temperature profiles in stratified lakes can be subdivided roughly into three parts (Hutter, 1984a):

Epilimnion: layer with an average surface temperature of about 18°C and several meters depth,

Metalimnion: layer containing the thermocline and experiencing strong temperature gradients,

Hypolimnion: layer with a lower temperature of about 6°C and several tens of meters depth.

This typical stratification can mainly be found during summer periods, when the surface layer is heated by solar irradiation. In a first approximation this situation is simplified by introducing a two layer system of which the interface represents the position of the thermocline (Figure 1). Subsequently,

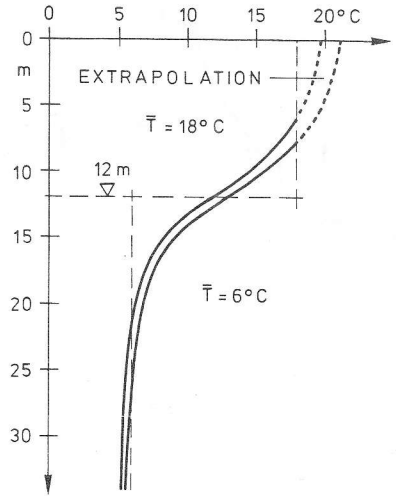

Figure 1

Upper and lower bound temperature profiles as measured in Lake of Zurich during August/September 1978. The dotted lines are extrapolations. Also shown are the two layer approximations with density discontinuity at 12 m depth and upper and lower layer temperatures 18°C and 6°C, respectively.

(From Hutter, 1984a)

the depth of the upper layer will be assumed much smaller than that of the lower layer.

Motions occur in both layers and are subject to a coupling by the thermocline. As we shall show later on, this coupling mechanism is weak in the sense that it is mainly one-way, i.e. the motion of the thermocline is driven by the barotropic transport. If the velocity fields in the two layers are unidirectional the motion is called barotropic. If they are in opposite directions it is baroclinic.

The configuration of the lake and the notation is summarized in Figure 2. Important in the depicted geometry are the vertical side walls that extend beyond the thermocline well into the hypolimnion. Application must, therefore, be limited to lakes with steep shores.

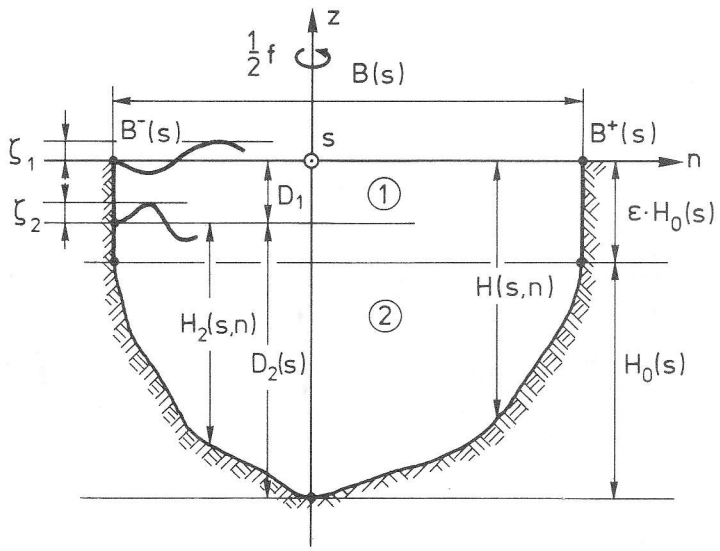

Figure 2

Side view of a cross section of the two layer lake in its natural coordinate system (s,n,z). Upper and lower layer variables are denoted by an index 1 or 2 respectively. The lake is within a rotating system of spatially constant angular velocity ½ f.

Lake topography varies in space only in the lower layer, i.e. the upper layer is confined by two vertical side walls, which must exceed the depth of the thermocline, i.e. $\varepsilon H_0(s) > D_1$ for all s. We accept the varying of the side walls with s because of analytical simplicity.

2.2 Governing equations

Basic idea in obtaining a description of the physical behaviour of our system is to formulate conservation equations for the fundamental physical processes, i.e. momentum, mass and energy. Since thermodynamic effects are of no concern in this study a closed system concept can be formulated, that is based on momentum and mass conservation for both layers. The full system is non-linear because of the advection terms, but they can be neglected by the argument of small Rossby numbers (geostrophic assumption). Furthermore, small elevations ζ_i in comparison to the depth of the upper layer will be considered. This approximation may be doubious in certain cases but is made for simplicity. Further, turbulence will be ignored but wind stress, distributed over the thin upper layer, and acting as a driving force will be considered.

Thus the equations of motion in components of a Cartesian system take on the form (Mysak, 1984, p. 87)

$$\begin{aligned} u_{1t} - f v_1 &= -g \zeta_{1x} + \tau^x/(\rho_1 D_1) \\ v_{1t} + f u_1 &= -g \zeta_{1y} + \tau^y/(\rho_1 D_1), \end{aligned} \tag{2.1}$$

$$D_1 (u_{1x} + v_{1y}) = \zeta_{2t} - \underline{\zeta_{1t}}, \tag{2.2}$$

$$\begin{aligned} u_{2t} - f v_2 &= -g \zeta_{1x} - g'(\zeta_{2x} - \underline{\zeta_{1x}}) \\ v_{2t} + f u_2 &= -g \zeta_{1y} - g'(\zeta_{2y} - \underline{\zeta_{1y}}) \end{aligned} \tag{2.3}$$

$$(H_2 u_2)_x + (H_2 v_2)_y = -\zeta_{2t}, \tag{2.4}$$

where g' is the reduced gravity $g' = g \cdot \frac{\rho_2 - \rho_1}{\rho_2}$. Everything that follows can be directly derived from equations (2.1) - (2.4).

2.3 Approximations

Equations (2.1) - (2.4) contain many aspects of motions in a lake. Here we are only interested in long-periodic oscillations, which can be isolated by performing the appropriate approximations.

2.3.1 Rigid lid approximation

It is known that to every wave type of the above system there exists an internal and an external variant. The periods of the latter are generally much smaller than those of the former and, by applying the rigid lid approximation, the external modes are impeded. This means, that compared to the interface elevation any surface elevation can be neglected, i.e. the underlined terms in (2.2) and (2.3) are ignored. With this, it follows from the mass conservations (2.2) and (2.4) that the quasi nondivergent velocity field can be replaced by the stream function ψ, through which the components of the integrated transport are given by

$$-\psi_y = D_1 u_1 + H_2 u_2, \qquad \psi_x = D_1 v_1 + H_2 v_2. \tag{2.5}$$

ψ is called the barotropic or mass transport stream function. Equations (2.1) - (2.4) can be transformed into a compact system in the variables ψ and $\zeta_2 \equiv \zeta$. The result -quoting Mysak (1984)- reads, assuming a constant Coriolis parameter f:

$$\begin{aligned} \nabla\cdot(H^{-1}\nabla\psi_t) + f(\nabla\Psi\times\nabla H^{-1})\cdot\hat{\underline{z}} &= -g' D_1 (\nabla\zeta\times\nabla H^{-1})\cdot\hat{\underline{z}} \\ &\quad + \frac{1}{\rho_1}\left[\nabla\times(\underline{\tau}H^{-1}) + \frac{H}{D_1}\underline{\tau}\times\nabla H^{-1}\right]\cdot\hat{\underline{z}}, \end{aligned} \tag{2.6}$$

$$\begin{aligned} H\nabla^2\zeta_t - \frac{H^2}{g' D_1 H_2} L\zeta_t + \frac{D_1}{H_2}\nabla\zeta_t\cdot\nabla H - \frac{f D_1}{H_2}(\nabla\zeta\times\nabla H)\cdot\hat{\underline{z}} \\ = \frac{1}{g' H_2}\left[\nabla(L\psi)\times\nabla H\right]\cdot\hat{\underline{z}} \\ - \frac{H}{\rho_1 g' D_1} f(\nabla\times L\underline{\tau})\cdot\hat{\underline{z}}, \end{aligned} \tag{2.7}$$

where the operator $L = \partial_{tt} + f^2$ has been introduced.

Mysak gives a detailed discussion of the physics of equations (2.6) and (2.7), which is now briefly summarized. In the absence of stratification ($g' = 0$) and wind forcing ($\underline{\tau} = \underline{0}$) (2.6) reduces to an equation that describes motions under conservation of potential vorticity (Hutter, 1984a, p. 26 ff). Stratification ($g' \neq 0$) in a lake with topography ($\nabla H \neq 0$) couples the barotropic part of (2.6) to baroclinic processes. Thus, the first term on the rhs of (2.6) represents the influence of baroclinic effects on barotropic motion. By the same argument the first term on the rhs of (2.7) describes the barotropic effects on the baroclinic motion. This means that there is in general a two-way coupling, the strength of which will be estimated below. We further recognize that, provided there is a constant depth within the lake and no wind forcing, equation (2.7) reveals internal gravity and Kelvin waves which propagate with the speed $c_i = (g' D_1 H_2 / H)^{1/2}$.

By deriving (2.6) and (2.7) from (2.1)-(2.4) two relations are obtained for the velocity fields as functions of ψ and ζ. These are

$$L\,\underline{u}_1 = \frac{1}{H}\left[\hat{\underline{z}}\times\nabla(L\psi) + H_2 g'(\nabla\zeta_t - f\hat{\underline{z}}\times\nabla\zeta) + \frac{H_2}{\rho_1 D_1}(\underline{\tau}_t - f\hat{\underline{z}}\times\tau)\right], \quad (2.8)_1$$

$$L\,\underline{u}_2 = \frac{1}{H}\left[\hat{\underline{z}}\times\nabla(L\psi) - D_1 g'(\nabla\zeta_t - f\hat{\underline{z}}\times\nabla\zeta) - \frac{1}{\rho_1}(\underline{\tau}_t - f\hat{\underline{z}}\times\tau)\right], \quad (2.8)_2$$

which are additively composed of three parts, i.e. a barotropic, a baroclinic and a wind forced component (see also § 2.5). The first are the same (and unidirectional) in both layers, and the second are in opposite directions and add up to vanishing total transport, reminiscent of barotropic and baroclinic behaviour, respectively.

2.3.2 Low frequency approximation

In equation (2.7) we realize that ζ appears with a third order time derivative. This means that (2.7) can contain three wave types. In fact a more precise analysis shows that there are two (internal) gravity waves and one topographic wave of

which the latter has the longest period. Because we want to study here topographic waves, we will search for solutions of (2.6), (2.7) with low frequency ω. For $\omega \ll f$ we may therefore neglect ω in comparison to f. Thus L reduces to $L \approx f^2$. Such an approximation, however, requires that periods are substantially greater than about 17 hours (the period corresponding to f). Parenthetically, we might also mention that this approximation holds only for lakes in which the internal seiche period (of a gravity or Kelvin wave) is considerably smaller than the period of topographic waves. Since the former increases with the lake dimension, the frequencies of gravity waves in larger lakes become of comparable order to those of topographic waves. For the lakes of Zurich and Lugano the approximation, however, is appropriate, see Table 1.

Lake	Surface length [km]	Period of internal gravity waves [h]	Period of internal topographic waves [h]
Lugano	17.2 [1]	≤ 28 [1]	74 [2]
Zurich	28 [1]	≤ 45 [1]	100 [2]
Geneva	72 [3]	78 [4]	72 - 96 [2]

[1] *Hutter, 1983*
[2] *Mysak, 1983*
[3] *Graf, 1983,*
[4] *Bäuerle, 1984*

Table 1

Table 1 showing that the gap between the eigenperiods of internal gravity and topographic waves depends on the lake dimension. The periods of the topographic waves are taken from an elliptical model.

2.4 Scaling

It is a general method in geophysics to simplify the often very complicated equations by estimating the importance of the individual terms. As a side result this process yields the important dimensionless parameters that govern the solutions of the equations (e.g. Reynolds number, Rossby number, etc.). By

scaling we mean a procedure that replaces any parameter ϕ of a set of equations by a product of its mean or characteristic value ϕ_0 and a dimensionless parameter (primed) which then is of order unity

$$\phi := \phi_0 \cdot \phi' \,. \tag{2.9}$$

2.4.1 Wind forcing mechanism

The true forcing mechanism in equations (2.6) and (2.7) is the wind. To estimate its relative importance consider the identity

$$\nabla \times (\underline{\tau} H^{-1}) + \frac{H}{D_1} \underline{\tau} \times \nabla H^{-1} = H^{-1} (\nabla \times \underline{\tau}) + (\nabla H^{-1}) \times \underline{\tau} + \frac{H}{D_1} \underline{\tau} \times \nabla H^{-1}. \tag{2.10}$$

The first term on the right can be neglected in comparison to the others, because the atmospheric length scale is in general much larger than the lake dimensions. Such a statement is tantamount to ignoring spatial variations of wind stress over the lake's domain. Further, comparing the last two terms it is seen that they differ by an order D_1/H which in view of our basic assumption is small (cf. Table 2). Consequently only the last term of (2.10) survives. In a way this is a strange result: only a lake with variable topography can be affected by the wind. This leads to the conclusion that the assumption on atmospheric length scales may be doubtful. Indeed, a varying topography in the vicinity of the lake may play a significant role as it can modify regional winds with atmospheric length scales to local winds with smaller length scales. An example is the topography around Lake of Lugano; but experimental evidence for the wind stress curl to be significant is so far lacking.

2.4.2 Gratton's scaling

Gratton (1983) considers lake stratifications with $D_1 \ll D_2$, i.e. a thin upper layer is based upon a deep hypolimnion. For this case he found that the baroclinic effect on the barotropic motion is of order D_1/D_2 smaller than the barotropic effect on

the baroclinic motion. So, to order D_1/D_2 the coupling becomes one-way. We omit the demonstration of the arguments here but suggest Mysak (1984, p. 92 ff) for further reading. The scaling is based on the substitutions following (2.9)

$$\psi := \psi_0 \psi', \quad \zeta := \zeta_0 \zeta', \quad \underline{\tau} := \tau_0 \underline{\tau}',$$
$$(x,y) := L(x',y'), \quad t := f^{-1} \cdot t', \qquad (2.11)$$
$$H := (D_1 + D_2)h', \quad H_2 := D_2 h_2,$$

where the primed variables are non-dimensional; L is a typical length scale of the considered waves (e.g. half the lake length). Higher wave modes, where cross variations are important, may require a (x,y)-scaling which is different for each spatial direction.

In the emerging equations terms of order D_1/D_2 are now ignored in comparison to those of order unity. Then (2.6), (2.7) transform to the non-dimensional equations (primes dropped)

$$\nabla \cdot (h^{-1} \nabla \psi_t) + (\nabla \psi \times \nabla h^{-1}) \cdot \hat{\underline{z}} = (h \underline{\tau} \times \nabla h^{-1}) \cdot \hat{\underline{z}}, \qquad (2.12)$$

$$(\nabla^2 - S^{-1}) \zeta_t = - (\nabla \psi \times \nabla h^{-1}) \cdot \hat{\underline{z}}, \qquad (2.13)$$

where S denotes a stratification parameter

$$S = \left(\frac{R_i}{L}\right)^2, \qquad (2.14)$$

with the internal Rossby radius

$$R_i^2 = \frac{g' D_1 D_2}{f^2 (D_1 + D_2)}. \qquad (2.15)$$

2.4.3 Scales in some Swiss lakes

Let us investigate now of which order these parameters are in nature. Table 2 collects the results partly quoted in the literature. Column 4 of this table demonstrates that neglecting terms of order D_1/D_2 in comparison to unity is certainly justified for Lake of Lugano and is still reasonable for all other lakes. Gratton's scale analysis also permits estimation

Lake	D_1 [m]	D_2^{mean} [m]	D_2^{max} [m]	$\frac{D_1}{D_2^{mean}}$	$\frac{\rho_2 - \rho_1}{\rho_2}$	R_i [km]	half length [km]	S^{-1}	ζ_0 [m]
Lugano	10[1]	183[1]	278[2]	0.055	$1.91 \cdot 10^{-3}$[1]	4.05	8.6	4.5	1.8[5]
Zurich	12[1]	52[1]	124[2]	0.231	$1.75 \cdot 10^{-3}$[1]	4.13	14	11.5	2.9[5]
Geneva	15[4]	153[4]	310[3]	0.098	$1.41 \cdot 10^{-3}$[4]	4.24	36	72.1	6.9[5]

1) *Hutter, 1984c, p. 78*
2) *Hutter, 1983, p. 108*
3) *Graf, 1983, p. 64*
4) *Bäuerle, 1984*
5) *Computed after Mysak, 1984, p. 94*

Table 2 Properties of Swiss lakes.

of the thermocline elevation amplitude (column 9) which is only a fraction of the epilimnion depth (column 1) and thus provides some a posteriori proof of the suitability of the linearized equations.

2.4.4 "Geometric optics" approximation

In equation (2.13) the stratification parameter S^{-1}, which is large in general, occurs together with ∇^2 which, in view of the scaling, is only of order unity. Because (2.13) has the form of a forced Helmholtz equation, neglection of ∇^2 in comparison to S^{-1} amounts to the geometric optics approximation (ray theory). To simplify the analysis of the baroclinic response we shall henceforth only deal with this approximation.

2.5 Scaled equations

Incorporating all above approximations the dimensionless field equations take on the form

$$\nabla \cdot (h^{-1} \nabla \psi_t) + (\nabla \psi \times \nabla h^{-1}) \cdot \hat{\underline{z}} = (h \underline{\tau} \times \nabla h^{-1}) \cdot \hat{\underline{z}} , \qquad (2.16)$$

$$S^{-1} \zeta_t = (\nabla \psi \times \nabla h^{-1}) \cdot \hat{\underline{z}} . \qquad (2.17)$$

Having solved this system for ψ and ζ enables us to calculate the velocity fields from (2.8) which now reduce to

$$\underline{u}_1 = \frac{1}{h}\left[\hat{\underline{z}}\times\nabla\psi + h(\nabla\zeta_t - \hat{\underline{z}}\times\nabla\zeta + \underline{\tau}_t - \hat{\underline{z}}\times\underline{\tau})\right], \qquad (2.18)_1$$

$$\underline{u}_2 = \frac{1}{h}\,\hat{\underline{z}}\times\nabla\psi\,. \qquad (2.18)_2$$

In this approximation the velocity field of the lower layer is merely barotropic, however, in the upper layer there are three components, viz. the barotropic, the baroclinic and the wind forced parts.

Mathematically, (2.16) is a linear, inhomogeneous partial differential equation for ψ in two dimensions. We first try to solve the homogeneous part of it and then study the modification due to simple wind forcings. Having determined ψ as the solution of (2.16) the thermocline elevation can be calculated from (2.17) and, in a last step, the velocity fields from (2.18).

2.6 Boundary conditions

Integration of the differential equations (2.16) and (2.17) requires prescription of boundary conditions. Let $\mathcal{D}$ be the lake domain and $\partial\mathcal{D}$ its boundary. Because of the vertical walls one boundary condition is no mass flux through the boundary

$$(D_1\,\underline{u}_1 + H_2\,\underline{u}_2)\cdot\hat{\underline{k}} = 0, \qquad (2.19)$$

where $\hat{\underline{k}}$ is the unit vector perpendicular to the boundary. Using (2.5) and the fact that $\hat{\underline{k}}\times\hat{\underline{z}}$ is a unit vector along $\partial\mathcal{D}$ (2.19) reduces to

$$\psi = 0 \quad \text{on} \quad \partial\mathcal{D}. \qquad (2.20)$$

In the same way we find a boundary condition for ζ by recognizing that $\underline{u}_i$ (i for upper and lower layer) must be tangential to $\partial\mathcal{D}$, $\underline{u}_i\cdot\hat{\underline{k}} = 0$. This again implies (2.19), but also $(\underline{u}_1 - \underline{u}_2)\cdot\hat{\underline{k}} = 0$, from which we find that to order D_1/D_2

$$\frac{\partial}{\partial k}\zeta_t - \frac{\partial\zeta}{\partial\ell} = -\hat{\underline{k}}\cdot\underline{\tau}_t + \hat{\underline{\ell}}\cdot\underline{\tau} \quad \text{on} \quad \partial\mathcal{D} \qquad (2.21)$$

must hold, where $\hat{\underline{\ell}}$ is the unit vector along $\partial\mathcal{D}$ and $\hat{\underline{k}}$ perpendicular to $\partial\mathcal{D}$.

2.7 Natural coordinates

It is convenient to describe a long but otherwise arbitrarily shaped lake in a natural curvilinear coordinate system. This means that we choose an orthogonal network which spans the lake domain in a natural way. The basis for this coordinate system is an axis, which follows more or less the thalweg of the lake. The arc length s along the axis forms the first coordinate of this system.

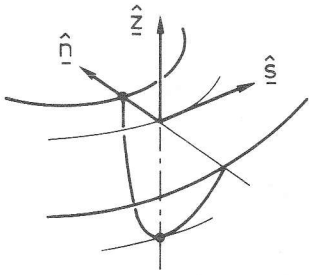

Figure 3

The position of the right handed natural coordinate system (s,n,z) in the lake basin.

$\hat{n}$ points to the positive center of curvature along $\hat{s}$.

In view of the restriction to elongated narrow lakes it is possible to choose a straight linear n-axis; so the system is curved only in the s-direction. In order to define the lake domain uniquely in terms of the coordinates the radius of curvature R(s) must exceed half the width of the lake B(s),

$$R(s) > \frac{1}{2} B(s). \qquad (2.22)$$

Sometimes R(s) may be too small to fulfil (2.22); then a different choice of the lake axis may yield better conditions.

2.7.1 Conversion of basis vectors

Let the lake axis be given by a parameter representation $(\tilde{x}(s), \tilde{y}(s))$ within a Cartesian system as shown in Figure 4. The coordinates of an arbitrary point P are then given by

$$\begin{aligned} x &= \tilde{x}(s) - n \sin\alpha(s), \\ y &= \tilde{y}(s) + n \cos\alpha(s), \end{aligned} \qquad (2.23)$$

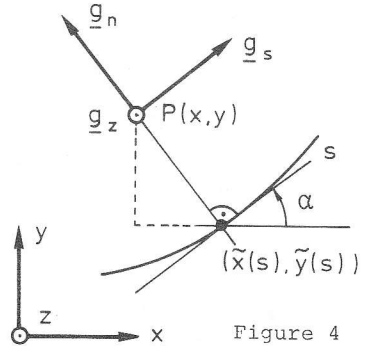

Figure 4

provided the n-axis is chosen to be straight. The set of basis vectors $\underline{g}_s$, $\underline{g}_n$ and $\underline{g}_z$ at the point P can be expressed in the form

$$\begin{aligned} \underline{g}_s &= \left(\frac{dx}{ds}, \frac{dy}{ds}, 0\right), \\ \underline{g}_n &= \left(\frac{dx}{dn}, \frac{dy}{dn}, 0\right), \\ \underline{g}_z &= (0, 0, 1), \end{aligned} \tag{2.24}$$

which is easily simplified to the form

$$\begin{aligned} \underline{g}_s &= (\tilde{x}' - n K \cos\alpha, \tilde{y}' - n K \cos\alpha, 0), \\ \underline{g}_n &= (-\sin\alpha, \cos\alpha, 0), \\ \underline{g}_z &\quad (0, 0, 1), \end{aligned} \tag{2.25}$$

using (2.23) and the fact that the curvature equals $K = \frac{d\alpha}{ds}$.

An important quantity for the characterization of a coordinate system is the arc element $d\underline{\ell}$. With the aid of Figure 5 it follows that $d\underline{\ell}$ takes on the form

$$\begin{aligned} d\underline{\ell} &= (J\, ds, dn, dz), \\ J &= 1 - Kn. \end{aligned} \tag{2.26}$$

This form is typical of an orthogonal metric.

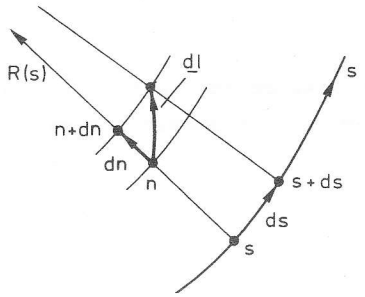

Figure 5
Arc element in a natural coordinate system.

2.7.2 Conversion of the ∇-operator

Let the arc element of an orthogonal metric be given by

$$d\underline{\ell} = (J_1\, dx_1, J_2\, dx_2, J_3\, dx_3), \tag{2.27}$$

see Table 3. Gradient, divergence and curl are then given by (see Pearson, 1974)

$$\text{grad}\, u = \left(\frac{1}{J_1}\frac{\partial u}{\partial x_1}; \frac{1}{J_2}\frac{\partial u}{\partial x_2}; \frac{1}{J_3}\frac{\partial u}{\partial x_3}\right), \tag{2.28}$$

$$\text{div}\, \underline{v} = \frac{1}{J_1 J_2 J_3}\left(\frac{\partial}{\partial x_1}(J_2 J_3 v_1) + \frac{\partial}{\partial x_2}(J_1 J_3 v_2) + \frac{\partial}{\partial x_3}(J_1 J_2 v_3)\right), \tag{2.29}$$

$$\text{curl } \underline{v} = \frac{1}{J_1 J_2 J_3}\Big[J_1 \frac{\partial}{\partial x_2}(J_3 v_3) - J_1 \frac{\partial}{\partial x_3}(J_2 v_2) \; ; \; J_2 \frac{\partial}{\partial x_3}(J_1 v_1) - J_2 \frac{\partial}{\partial x_1}(J_3 v_3) \; ; \; J_3 \frac{\partial}{\partial x_1}(J_2 v_2) - J_3 \frac{\partial}{\partial x_2}(J_1 v_1)\Big] , \tag{2.30}$$

v_1, v_2, v_3 are components of the vector $\underline{v}$ in the x_1, x_2, x_3 directions, respectively. Choosing the above coordinate system requires the identifications

$$J_1 = 1 - Kn, \quad J_2 = 1, \quad J_3 = 1. \tag{2.31}$$

System	Coordinates	J_1	J_2	J_3	
Cartesian	(x, y, z)	1	1	1	
cylindric	(r, ϕ, z)	1	r	1	
elliptic	(ξ, η, z)	J	J	1	, where $J = a(\mathrm{Sh}^2 \xi + \sin^2 \eta)^{1/2}$
natural	(s, n, z)	J	1	1	, where $J = 1 - K(s) \cdot n$

Table 3 Listing the coordinate systems that are often used in lake hydrodynamics.

2.8 Equations in natural coordinates

With the aid of (2.27), (2.28), (2.29) the equations (2.16), (2.17) take on the form

$$\frac{1}{J}\Big[\frac{\partial}{\partial s}\Big(\frac{h^{-1}}{J}\frac{\partial \psi_t}{\partial s}\Big) + J \frac{\partial}{\partial n}\Big(h^{-1}\frac{\partial \psi_t}{\partial n}\Big) - K h^{-1}\frac{\partial \psi_t}{\partial n} + \frac{\partial \psi}{\partial s}\frac{\partial h^{-1}}{\partial n} - \frac{\partial \psi}{\partial n}\frac{\partial h^{-1}}{\partial s}\Big] = h\Big[\tau_s \frac{\partial h^{-1}}{\partial n} - \tau_n \frac{1}{J}\frac{\partial h^{-1}}{\partial s}\Big], \tag{2.32}$$

$$S^{-1}\zeta_t = \frac{1}{J}\Big[\frac{\partial \psi}{\partial s}\frac{\partial h^{-1}}{\partial n} - \frac{\partial \psi}{\partial n}\frac{\partial h^{-1}}{\partial s}\Big], \tag{2.33}$$

where we have also used (2.26).

3. METHOD OF WEIGHTED RESIDUALS

3.1 Breakdown of simple separation

The number of known exact solutions of the topographic wave operator for enclosed basins is relatively small (Lamb, 1932; Ball, 1965; Saylor et al., 1980; Mysak, 1983, 1984). The reason is that the homogeneous part of (2.16) does not permit separable solutions for an arbitrary topography. Let us demonstrate this in a coordinate system (x_1, x_2, x_3) where the arc element $d\ell$ is given by (2.27). We select the separations

$$\psi(x_1, x_2, t) = e^{i\omega t} \cdot \psi_1(x_1) \cdot \psi_2(x_2),$$

$$h^{-1}(x_1, x_2) = h^{-1}(x_1) \cdot h_2^{-1}(x_2),$$

$$\frac{J_1(x_1, x_2)}{J_2(x_1, x_2)} = a_1(x_1) \cdot a_2(x_2),$$

and then obtain, with the aid of (2.28) and (2.29), for the homogeneous part of (2.16)

$$\frac{h_1}{a_1 \psi_1} \frac{\partial}{\partial x_1}\left(h_1^{-1} a_1^{-1} \frac{\partial \psi_1}{\partial x_1}\right) + \frac{h_2 a_2}{\psi_2} \frac{\partial}{\partial x_2}\left(h_2^{-1} a_2 \frac{\partial \psi_1}{\partial x_2}\right)$$
$$+ \frac{1}{i\omega} \frac{a_2}{a_1}\left[\frac{h_2}{\psi_1} \frac{\partial \psi_1}{\partial x_1} \frac{\partial h_2^{-1}}{\partial x_2} - \frac{h_1}{\psi_2} \frac{\partial \psi_2}{\partial x_2} \frac{\partial h_1^{-1}}{\partial x_1}\right] = 0. \qquad (3.1)$$

Lamb, Saylor and Mysak selected a wavelike structure

$$\psi_2(x_2) = e^{i\alpha x_2},$$

and a topography that varied only in the x_1-direction. Thus (3.1) reduces to

$$\frac{h_1}{a_1 \psi_1} \frac{\partial}{\partial x_1}\left(h_1^{-1} a_1^{-1} \frac{\partial \psi_1}{\partial x_1}\right)$$
$$+ a_2 e^{-i\alpha x_2} \frac{\partial}{\partial x_2}\left(a_2 i\alpha e^{i\alpha x_2}\right) - \frac{\alpha}{\omega} \frac{a_2}{a_1} h_1 \frac{\partial h_1^{-1}}{\partial x_1} = 0, \qquad (3.2)$$

which is separable provided a_2/a_1 is only a function of x_1. Thus, Saylor and Mysak who used cylindric and elliptic coordinate systems, respectively, were able to find separable solutions of (3.2). In this study we do not want to be restricted to topographies that vary only in one direction. Further,

we make use of a natural coordinate system which in general does not allow separation. The next sections demonstrate the application of the method of Weighted Residuals, see Finlayson (1972), on the topographic wave problem represented by equation (2.16).

3.2 Generalized ansatz of separation

Just having shown that simple separation fails, we now try to use the impossible anyhow, yet in approximate fashion. We do no longer require strict separability but rather prescribe the functional dependence in one direction. This functional dependence shall be described by a well-chosen set of linear independent basis functions that may already fulfil the boundary conditions. It is obvious that our problem then reduces to a problem in only one dimension, since its behaviour in the other is already chosen.

At this point, it seems appropriate to motivate the use of the coordinate system (s, n, z). It naturally selects the small direction n; it is this direction for which the basis functions are selected, because the true behaviour can most likely best be approximated in this direction, see however later developments.

Let $\{P_\alpha(s, n)\}$ be a convenient set of known basis functions indexed by α, and let $\psi(s, n, t)$ be decomposed into these basis functions as follows:

$$\psi(s,n,t) = \sum_{\alpha=1}^{N} P_\alpha(s,n) \cdot \psi^\alpha(s,t). \qquad (3.3)$$

Each basis function is weighted by a function $\psi^\alpha(s,t)$ that is assumed not to depend on n. In other words, all n-dependence has been thrown into the known prescribed system $\{P_\alpha\}$, which preferably is chosen from a complete set. If $N < \infty$, (3.3) is an approximation in so far as there exists a certain limitation in the variation of ψ, i.e. the set $\{P_\alpha\}$ looses its completeness. It is hoped that truncating (3.3) for very small N will already provide the essentials of the physical behaviour.

3.3 Integrated representation of the equations

Let $\mathbb{D}$ and $\mathbb{B}$ be a linear differential operator and a boundary operator, respectively, e.g. for $\underline{\tau} = \underline{0}$ in (2.16) $\mathbb{D} = \nabla \cdot h^{-1} \nabla \frac{\partial}{\partial t} - \underline{\hat{z}} \cdot (\nabla h^{-1}) \times \nabla$ and $\mathbb{B} = \mathbb{1}$. Equation (2.16) with its boundary condition (2.20) reads then

$$\mathbb{D}\psi = 0, \quad \text{in} \quad \mathcal{D}, \tag{3.4}$$

$$\mathbb{B}\psi = 0, \quad \text{on} \quad \partial\mathcal{D}, \tag{3.5}$$

A weak form of (3.4), (3.5) can be obtained by a weighted integration over the respective domains

$$\int_{\mathcal{D}} (\mathbb{D}\,\psi)\,\delta\phi_{\mathcal{D}}\,da + \oint_{\partial\mathcal{D}} (\mathbb{B}\,\psi)\,\delta\,\phi_{\partial\mathcal{D}}\,d\ell = 0. \tag{3.6}$$

Here $\delta\phi_{\mathcal{D}}$ and $\delta\phi_{\partial\mathcal{D}}$ are weighting functions defined over $\mathcal{D}$ and $\partial\mathcal{D}$, respectively, and δ is a symbol to remind the reader that in the space of generalized functions the functions are arbitrary. (3.6) follows directly from (3.4) and (3.5). Conversely, (3.4), (3.5) follow from (3.6) only if (3.6) holds for any function $\delta\phi$. This is a consequence of the fundamental lemma of Calculus of Variation (see Courant & Hilbert, 1967).

We now insert (3.3) for ψ and a similar expression for $\delta\phi$,

$$\delta\phi = \sum_{\beta=1}^{M} Q_\beta(s, n)\,\delta\phi^\beta(s, t), \tag{3.7}$$

into (3.6) and obtain an expression of the form

$$\int_{\mathcal{D}} (\mathbb{D}\,P_\alpha\underline{\psi^\alpha})\,Q_\beta\,\underline{\delta\phi^\beta_{\mathcal{D}}}\,da + \oint_{\partial\mathcal{D}} (\mathbb{B}\,P_\alpha\underline{\psi^\alpha})\,Q_\beta\,\underline{\delta\phi^\beta_{\partial\mathcal{D}}}\,d\ell = 0, \tag{3.8}$$

in which summation over identical upper and lower indices is understood. The underlined functions are independent of n. Selecting $M = N < \infty$ and sets $\{P_\alpha\}$ and $\{Q_\beta\}$ which already fulfil the boundary conditions

$$P_\alpha\Big|_{\partial\mathcal{D}} = 0, \quad Q_\beta\Big|_{\partial\mathcal{D}} = 0, \tag{3.9}$$

the second integral in (3.8) vanishes automatically, except

perhaps where the lake axis intersects the boundary $\partial\mathcal{D}$. We denote these points by $s = 0$ and $s = L$ and call them the end points, see Figure 6.

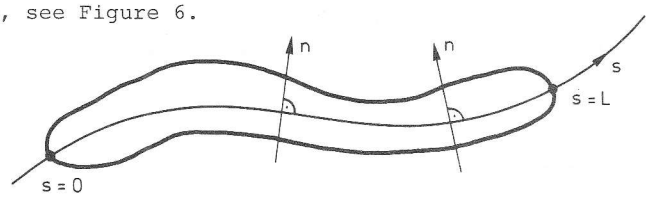

Figure 6
Configuration of an elongated lake.

So the only possible contribution of the second integration in (3.8) could be

$$\oint_{0^+}^{0^-} \mathbb{B}\,(P_\alpha \psi^\alpha)\, Q_\beta\, \delta\phi^\beta_{\partial\mathcal{D}}\, d\ell + \oint_{L^-}^{L^+} \mathbb{B}\,(P_\alpha \psi^\alpha)\, Q_\beta\, \delta\phi^\beta_{\partial\mathcal{D}}\, d\ell,$$

which vanishes for all $\delta\phi^\beta_{\partial\mathcal{D}}$ only if we impose on ψ^α the boundary condition $\psi^\alpha = 0$ at $s = 0$ and $s = L$. If it is further recognized that

$$da = J\, dn\, ds, \tag{3.10}$$

in view of Figure 5, equation (3.8) will take on the form

$$\int_s \left(\int_n (\mathbb{D}\, P_\alpha \psi^\alpha)\, Q_\beta\, J\, dn \right) \delta\phi^\beta_{\mathcal{D}}\, ds = 0. \tag{3.11}$$

The inner most integral of (3.11) can be expressed as a matrix element operator $\mathbb{M}_{\beta\alpha}$ on ψ^α so that (3.11) becomes

$$\int_s \mathbb{M}_{\beta\alpha}\, \psi^\alpha\, \delta\phi^\beta_{\mathcal{D}}\, ds = 0, \tag{3.12}$$

which must hold for any $\delta\phi^\beta_{\mathcal{D}}$. Invoking the fundamental lemma of the Calculus of Variations, (3.12) reduces to the two-point boundary value problem

$$\begin{aligned} \mathbb{M}_{\beta\alpha}\, \psi^\alpha(s,t) &= 0, \quad \alpha, \beta = 1, \ldots, N, \quad 0 < s < L, \\ \psi^\alpha(s,t) &= 0, \qquad\qquad\qquad\quad s = 0, L. \end{aligned} \tag{3.13}$$

So, our inherent two dimensional problem (2.16) has been reduced to a finite set of coupled spatially one-dimensional linear

differential equations $(3.13)_1$ with boundary conditions $(3.13)_2$. This procedure will now be applied to (2.32), by first assuming homogeneity, i.e. no wind stress, $\underline{\tau} = \underline{0}$, and then calculating the matrix elements $M_{\beta\alpha}$ for a given lake topography.

3.4 Matrix elements

Substituting (3.3) into the homogeneous system (2.32) (with no wind forcing) and performing (3.6), thereby incorporating (3.7), we obtain

$$0 = \iint_{\mathcal{D}} \Big[\underbrace{\frac{\partial}{\partial s}\Big(\frac{h^{-1}}{J}\,\frac{\partial}{\partial s}(P_\alpha\,\psi_t^\alpha)\Big)}_{(1)} + \underbrace{\frac{\partial}{\partial n}\,h^{-1}\,J\,\frac{\partial}{\partial n}(P_\alpha\,\psi_t^\alpha)}_{(2)} + \underbrace{\frac{\partial h^{-1}}{\partial n}\,\frac{\partial}{\partial s}(P_\alpha\,\psi^\alpha)}_{(3)} - \underbrace{\frac{\partial h^{-1}}{\partial s}\,\frac{\partial}{\partial n}(P_\alpha\,\psi^\alpha)}_{(4)} \Big] Q_\beta\,\delta\phi_{\mathcal{D}}^\beta\,dn\,ds, \tag{3.14}$$

where use of the summation convention has been made. Each term in this expression will be evaluated separately and boundaries for the integration in the transverse direction will be denoted by $B^-(s)$ and $B^+(s)$ as shown in Figure 2. In the following deductions use will be made of Leibnitz' integration rule

$$\begin{aligned} \int_{B^-(s)}^{B^+(s)} \frac{\partial F}{\partial s}\,G\,dn &= \int_{B^-(s)}^{B^+(s)} \frac{\partial}{\partial s}(FG)\,dn - \int_{B^-(s)}^{B^+(s)} F\,\frac{\partial G}{\partial s}\,dn \\ &= \frac{\partial}{\partial s}\int_{B^-(s)}^{B^+(s)} FG\,dn - (FG)\Big|_{B^+}\cdot\frac{\partial B^+}{\partial s} + (FG)\Big|_{B^-}\cdot\frac{\partial B^-}{\partial s} - \int_{B^-}^{B^+} F\,\frac{\partial G}{\partial s}\,dn, \end{aligned} \tag{3.15}$$

where F and G are arbitrary, differentiable functions of s and n.

With these preliminaries the terms (1) to (4) can now be evaluated. The rule of transformation is to remove differentiations of the topography h as far as possible, which can be achieved by integration by parts:

Term (1):

$$(1) = \int \frac{\partial}{\partial s}\left(\frac{h^{-1}}{J}\frac{\partial}{\partial s}(P_\alpha \psi_t^\alpha)\right) Q_\beta \, dn$$

$$= \frac{\partial}{\partial s}\int \frac{h^{-1}}{J}\frac{\partial}{\partial s}(P_\alpha \psi_t^\alpha) Q_\beta \, dn - \int \frac{h^{-1}}{J}\frac{\partial}{\partial s}(P_\alpha \psi_t^\alpha)\frac{\partial Q_\beta}{\partial s} \, dn$$

$$= \frac{\partial}{\partial s}\left[\psi_t^\alpha \int \frac{h^{-1}}{J}\frac{\partial P_\alpha}{\partial s} Q_\beta \, dn + \frac{\partial \psi_t^\alpha}{\partial s}\int \frac{h^{-1}}{J} P_\alpha Q_\beta \, dn\right]$$

$$- \psi_t^\alpha \int \frac{h^{-1}}{J}\frac{\partial P_\alpha}{\partial s}\frac{\partial Q_\beta}{\partial s} \, dn - \frac{\partial \psi_t^\alpha}{\partial s}\int \frac{h^{-1}}{J} P_\alpha \frac{\partial Q_\beta}{\partial s} \, dn \qquad (3.16)$$

$$= \psi_t^\alpha\left[\frac{\partial}{\partial s}\int \frac{h^{-1}}{J}\frac{\partial P_\alpha}{\partial s} Q_\beta \, dn - \int \frac{h^{-1}}{J}\frac{\partial P_\alpha}{\partial s}\frac{\partial Q_\beta}{\partial s} \, dn\right]$$

$$+ \frac{\partial \psi_t^\alpha}{\partial s}\left[\int \frac{h^{-1}}{J}\frac{\partial P_\alpha}{\partial s} Q_\beta \, dn + \frac{\partial}{\partial s}\int \frac{h^{-1}}{J} P_\alpha Q_\beta \, dn\right.$$

$$\left. - \int \frac{h^{-1}}{J} P_\alpha \frac{\partial Q_\beta}{\partial s} \, dn\right] + \frac{\partial^2 \psi_t^\alpha}{\partial s^2}\int \frac{h^{-1}}{J} P_\alpha Q_\beta \, dn ,$$

Term (2):

$$(2) = \int \frac{\partial}{\partial n}\left[h^{-1} J \frac{\partial}{\partial n}(P_\alpha \psi_t^\alpha)\right] Q_\beta \, dn$$

$$= - \int h^{-1} J \frac{\partial}{\partial n}(P_\alpha \psi_t^\alpha)\frac{\partial Q_\beta}{\partial n} \, dn \qquad (3.17)$$

$$= - \psi_t^\alpha \int h^{-1} J \frac{\partial P_\alpha}{\partial n}\frac{\partial Q_\beta}{\partial n} \, dn,$$

Term (3):

$$(3) = \int \frac{\partial h^{-1}}{\partial n}\frac{\partial}{\partial s}(P_\alpha \psi^\alpha) Q_\beta \, dn$$

$$= - \int \frac{\partial}{\partial n}\left(\frac{\partial}{\partial s}(P_\alpha \psi^\alpha) Q_\beta\right)\cdot h^{-1} \, dn \qquad (3.18)$$

$$= -\psi^\alpha \int h^{-1}\frac{\partial}{\partial n}\left(\frac{\partial P_\alpha}{\partial s} Q_\beta\right) dn - \frac{\partial \psi^\alpha}{\partial s}\int h^{-1}\frac{\partial}{\partial n}(P_\alpha Q_\beta) \, dn,$$

Term (4):

$$(4) = -\int \frac{\partial h^{-1}}{\partial s}\frac{\partial}{\partial n}(P_\alpha \psi^\alpha) Q_\beta \, dn$$

$$= - \frac{\partial}{\partial s}\int h^{-1}\frac{\partial}{\partial n}(P_\alpha \psi^\alpha) Q_\beta \, dn + \int h^{-1}\frac{\partial}{\partial s}\left(\frac{\partial}{\partial n}(P_\alpha \psi^\alpha) Q_\beta\right) dn$$

$$= - \frac{\partial \psi^\alpha}{\partial s}\int h^{-1}\frac{\partial P_\alpha}{\partial n} Q_\beta \, dn - \psi^\alpha \frac{\partial}{\partial s}\int h^{-1}\frac{\partial P_\alpha}{\partial n} Q_\beta \, dn \qquad (3.19)$$

$$+ \psi^\alpha \int h^{-1}\frac{\partial}{\partial s}\left(\frac{\partial P_\alpha}{\partial n} Q_\beta\right) dn + \frac{\partial \psi^\alpha}{\partial s}\int h^{-1}\frac{\partial P_\alpha}{\partial n} Q_\beta \, dn.$$

Parenthetically we may remark that the process of this evaluation is more complex when the basis functions are not restricted by the condition that they vanish along the shore, because further integration by parts is necessary in that case. Insering (3.16) - (3.19) into (3.14) yields the required form (3.12) of (3.14), namely

$$
\begin{aligned}
0 = \int_{s=0}^{s=L} ds\ \delta\phi^{\beta} \Bigg[& \frac{\partial^2 \psi_t^{\alpha}}{\partial s^2} \Big[\int \frac{h^{-1}}{J} P_{\alpha} Q_{\beta}\, dn \Big] \\
& + \frac{\partial \psi_t^{\alpha}}{\partial s} \Big[\int \frac{h^{-1}}{J} \frac{\partial P_{\alpha}}{\partial s} Q_{\beta}\, dn + \frac{\partial}{\partial s} \int \frac{h^{-1}}{J} P_{\alpha} Q_{\beta}\, dn - \int \frac{h^{-1}}{J} P_{\alpha} \frac{\partial Q_{\beta}}{\partial s}\, dn \Big] \\
& + \psi_t^{\alpha} \Big[\frac{\partial}{\partial s} \int \frac{h^{-1}}{J} \frac{\partial P_{\alpha}}{\partial s} Q_{\beta}\, dn - \int \frac{h^{-1}}{J} \frac{\partial P_{\alpha}}{\partial s} \frac{\partial Q_{\beta}}{\partial s}\, dn - \int h^{-1} J \frac{\partial P_{\alpha}}{\partial n} \frac{\partial Q_{\beta}}{\partial n}\, dn \Big] \\
& + \frac{\partial \psi^{\alpha}}{\partial s} \Big[- \int h^{-1} \frac{\partial P_{\alpha}}{\partial n} Q_{\beta}\, dn - \int h^{-1} P_{\alpha} \frac{\partial Q_{\beta}}{\partial n}\, dn \Big] \\
& + \psi^{\alpha} \Big[\int h^{-1} \frac{\partial P_{\alpha}}{\partial n} \frac{\partial Q_{\beta}}{\partial s}\, dn - \int h^{-1} \frac{\partial P_{\alpha}}{\partial s} \frac{\partial Q_{\beta}}{\partial n}\, dn - \frac{\partial}{\partial s} \int h^{-1} \frac{\partial P_{\alpha}}{\partial n} Q_{\beta}\, dn \Big] \Bigg].
\end{aligned}
\tag{3.20}
$$

The inner most integrals are understood as $\int_{B^-(s)}^{B^+(s)}$. Since (3.20) must hold for any $\delta\phi_{\mathcal{D}}^{\beta}$, it follows that

$$
\begin{aligned}
M_{\beta\alpha}\, \psi^{\alpha} &= 0, \quad \alpha, \beta = 1,2,\ldots,N, \quad 0 < s < L, \\
\psi^{\alpha} &= 0, \qquad\qquad\qquad\quad s = 0, L,
\end{aligned}
\tag{3.21}
$$

where the linear matrix operator $M_{\beta\alpha}$ is given by

$$
\begin{aligned}
M_{\beta\alpha} = \quad & M_{\beta\alpha}^{00} \frac{\partial^3}{\partial s^2\, \partial t} \\
& + (M_{\beta\alpha}^{10} + \frac{\partial}{\partial s} M_{\beta\alpha}^{00} - M_{\beta\alpha}^{01}) \frac{\partial^2}{\partial s\, \partial t} \\
& + (\frac{\partial}{\partial s} M_{\beta\alpha}^{10} - M_{\beta\alpha}^{11} - M_{\beta\alpha}^{22}) \frac{\partial}{\partial t} \\
& + (- M_{\beta\alpha}^{20} - M_{\beta\alpha}^{02}) \frac{\partial}{\partial s} \\
& + (M_{\beta\alpha}^{21} - M_{\beta\alpha}^{12} - \frac{\partial}{\partial s} M_{\beta\alpha}^{20}),
\end{aligned}
\tag{3.22}
$$

with

$$M^{00}_{\beta\alpha} = \int h^{-1} J^{-1} P_\alpha Q_\beta \, dn,$$

$$M^{10}_{\beta\alpha} = \int h^{-1} J^{-1} \frac{\partial P_\alpha}{\partial s} Q_\beta \, dn, \qquad M^{01}_{\beta\alpha} = \int h^{-1} J^{-1} P_\alpha \frac{\partial Q_\beta}{\partial s} \, dn,$$

$$M^{20}_{\beta\alpha} = \int h^{-1} \frac{\partial P_\alpha}{\partial n} Q_\beta \, dn, \qquad M^{02}_{\beta\alpha} = \int h^{-1} P_\alpha \frac{\partial Q_\beta}{\partial n} \, dn, \qquad (3.23)$$

$$M^{11}_{\beta\alpha} = \int h^{-1} J^{-1} \frac{\partial P_\alpha}{\partial s} \frac{\partial Q_\beta}{\partial s} \, dn, \qquad M^{22}_{\beta\alpha} = \int h^{-1} J \frac{\partial P_\alpha}{\partial n} \frac{\partial Q_\beta}{\partial n} \, dn,$$

$$M^{12}_{\beta\alpha} = \int h^{-1} \frac{\partial P_\alpha}{\partial s} \frac{\partial Q_\beta}{\partial n} \, dn, \qquad M^{21}_{\beta\alpha} = \int h^{-1} \frac{\partial P_\alpha}{\partial n} \frac{\partial Q_\beta}{\partial s} \, dn.$$

The individual components $M^{ij}_{\beta\alpha}$ in (3.22) are known functions of s and depend on the topography of the lake, h, on the metric of the natural coordinate system, J(s, n), on the shape of the lake shore, $B^{\pm}(s)$, and on the sets of basis functions $\{P_\alpha(s,n)\}$ and $\{Q_\beta(s,n)\}$.

3.5 Incorporation of the wind

If, instead of searching for the free modes, we want to consider the response of the lake to external wind forcing, the homogeneous two-point boundary value problem must be replaced by the inhomogeneous set

$$\begin{aligned} M_{\beta\alpha} \, \psi^\alpha &= W_\beta, \quad \beta = 1,2,\ldots,N, \qquad 0 < s < L \\ \psi^\alpha &= 0, \qquad\qquad\qquad\qquad\quad s = 0, L \end{aligned} \qquad (3.24)$$

where for prescribed wind $\underline{\tau}$, W_β is a known vector. Applying to the rhs of (2.32) the procedure that is described in section 3.3 yields

$$W_\beta = \int Jh(\tau_s \frac{\partial h^{-1}}{\partial n} - \tau_n \frac{1}{J} \frac{\partial h^{-1}}{\partial s}) Q_\beta \, dn, \qquad (3.25)$$

which can be calculated for a given lake and wind field.

4. APPLICATION TO SPECIAL TOPOGRAPHIES

4.1 Basic Assumptions

Consider now a straight lake with symmetric cross sections, thus

$$K(s) = 0, \qquad h(s,n) = h(s,-n)\,. \tag{4.1}$$

With the aid of Figure 2 it follows that

$$|B^+(s)| = |B^-(s)| = \frac{1}{2}B(s)\,. \tag{4.2}$$

The effects of the topography of the lake on the waves will be incorporated by choosing a profile of the form (cf. Saylor et al., 1980)

$$h(s,n) = h_0(s)\cdot h_1(s,n,q,\varepsilon),$$
$$h_1(s,n,q,\varepsilon) = 1+\varepsilon - \left|\frac{2n}{B(s)}\right|^q, \tag{4.3}$$

where the topography parameter q and the sidewall parameter ε have been introduced. Their effects on the topography are shown in Figure 7. Usually the sidewalls of the basin are chosen to be of constant depth, but here we prefer an expression of the form (4.3) because of analytical simplicity. We require $\varepsilon > D_1/D_2$ (cf. Figure 2) which yields for ε the values listed in Table 4. There are two reasons why the introduction of sidewalls is necessary. Physically we require vertical boundaries, otherwise all waves impinging on the shore would break. That means that nonlinear effects would be important. Mathematically $\varepsilon \neq 0$ prevents some of the matrix elements (3.23) from becoming

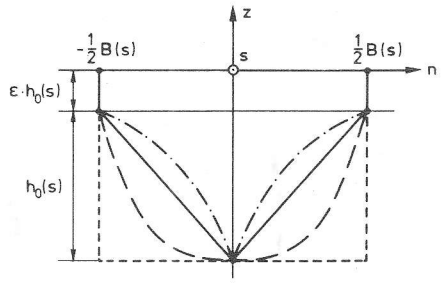

—·—·— 0 < q < 1
——— q = 1
— — — q > 1
- - - - - q → ∞

Figure 7

Cross sections of the lake basin.

Lake	D_1[m]	D_2^{mean} [m]	$\varepsilon = \frac{D_1}{D_2^{mean}}$
Lugano	10	183	0.055
Zürich	12	52	0.231
Geneva	15	153	0.098

Table 4

Magnitudes for the sidewall parameter ε, calculated from Table 2.

non-integrable. It will have to be tested later on how strongly the results will depend on this sidewall parameter ε.

4.2 Symmetrization

That the lake bathymetry has been restricted to symmetric cross sections suggests to split the motion, described by ψ, into two parts, viz. a symmetric part ψ_+ and a skew-symmetric part ψ_-, whereby $n = 0$ is meant to be the center of symmetry:

$$\psi(s,n,t) = \psi_+(s,n,t) + \psi_-(s,n,t)\,, \tag{4.4}$$

with

$$\begin{aligned} \psi_+(s,n,t) &= \psi_+(s,-n,t)\,, \\ \psi_-(s,n,t) &= -\psi_-(s,-n,t)\,. \end{aligned} \tag{4.5}$$

The separations (4.4) and (4.5) require that the set of basis functions $\{P_\alpha(s,n)\}$ and $\{Q_\beta(s,n)\}$ will have to be split accordingly into these two parts, since only the basis functions contain an n-dependence (cf. (3.3), (3.7)). As a result, the matrix elements (3.23) will be split into parts that act only on symmetric or skew-symmetric stream functions ψ. Let us demonstrate this by using

$$\begin{aligned} P_\alpha(s,n) &= P_\alpha^+(s,n) + P_\alpha^-(s,n)\,, \\ Q_\beta(s,n) &= Q_\beta^+(s,n) + Q_\beta^-(s,n)\,, \end{aligned} \qquad (\alpha,\beta = 1,\ldots,N) \tag{4.6}$$

as basis functions. Then for $M_{\beta\alpha}^{00}$ we obtain

$$\begin{aligned} M_{\beta\alpha}^{00} &= \int h^{-1}(P_\alpha^+ + P_\alpha^-)(Q_\beta^+ + Q_\beta^-)\,dn \\ &= \int h^{-1}\, P_\alpha^+\, Q_\beta^+\, dn + \int h^{-1}\, P_\alpha^-\, Q_\beta^-\, dn \\ &\quad + \int h^{-1}\, P_\alpha^-\, Q_\beta^+\, dn + \int h^{-1}\, P_\alpha^+\, Q_\beta^-\, dn, \end{aligned} \tag{4.7}$$

where the last two summands vanish because the integration of a skew-symmetric function over a symmetric domain always vanishes. Similar properties hold for the other matrices.

It is now advantageous to introduce the separations into symmetric and skew-symmetric functions for the solution functions ψ^α. In other words, the vector $\underline{\psi}$ will now have the form

$$\underline{\psi} = (\underbrace{\psi_+^1, \psi_+^2, \ldots, \psi_+^N}_{\text{symmetric components}}; \underbrace{\psi_-^1, \psi_-^2, \ldots, \psi_-^N}_{\text{skew-symmetric components}}). \tag{4.8}$$

This is tantamount to splitting the solution space of ψ into the direct sum of symmetric and skew-symmetric subspaces, and it corresponds to the recognition that P_α^+, P_α^- and Q_β^+, Q_β^- contribute to different submatrices in the matrices $M_{\beta\alpha}^{ij}$. For instance, in the notation of (4.8) the matrix operator $\underline{M}^{00}$ can be written in the quasi diagonal form

$$\underline{M}^{00} = \begin{bmatrix} \underline{M}^{00++} & 0 \\ 0 & \underline{M}^{00--} \end{bmatrix}, \tag{4.9}$$

where $\underline{M}^{00++}$ and $\underline{M}^{00--}$ are given by

$$\begin{aligned} M_{\beta\alpha}^{00++} &= \int h^{-1} P_\alpha^+ Q_\beta^+ \, dn, \\ M_{\beta\alpha}^{00--} &= \int h^{-1} P_\alpha^- Q_\beta^- \, dn. \end{aligned} \tag{4.10}$$

Matrix operators that take on this form can not couple the symmetric and skew-symmetric part of the motion. Considering, on the other hand, the matrix element $M_{\beta\alpha}^{20}$, or

$$\begin{aligned} M_{\beta\alpha}^{20} = &\int h^{-1} \frac{\partial P_\alpha^+}{\partial n} Q_\beta^- \, dn + \int h^{-1} \frac{\partial P_\alpha^-}{\partial n} Q_\beta^+ \, dn \\ &+ \int h^{-1} \frac{\partial P_\alpha^+}{\partial n} Q_\beta^+ \, dn + \int h^{-1} \frac{\partial P_\alpha^-}{\partial n} Q_\beta^- \, dn, \end{aligned} \tag{4.11}$$

shows that here the last two summands vanish because the derivative in the n-direction changes the symmetry. Thus, matrix

elements (3.23) that contain an odd number of derivatives in the n-direction take on the form

$$\underline{M}^{20} = \begin{bmatrix} 0 & \underline{M}^{20-+} \\ \underline{M}^{20+-} & 0 \end{bmatrix}, \tag{4.12}$$

where the elements are given by

$$\begin{aligned} M^{20+-}_{\beta\alpha} &= \int h^{-1} \frac{\partial P^{+}_{\alpha}}{\partial n} Q^{-}_{\beta} \, dn, \\ M^{20-+}_{\beta\alpha} &= \int h^{-1} \frac{\partial P^{-}_{\alpha}}{\partial n} Q^{+}_{\beta} \, dn. \end{aligned} \tag{4.13}$$

Matrix operators of the type (4.12) couple symmetric and skew-symmetric motion, which is necessary for wave solutions to exist. To make this explicit, note that (3.21) can be written as

$$\left(i\omega \begin{bmatrix} \underline{M}^{++} & 0 \\ 0 & \underline{M}^{--} \end{bmatrix} + \begin{bmatrix} 0 & \underline{M}^{-+} \\ \underline{M}^{+-} & 0 \end{bmatrix} \right) \begin{bmatrix} \underline{\psi}_{+} \\ \underline{\psi}_{-} \end{bmatrix} = 0, \tag{4.14}$$

where the operator $\partial/\partial t$ has been replaced by $i\omega$ through a harmonic time dependence $e^{i\omega t}$ of the solution. The assumption of e.g. a purely symmetric motion, i.e. $\underline{\psi}_{-} = 0$, leads to the system

$$\begin{aligned} i\omega \, M^{++}_{\beta\alpha} \, \psi^{\alpha}_{+} &= 0, \\ M^{+-}_{\beta\alpha} \, \psi^{\alpha}_{+} &= 0, \end{aligned} \qquad \alpha,\beta = 1,\ldots,N \tag{4.15}$$

which, in terms of (2.16), corresponds to

$$\begin{aligned} i\omega \, \nabla\cdot(h^{-1} \nabla\psi_{+}) &= 0 \qquad \text{on } \mathcal{D} \\ (\nabla\psi_{+} \times \nabla h^{-1})\cdot\hat{\underline{z}} &= 0 \qquad \text{on } \mathcal{D} \\ \psi_{+} &= 0 \qquad \text{on } \partial\mathcal{D} \end{aligned} \tag{4.16}$$

A non-trivial ψ_{+} satisfying this set of equations permits only $\omega = 0$, as proved in Appendix B, which shows that there exists no wave in this case. An analogous conclusion prevails when $\underline{\psi}_{+} = 0$ and $\underline{\psi}_{-} \neq 0$ is assumed. Proper topographic waves must therefore have both non-trivial $\underline{\psi}_{+}$ and $\underline{\psi}_{-}$ functions.

Thus, we have demonstrated, that -within our approximate

formalism - the behaviour of topographic waves is well incorporated. Indeed, corresponding to the results of Ball (1965) and Mysak (1983), we obtain the correct features of these waves. ψ-functions which are solutions of (3.21) are necessarily a mixture of symmetric and skew-symmetric components. At certain times plots of the streamlines are skew-symmetric, at others they are symmetric and in between they are a combination of the two (cf. Figure 8).

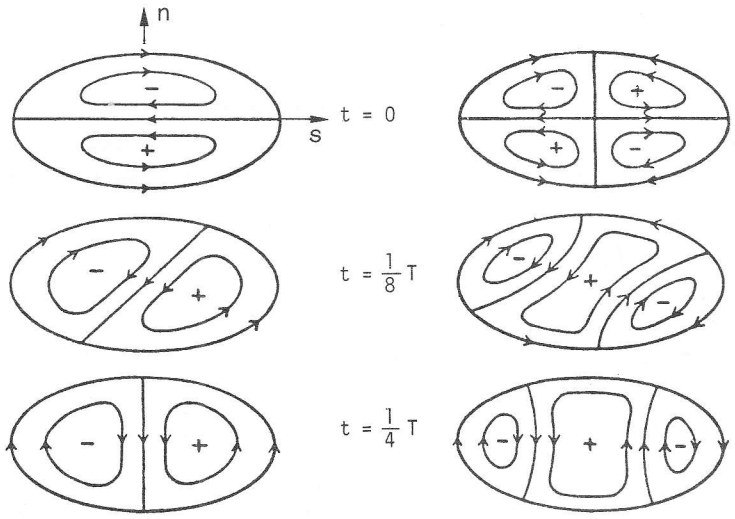

Figure 8

Showing the symmetric and skew-symmetric aspect of the motion of topographic waves (from Ball, 1965). For $t = 0$ the motion is purely skew-symmetric in the n-direction and for $t = 1/4\ T$, where T is the period of the motion, it is purely symmetric. At intermediate times there is a mixture of both aspects. This feature can be seen both in the ground mode (left) and a higher mode (right). Note that the modal structure of the higher mode (right) changes in time

We regard this as one of the essential features of topographic waves, and the fact that the equations (4.14) qualitatively exhibit these properties may serve as a partial corroboration of the appropriateness of the approximate model.

4.3 Basis Functions

The above procedure requires a set of basis functions that fulfills the boundary conditions (3.9). Further, we split the set into a symmetric and skew-symmetric part, and for simplicity also choose $\{P_\alpha\}$ and $\{Q_\beta\}$ from the same set (Galerkin procedure). The simplest choice is then to take trigonometric functions, sin and cos, which form a complete set and in the form

$$P_\alpha^+(s,n) = \cos\left(\pi(\alpha-\tfrac{1}{2})\,\frac{2n}{B(s)}\right), \quad P_\alpha^-(s,n) = \sin\left(\pi\alpha\,\frac{2n}{B(s)}\right),$$
$$Q_\beta^+(s,n) = \cos\left(\pi(\beta-\tfrac{1}{2})\,\frac{2n}{B(s)}\right), \quad Q_\beta^-(s,n) = \sin\left(\pi\beta\,\frac{2n}{B(s)}\right), \tag{4.17}$$
$$(\alpha,\beta = 1,2,\ldots,N)$$

they satisfy the boundary conditions (cf. Figure 9).

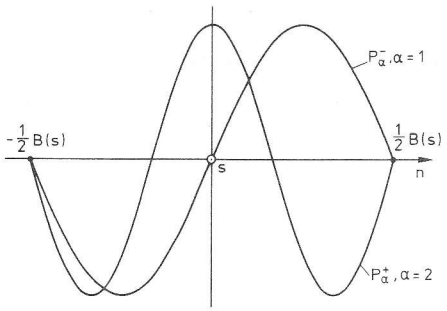

Figure 9

Basis functions.

4.4 Calculation of the matrix elements

With (4.3) and (4.17) the matix elements (3.23) can be calculated. Simplifications are obtained with the substitution

$$x := \frac{2n}{B(s)}, \qquad dx = \frac{2}{B(s)}\,dn. \tag{4.18}$$

Straightforward calculation, using the definition (3.23), (4.1), (4.2), (4.3), (4.6) and (4.17), yields

$$M_{\beta\alpha}^{00++} = B\, h_0^{-1} \int h^{-1} \cos\pi(\alpha-\tfrac{1}{2})x \cos\pi(\beta-\tfrac{1}{2})x\, dx\,,$$

$$M_{\beta\alpha}^{00--} = B\, h_0^{-1} \int h^{-1} \sin\pi\alpha x \sin\pi\beta x\, dx\,, \tag{4.19}$$

$$M_{\beta\alpha}^{10++} = \pi(\alpha-\tfrac{1}{2}) \frac{\partial B}{\partial s} h_0^{-1} \int x\, h^{-1} \sin\pi(\alpha-\tfrac{1}{2})x \cos\pi(\beta-\tfrac{1}{2})x\, dx,$$

$$M_{\beta\alpha}^{10--} = -\pi\alpha \frac{\partial B}{\partial s} h_0^{-1} \int x\, h^{-1} \cos\pi\alpha x \sin\pi\beta x\, dx, \tag{4.20}$$

$$M_{\beta\alpha}^{01++} = \pi(\beta-\tfrac{1}{2}) \frac{\partial B}{\partial s} h_0^{-1} \int x\, h^{-1} \cos\pi(\alpha-\tfrac{1}{2})x \sin\pi(\beta-\tfrac{1}{2})x\, dx,$$

$$M_{\beta\alpha}^{01--} = -\pi\beta \frac{\partial B}{\partial s} h_0^{-1} \int x\, h^{-1} \sin\pi\alpha x \cos\pi\beta x\, dx, \tag{4.21}$$

$$M_{\beta\alpha}^{20+-} = -2\pi(\alpha-\tfrac{1}{2}) h_0^{-1} \int h^{-1} \sin\pi(\alpha-\tfrac{1}{2})x \sin\pi\beta x\, dx\,,$$

$$M_{\beta\alpha}^{20-+} = 2\pi\alpha\, h_0^{-1} \int h^{-1} \cos\pi\alpha x \cos\pi(\beta-\tfrac{1}{2})x\, dx\,, \tag{4.22}$$

$$M_{\beta\alpha}^{02+-} = 2\pi\beta\, h_0^{-1} \int h^{-1} \cos\pi(\alpha-\tfrac{1}{2})x \cos\pi\beta x\, dx\,,$$

$$M_{\beta\alpha}^{02-+} = -2\pi(\beta-\tfrac{1}{2}) h_0^{-1} \int h^{-1} \sin\pi\alpha x \sin\pi(\beta-\tfrac{1}{2})x\, dx, \tag{4.23}$$

$$M_{\beta\alpha}^{11++} = \pi^2(\alpha-\tfrac{1}{2})(\beta-\tfrac{1}{2}) B^{-1} (\frac{\partial B}{\partial s})^2 h_0^{-1} \int x^2 h^{-1} \sin\pi(\alpha-\tfrac{1}{2})x \sin\pi(\beta-\tfrac{1}{2})x\, dx,$$

$$M_{\beta\alpha}^{11--} = \pi^2 \alpha\beta\, B^{-1} (\frac{\partial B}{\partial s})^2 h_0^{-1} \int x^2 h^{-1} \cos\pi\alpha x \cos\pi\beta x\, dx, \tag{4.24}$$

$$M_{\beta\alpha}^{22++} = 4\pi^2(\alpha-\tfrac{1}{2})(\beta-\tfrac{1}{2}) B^{-1} h_0^{-1} \int h^{-1} \sin\pi(\alpha-\tfrac{1}{2})x \sin\pi(\beta-\tfrac{1}{2})x\, dx,$$

$$M_{\beta\alpha}^{22--} = 4\pi^2 \alpha\beta B^{-1} h_0^{-1} \int h^{-1} \cos\pi\alpha x \cos\pi\beta x\, dx, \tag{4.25}$$

$$M_{\beta\alpha}^{12+-} = 2\pi^2(\alpha-\tfrac{1}{2})\beta B^{-1} \frac{\partial B}{\partial s} h_0^{-1} \int x\, h^{-1} \sin\pi(\alpha-\tfrac{1}{2})x \cos\alpha\beta x\, dx,$$

$$M_{\beta\alpha}^{12-+} = 2\pi^2\alpha(\beta-\tfrac{1}{2}) B^{-1} \frac{\partial B}{\partial s} h_0^{-1} \int x\, h^{-1} \cos\pi\alpha x \sin\pi(\beta-\tfrac{1}{2})x\, dx, \tag{4.26}$$

$$M^{21+-}_{\beta\alpha} = 2\pi^2 (\alpha - \tfrac{1}{2})\, \beta\, B^{-1} \frac{\partial B}{\partial s} h_0^{-1} \int x\, h^{-1} \sin\pi(\alpha - \tfrac{1}{2})x \cos \pi\beta x \, dx,$$

$$M^{21-+}_{\beta\alpha} = 2\pi^2 \alpha (\beta - \tfrac{1}{2}) B^{-1} \frac{\partial B}{\partial s} h_0^{-1} \int x\, h^{-1} \cos\pi\alpha x \sin\pi(\beta - \tfrac{1}{2})x \, dx, \qquad (4.27)$$

$$(\alpha, \beta = 1, \ldots, N)$$

where the index 1 at h^{-1} has been dropped and the integration $\int_0^1$ is meant. For a prescribed topography, i.e. for selected ε and q, the integrals in (4.19)-(4.27) can be worked out once and for all. The matrix elements are composed only of five different integrals which must be calculated on a computer or pocket calculator. To this end we define the functions

$$I_i(a,b,q,\varepsilon), \qquad (4.28)$$

according to

$$I_0 = \int_0^1 h^{-1} \sin\pi ax \sin\pi bx \, dx,$$

$$I_1 = \int_0^1 h^{-1} \cos\pi ax \cos\pi bx \, dx,$$

$$I_2 = \int_0^1 x\, h^{-1} \cos\pi ax \sin\pi bx \, dx, \qquad (4.29)$$

$$I_3 = \int_0^1 x^2 h^{-1} \cos\pi ax \cos\pi bx \, dx,$$

$$I_4 = \int_0^1 x^2 h^{-1} \sin\pi(a-\tfrac{1}{2})x \sin\pi(b-\tfrac{1}{2})x \, dx,$$

where h is given by $(4.3)_2$

$$h = 1 + \varepsilon - x^q. \qquad (4.30)$$

The matrix elements (4.19)-(4.27) expressed in terms of these are

$$M^{00++}_{\beta\alpha} = B\, h_0^{-1}\, I_1(\alpha - \tfrac{1}{2}, \beta - \tfrac{1}{2}),$$

$$M^{00--}_{\beta\alpha} = B\, h_0^{-1}\, I_0(\alpha, \beta),$$

$$M^{10++}_{\beta\alpha} = \pi(\alpha - \tfrac{1}{2}) \frac{\partial B}{\partial s} h_0^{-1}\, I_2(\beta - \tfrac{1}{2}, \alpha - \tfrac{1}{2}), \qquad (4.31)$$

$$M^{10--}_{\beta\alpha} = -\pi\alpha \frac{\partial B}{\partial s} h_0^{-1}\, I_2(\alpha, \beta)$$

cont. →

$$M_{\beta\alpha}^{01++} = \pi(\beta - \tfrac{1}{2}) \frac{\partial B}{\partial s} h_0^{-1} I_2(\alpha - \tfrac{1}{2}, \beta - \tfrac{1}{2}),$$

$$M_{\beta\alpha}^{01--} = -\pi\beta \frac{\partial B}{\partial s} h_0^{-1} I_2(\beta, \alpha),$$

$$M_{\beta\alpha}^{20+-} = -2\pi(\alpha - \tfrac{1}{2}) h_0^{-1} I_0(\alpha - \tfrac{1}{2}, \beta),$$

$$M_{\beta\alpha}^{20-+} = 2\pi\alpha h_0^{-1} I_1(\alpha, \beta - \tfrac{1}{2}),$$

$$M_{\beta\alpha}^{02+-} = 2\pi\beta h_0^{-1} I_1(\alpha - \tfrac{1}{2}, \beta),$$

$$M_{\beta\alpha}^{02-+} = -2\pi(\beta - \tfrac{1}{2}) h_0^{-1} I_0(\alpha, \beta - \tfrac{1}{2}),$$

$$M_{\beta\alpha}^{11++} = \pi^2(\alpha - \tfrac{1}{2})(\beta - \tfrac{1}{2}) B^{-1} (\frac{\partial B}{\partial s})^2 h_0^{-1} I_4(\alpha, \beta),$$

$$M_{\beta\alpha}^{11--} = \pi^2\alpha\beta B^{-1} (\frac{\partial B}{\partial s})^2 h_0^{-1} I_3(\alpha, \beta),$$

$$M_{\beta\alpha}^{22++} = 4\pi^2(\alpha - \tfrac{1}{2})(\beta - \tfrac{1}{2}) B^{-1} h_0^{-1} I_0(\alpha - \tfrac{1}{2}, \beta - \tfrac{1}{2}),$$

$$M_{\beta\alpha}^{22--} = 4\pi^2\alpha\beta B^{-1} h_0^{-1} I_1(\alpha, \beta),$$

$$M_{\beta\alpha}^{12+-} = 2\pi^2(\alpha - \tfrac{1}{2})\beta B^{-1} (\frac{\partial B}{\partial s}) h_0^{-1} I_2(\beta, \alpha - \tfrac{1}{2}),$$

$$M_{\beta\alpha}^{12-+} = 2\pi^2\alpha(\beta - \tfrac{1}{2}) B^{-1} (\frac{\partial B}{\partial s}) h_0^{-1} I_2(\alpha, \beta - \tfrac{1}{2}),$$

$$M_{\beta\alpha}^{21+-} = M_{\beta\alpha}^{12+-},$$

$$M_{\beta\alpha}^{21-+} = M_{\beta\alpha}^{12-+}, \qquad (\alpha, \beta = 1, \ldots, N)$$

having omitted the parameters ε and q as arguments of I_i. The numerical evaluation of the constant part was performed on a computer using the IMSL-library subroutines. The results, with a relative accuracy of 10^{-6}, for selected ε and q up to order 4 are listed in Appendix E.

5. CHANNEL MODELS

5.1 Basic equations

The restricted model, which has been presented in chapter 4, is now applied in a first step to straight channels, which have in their cross direction a topography of the form (4.3), see Figure 10. Such channels have also been considered by Gratton (1983), but using a different method.

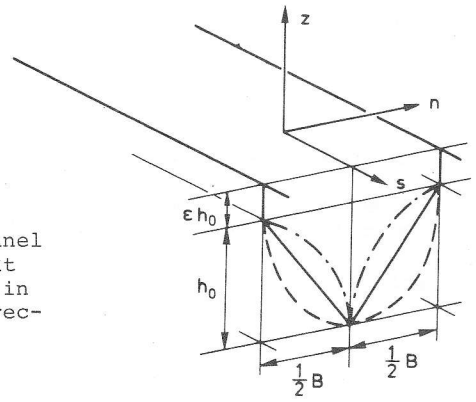

Figure 10

Infinite channel with different topographies in the cross direction.

The channel is assumed not to have a mean flow along the s-direction. The considerations regarding the temporal sequence of the symmetric and skew-symmetric parts of the solution (4.8) lead straightforwardly to a harmonic time dependence of the form

$$\underline{\psi} = (\underline{\psi}_+(s) \sin\omega t;\ \underline{\psi}_-(s) \cos\omega t), \qquad (5.1)$$

with strictly real ω. There is a phase shift of $\pi/2$ -corresponding to 1/4 T- between both components, which is in accordance with the results found by Ball (1965), see Figure 8, and Mysak (1983, 1984). Introducing the definitions

$$M^{00}_{\beta\alpha} = B\, h_0^{-1}\, K^{00}_{\beta\alpha},$$

$$M^{10}_{\beta\alpha} = \frac{\partial B}{\partial s}\, h_0^{-1}\, K^{10}_{\beta\alpha},$$

$$M^{01}_{\beta\alpha} = \frac{\partial B}{\partial s}\, h_0^{-1}\, K^{01}_{\beta\alpha}, \qquad \text{cont.} \rightarrow$$

$$M^{20}_{\beta\alpha} = h_0^{-1} K^{20}_{\beta\alpha},$$

$$M^{02}_{\beta\alpha} = h_0^{-1} K^{02}_{\beta\alpha},$$

$$M^{11}_{\beta\alpha} = B^{-1} \left(\frac{\partial B}{\partial s}\right)^2 h_0^{-1} K^{11}_{\beta\alpha},$$

$$M^{22}_{\beta\alpha} = B^{-1} h_0^{-1} K^{22}_{\beta\alpha},$$

with constant $K^{ij}_{\beta\alpha}$ the matrix operator $\underline{M}$ (3.22) may be written as

$$\begin{aligned}\underline{M} = {} & B h_0^{-1} \underline{K}^{00} \frac{\partial^3}{\partial s^2 \partial t} \\ & + \left(\frac{\partial B}{\partial s} h_0^{-1} (\underline{K}^{10} - \underline{K}^{01}) + \frac{\partial}{\partial s} (B h_0^{-1}) \underline{K}^{00}\right) \frac{\partial^2}{\partial s \partial t} \\ & + \left(\frac{\partial}{\partial s}\left(\frac{\partial B}{\partial s} h_0^{-1}\right) \underline{K}^{10} - B^{-1} \left(\frac{\partial B}{\partial s}\right)^2 h_0^{-1} \underline{K}^{11} - B^{-1} h_0^{-1} \underline{K}^{22}\right) \frac{\partial}{\partial t} \\ & + h_0^{-1} (-\underline{K}^{20} - \underline{K}^{02}) \frac{\partial}{\partial s} \\ & - \frac{\partial h_0^{-1}}{\partial s} \underline{K}^{20}.\end{aligned} \tag{5.2}$$

With a constant width B(s), which after all was also the choice of Lamb (1932) and Mysak (1983, 1984) in their coordinate systems, (5.2) reduces to

$$\begin{aligned}\tilde{\underline{M}} = B h_0 \underline{M} = {} & B^2 \underline{K}^{00} \frac{\partial^3}{\partial s^2 \partial t} + B^2 h_0 \frac{\partial h_0^{-1}}{\partial s} \underline{K}^{00} \frac{\partial^2}{\partial s \partial t} \\ & - \underline{K}^{22} \frac{\partial}{\partial t} + B(-\underline{K}^{20} - \underline{K}^{02}) \frac{\partial}{\partial s} - B h_0 \frac{\partial h_0^{-1}}{\partial s} \underline{K}^{20}.\end{aligned} \tag{5.3}$$

Because (3.21) is a homogeneous system the operator $\underline{M}$ can be multiplied by any non-zero function without changing the solution ψ^α. Therefore $\tilde{\underline{M}}$ is a differential operator with constant coefficients only if

$$h_0 \frac{\partial h_0^{-1}}{\partial s} = \text{constant} =: \frac{c}{L}.$$

For such a case the profile $h_0(s)$ must take on the form

$$h_0(s) \sim e^{-\frac{c}{L} s}. \tag{5.4}$$

$c = 0$ yields constant depth in the s-direction and $c \neq 0$ exhi-

bits the same features as these already considered by Mysak (1984, p. 102). However, when $c \neq 0$, in order to obtain reasonable lake topographies, the lake must be subdivided into at least three adjoining parts as shown in Figure 11.

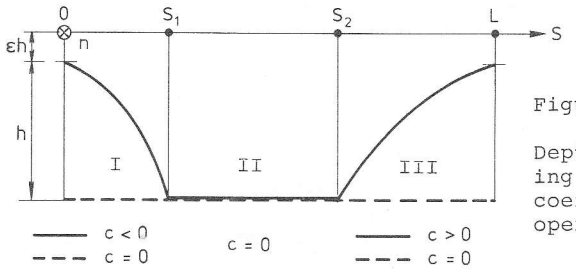

Figure 11

Depth profiles yielding piecewise constant coefficients for the operator $\underline{\tilde{M}}$ (5.3).

Obviously when $c \neq 0$ the solutions to each subsection must fulfil matching conditions, which complicates calculations considerably. We therefore choose $c = 0$, a depth profile which is constant in the s-direction for all $s \in (0,L)$.

The operator then reads

$$\underline{\tilde{M}} = B^2 \underline{K}^{00} \frac{\partial^3}{\partial s^2 \partial t} - \underline{K}^{22} \frac{\partial}{\partial t} - B(\underline{K}^{20} + \underline{K}^{02}) \frac{\partial}{\partial s} . \qquad (5.5)$$

With a harmonic time dependence of the form (5.1) the boundary-value-problem (3.21) becomes

$$\begin{aligned}
&\omega(B^2 \underline{K}^{00++} \frac{d^2}{ds^2} - \underline{K}^{22++}) \underline{\psi}_+ \\
&- B(\underline{K}^{20-+} + \underline{K}^{02-+}) \frac{d}{ds} \underline{\psi}_- = 0, \qquad 0 < s < L \\
&\omega(B^2 \underline{K}^{00--} \frac{d^2}{ds^2} - \underline{K}^{22--}) \underline{\psi}_- \\
&+ B(\underline{K}^{20+-} + \underline{K}^{02+-}) \frac{d}{ds} \underline{\psi}_+ = 0, \qquad 0 < s < L \qquad (5.6) \\
&\underline{\psi}_+(s) = \left(\psi_+^1(s), \ldots, \psi_-^N(s)\right) = 0, \qquad s = 0,L \\
&\underline{\psi}_-(s) = \left(\psi_-^1(s), \ldots, \psi_-^N(s)\right) = 0, \qquad s = 0,L
\end{aligned}$$

in which the $\underline{K}$'s are constant (N×N)-matrices, of which the values depend on the choice of the basis functions P_α and Q_β and the topography in the n-direction. Equations $(5.6)_{1,2}$ form a system of ordinary second order linear differential equations, which can be transformed into a system of algebraic equations by writing

$$\underline{\psi} = (\underline{\psi}_+ ; \underline{\psi}_-) = e^{i\frac{k}{L}s} (c_1, \ldots, c_N ; c_{N+1}, \ldots, c_{2N}), \qquad (5.7)$$

where k and c_α are complex constants. Equations $(5.6)_1$ and $(5.6)_2$ can then be written in the compact algebraic form

$$C_{\beta\alpha}(\omega,k)c_\alpha = 0, \qquad \alpha,\beta = 1,\ldots,2N, \qquad (5.8)$$

where the matrix elements $C_{\beta\alpha}$ are given by

$$\begin{aligned}
C_{\beta\alpha} &= \omega\left((rk)^2 K^{00++}_{\beta\alpha} + K^{22++}_{\beta\alpha}\right), && \alpha,\beta=1,\ldots,N \\
C_{\beta\alpha} &= i(rk)\left(K^{20-+}_{\beta,\alpha-N} + K^{02-+}_{\beta,\alpha-N}\right), && \begin{matrix}\beta=1,\ldots,N\\ \alpha=N+1,\ldots,2N\end{matrix} \\
C_{\beta\alpha} &= -i(rk)\left(K^{20+-}_{\beta-N,\alpha} + K^{02+-}_{\beta-N,\alpha}\right), && \begin{matrix}\alpha=1,\ldots,N\\ \beta=N+1,\ldots,2N\end{matrix} \\
C_{\beta\alpha} &= \omega\left((rk)^2 K^{00--}_{\beta-N,\alpha-N} + K^{22--}_{\beta-N,\alpha-N}\right), && \alpha,\beta=N+1,\ldots,2N
\end{aligned} \qquad (5.9)$$

whereby the aspect ratio r = B/L has been introduced. A non-trivial $\underline{\psi}$ requires

$$\det \underline{C}(\omega,k) = 0. \qquad (5.10)$$

This is the dispersion relation for $\omega(k)$. Remember that k is allowed to be complex, whereas ω is considered to be real. Should k, as determined by (5.10) be real, then ψ is purely harmonic both in space and time and (5.7) corresponds to a harmonic wave travelling in the s-direction. For complex k, ψ still oscillates in s but is attenuated or amplified depending on whether $\mathrm{Im}(\frac{k}{L}s) > 0$ or < 0. Purely imaginary k yields a ψ with no oscillations along the s-direction. For infinite channels only the first of these solutions is reasonable, but the other solutions are equally meaningful in channels of finite extent and will also be analyzed. At the moment the boundary conditions $(5.6)_3$ and $(5.6)_4$ will not be satisfied because

infinite channels are considered (Gratton, 1983). For such a case $\omega(k)$ is a continuous function of k. Fulfilling boundary conditions in a further step only breaks this continuity of the dispersion relation, selects isolated points on this curve and yields the eigenfrequencies for an intersected, finite channel, i.e. a lake.

It is demonstrated later on that, by selecting ω, the wavenumber k falls into different regimes, a real regime, a complex regime and an imaginary regime, each of which corresponds to different frequency intervals. Equations (5.8)-(5.10) require further remarks:

1) The dispersion relation $\omega(k)$ depends only on $r \cdot k$, therefore the horizontal dimensions are only important through their aspect ratio. Without loss of generality, the aspect ratio for channels may be set to unity, $r := 1$.

2) (5.10) yields a polynomial of order 4N in the complex variable k with real coefficients depending on ω. Therefore, by invoking the Fundamental Theorem of Algebra, there are 4N roots for a given ω.

3) The structure of $C_{\beta\alpha}$ leads to a polynomial in only even powers of k.

4) By these arguments we find that the 4N roots consist of both $\pm k$ and their complex conjugates.

5) Taking the limit $\omega \to \infty$ the dispersion relation will eventually be independent of ω, therefore there exist asymptotic wavenumbers.

The dispersion relation $\omega(k)$, obtained from (5.10), enables us to build up channel solutions. To demonstrate this, let

$$\{k_\gamma\}, \quad k_\gamma \in \mathbb{C}, \quad \gamma = 1,\ldots,4N, \tag{5.11}$$

be the set of roots of (5.10) to a given frequency ω. Since k_γ satisfies (5.10), there exists for each $\gamma = 1,\ldots,4N$ a non-trivial solution vector of (5.8),

$$c_{\alpha\gamma} \in \mathbb{C}, \qquad \begin{matrix}\alpha = 1, \ldots, 2N, \\ \gamma = 1, \ldots, 4N,\end{matrix}$$

which fulfils

$$C_{\beta\alpha}(\omega, k_\gamma)\, c_{\alpha\gamma} = 0, \qquad \beta = 1, \ldots, 2N.$$

Therefore, for selected ω and γ, the channel solution $\underline{\psi} = (\underline{\psi}_+ ; \underline{\psi}_-)$ of $(5.6)_{1,2}$ reads

$$\begin{aligned} \psi_+^\alpha(\omega,\gamma) &= c_{\alpha\gamma}\, e^{i\frac{k_\gamma}{L}s}, \qquad \alpha = 1, \ldots, N, \\ \psi_-^{\alpha-N}(\omega,\gamma) &= c_{\alpha\gamma}\, e^{i\frac{k_\gamma}{L}s}, \qquad \alpha = N+1, \ldots, 2N, \end{aligned} \qquad \begin{matrix}\text{no sum over } \gamma \\ \gamma = 1, \ldots, 4N.\end{matrix}$$

However, since equation $(5.6)_{1,2}$ form a linear system, a general channel solution can be obtained by an arbitrary linear combination of solutions corresponding to different wavenumbers k_γ. With arbitrary

$$d_\gamma \in \mathbb{C}, \qquad \gamma = 1, \ldots, 4N,$$

the superpositions

$$\begin{aligned} \psi_+^\alpha &= \sum_\gamma e^{i\frac{k_\gamma}{L}s}\, c_{\alpha\gamma}\, d_\gamma, \qquad \alpha = 1, \ldots, N, \\ \psi_-^{\alpha-N} &= \sum_\gamma e^{i\frac{k_\gamma}{L}s}\, c_{\alpha\gamma}\, d_\gamma, \qquad \alpha = N+1, \ldots, 2N, \end{aligned} \tag{5.12}$$

form a general solution of $(5.6)_{1,2}$.

From equations (5.12) the approximate solution $\psi(s,n,t)$ of the form (3.3) of equation (2.16) can now readily be constructed. Using (3.3), (4.8), (5.10) and (5.12) yields

$$\begin{aligned} \psi(s,n,t) = \sin\omega t \Bigg[\sum_{\alpha=1}^{N} p_\alpha^+(s,n) \cdot \sum_{\gamma=1}^{4N} e^{i\frac{k_\gamma}{L}s}\, c_{\alpha\gamma}\, d_\gamma \Bigg] \\ + \cos\omega t \Bigg[\sum_{\alpha=N+1}^{2N} p_{\alpha-N}^-(s,n) \cdot \sum_{\gamma=1}^{4N} e^{i\frac{k_\gamma}{L}s}\, c_{\alpha\gamma}\, d_\gamma \Bigg] \end{aligned} \tag{5.13}$$

where, in an infinite channel, $d_\gamma \in \mathbb{C}$ is arbitrary.

5.2 Dispersion relation

The dispersion relation, which is obtained by fulfilling (5.10) can be plotted in a coordinate system (Re(k), Im(k),ω). The resulting curves ω(k) are then symmetric to both Re(k) = 0 and Im(k)=0. Figure 12 displays a schematic plot of the dispersion relation for an infinite channel in a first order model. For graphical transparency ε = 0.05 and q = 0.5 have been chosen.

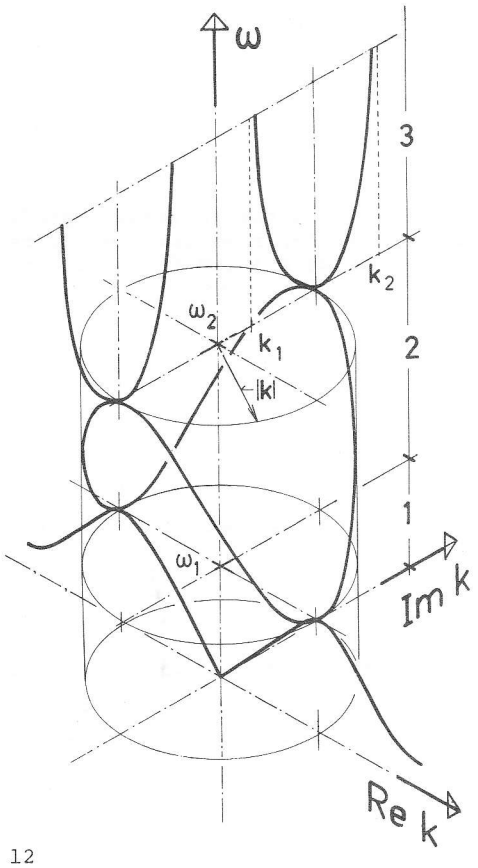

Figure 12

Schematic plot of the complex dispersion relation ω(k), $k \in \mathbb{C}$ for an infinite channel with ε = 0.05 and q = 0.5 in a first order model. In regime 1 k is real, in regime 2 it is complex and in regime 3 k is purely imaginary.

Three regimes 1 - 3 can be distinguished which are separated at the periods listed in Table 5. In these three regimes the wave numbers k belong to different mathematical fields (see Table 6) each of which determines the structure of the solution (5.7) in the s-direction. In the first regime, where $0 < \omega < \omega_1$

q	T_1[h]		T_2[h]	
	$\varepsilon = 0.05$	$\varepsilon = 0.10$	$\varepsilon = 0.05$	$\varepsilon = 0.10$
0.5	52.8	58.3	10.5	11.8
1.0	60.5	64.3	13.2	14.4
2.0	83.0	88.2	22.0	22.6
5.0	174	199	58.2	61.8

Table 5

Periods, which separate the regimes, depending on topography- and sidewall-parameters q and ε, respectively. The period T is calculated from the dimensionless ω using the scaling (2.11) and $\frac{1}{2\pi} f = 1/16.9$ h according to 45° latitude.

q	1	2	3
0.5 1.5 2.0 5.0	4 $\mathbb{R}$	4 $\tilde{\mathbb{C}}$	4 $\mathbb{J}$

Table 6

Fields to which wavenumbers belong in the different regimes 1, 2, 3 of a first order model. $\mathbb{R}$ and $\mathbb{C}$ are the real and complex fields and $\mathbb{J} = i\mathbb{R}$; further $\tilde{\mathbb{C}} = \mathbb{C} \setminus (\mathbb{R} \cup \mathbb{J})$. The figure 4 indicates that four roots belong to that field.

or $T > T_1$, k must be a real number, since $\psi \sim \exp(i\frac{k}{L} s)$ according to (5.7), the spatial behaviour in the s-direction is purely periodic. Typically of Rossby-waves there are always two wavenumbers for a given frequency, i.e. both large and small wavelengths occur.

In the second regime, $\omega_1 < \omega < \omega_2$ or $T_2 < T < T_1$, k must take on complex values in order to fulfil (5.10). Therefore, solutions are products of both exponential and periodic dependence. Because of the exponential growth or decay of the solutions, they have no physical meaning in an infinite channel.

However, in lakes, which are of finite extent also in the s-direction, they may well be considered. It is characteristic, of a first order model that in regime 2 and for all studied topographies the modulus of k does not depend on ω. This can easily be shown from (5.10) using (5.9) and Vieta's theorem for a quadratic polynomial. Therefore, the dispersion curve $\omega(k)$ is located on the mantle surface of a circular cylinder of which the radius, however, depends on both, ε and q, see Table 7. In the third regime, i.e. for $\omega > \omega_2$ or $T < T_2$, k must be imaginary. Therefore, the solutions exhibit pure exponential character. Again in the channel these types of solutions can not make physical sense. Moreover, as $\omega \to \infty$, the wavenumbers take on the asymptotic values k_1 and k_2 listed in Table 7. In a first order model the dispersion curves $\omega(k)$ allow for

q	$\lvert k \rvert$ in 2		$-i\,k_1$ in 3		$-i\,k_2$ in 3	
	$\varepsilon = 0.05$	$\varepsilon = 0.10$	$\varepsilon = 0.05$	$\varepsilon = 0.10$	$\varepsilon = 0.05$	$\varepsilon = 0.10$
0.5	6.6	5.9	5.5	4.9	8.0	7.3
1.0	6.9	6.2	5.6	5.0	8.6	7.8
2.0	6.8	6.3	5.2	4.8	8.9	8.2
5.0	6.1	5.8	4.4	4.1	8.5	8.0

Table 7

Characteristic wave numbers $\lvert k \rvert$, k_1 and k_2, of the first order model as defined in Figure 12 tabulated for values of q and ε.

each ω 4 wavenumbers k, except when $\omega = \omega_1$ and $\omega = \omega_2$, where two distinct regimes merge together forming double roots. At these critical frequencies the solutions, satisfying (5.6) are not only of the form $\exp(i\frac{k}{L}s)$, see (5.7), but also

$$(\frac{k}{L}s)\exp(i\frac{k}{L}s), \qquad (5.14)$$

so that again 4N linear independent solutions exist, although there are only 2N different roots k. For later use, the union of the three regimes 1, 2, 3 of the dispersion relation in Figure 12 will be called a *mode unit*.

The second order model is more complicated. According to (5.11), to each frequency there are now 8 wavenumbers k, for which (5.10) is satisfied. In Figure 13 its dispersion relation $\omega(k)$, $k \in \mathbb{C}$ is shown. Except for distortions of the cylinder it consists of two *mode units* placed into each other. Thus, there are now two branches with real, complex and imaginary k's, respectively. Because the transitions from real to com-

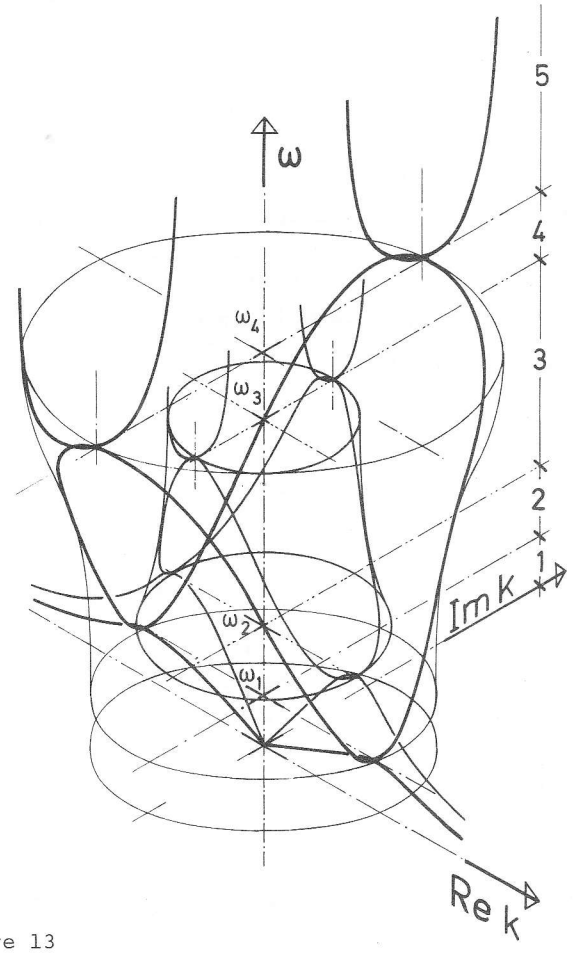

Figure 13

Schematic plot of the dispersion relation $\omega(k)$, $k \in \mathbb{C}$ for an infinite channel with $\varepsilon = 0.05$ and $q = 0.5$ in a second order model.

plex and from complex to imaginary k's on the two mode units take place at different frequencies, five distinctive regimes 1 - 5 must be considered, which are separated at the periods listed in Table 8.

q	T_1 [h]		T_2 [h]		T_3 [h]		T_4 [h]	
	ε=0.05	ε=0.10	ε=0.05	ε=0.10	ε=0.05	ε=0.10	ε=0.05	ε=0.10
0.5	94.5	109	49.8	54.6	10.7	12.1	8.8	11.9
1.0	126	132	55.0	60.0	17.3	18.6	8.9	11.5
2.0	245	269	64.5	69.0	45.8	47.0	10.0	11.8
5.0	~1400	~1800	470	530	101	109	15.8	17.3

Table 8 Periods, which separate five distinct regimes in the second order model.

The relative size of the mode units, whether the belly-shaped surfaces intersect and change their spatial position within the (k,ω)-coordinate system depends crucially upon the topography. This will be discussed in a further section. The cylindrical surface of the first order degenerates to a smaller belly-shaped surface, i.e. the modulus of k in the complex branch now depends on the frequency. Moreover, the second mode unit forms an outer shell, which here has the form of a cone. Again, the shape and position of these surfaces are strongly governed by the topography of the channel and much less by the sidewall-parameter. The structure of the 5 regimes depends on the topography, but the solutions can take on the three types: periodic, periodic-exponential or exponential dependence in the s-direction, however, for the situation of Figure 13 they occur in different combinations, see Table 9:

q	1	2	3	4	5
0.5 1.0 2.0	$8\,\mathbb{R}$	$4\,\mathbb{R}$, $4\,\tilde{\mathbb{C}}$	$8\,\tilde{\mathbb{C}}$	$4\,\tilde{\mathbb{C}}$, $4\,\mathbb{J}$	$8\,\mathbb{J}$
5.0	$8\,\mathbb{R}$	$4\,\mathbb{R}$, $4\,\tilde{\mathbb{C}}$	$4\,\mathbb{R}$, $4\,\mathbb{J}$	$4\,\tilde{\mathbb{C}}$, $4\,\mathbb{J}$	$8\,\mathbb{J}$

Table 9 The fields to which the wavenumbers belong in the 5 regimes of a second order model for various profiles.

Channel solutions which are physically meaningful occur in regime 1 and 2, and 3 only for $q = 5.0$. Figures 12 and 13 also indicate, how the graph of the dispersion relation of a Nth order model will qualitatively look like.

Figure 14 displays the modulus $|k|$ as a function of ω for a third order model. In the (k,ω)-space three mode units are now placed within each other, and each mode unit has a real, a complex and an imaginary branch, which are represented in Figure 14 by the three distictly different types of dispersion curves. In the situation of Figure 14, 7 regimes may be differentiated.

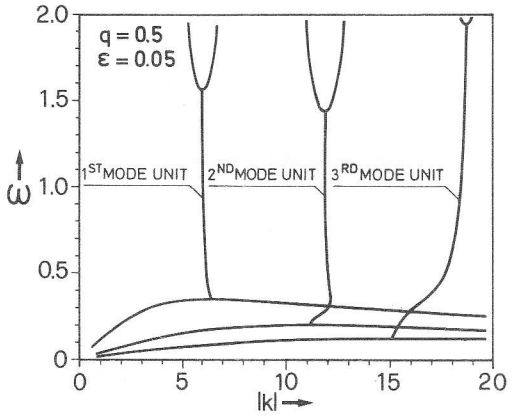

Figure 14

Modulus $|k|$ of the third order dispersion relation for an infinite channel with $\varepsilon = 0.05$ and $q = 0.5$.

Summarizing the main points, we remark:

- The dispersion relation resulting from a Nth order model can be separated into $2N + 1$ consecutive regimes, in which individual wavenumbers belong to $\mathbb{R}$, $\tilde{\mathbb{C}}$ or $\mathbb{J}$, respectively.

- Solutions for channels, which are physically meaningful, can only be constructed from wavenumbers k such that $k \in \mathbb{R}$. Therefore, there exist maximum frequencies, for which channel solutions may occur (see Tables 5, 9). At these maxima energy cannot propagate; for smaller k's group and phase velocities are unidirectional, for larger k's they are anti-parallel.

- Solutions in domains, which are of finite extent also in the s-direction (lakes), can be constructed from any wavenumber k. Their spatial dependence is either periodic when $k \in \mathbb{R}$, periodic-exponential for $k \in \tilde{\mathbb{C}}$ or exponential when $k \in \mathbb{J}$.
- From this point of view, lake solutions occur for all $0 < \omega < \infty$. However it must be remembered, that in section 2.3.2 a low-frequency approximation $\omega^2 << f^2$ was made. Therefore, using the scaling (2.11), the dimensionless frequency ω must fulfil the inequality

$$0 < \omega < 1. \qquad (5.15)$$

The real branches of each mode unit exhibit qualitatively the same structure as Rossby waves in the atmosphere (Holton, 1979). The atmospherical Rossby waves are governed by the rotation f and its latitudinal variation β. This β-effect plays the very same role as the topography variations in channels and lakes. Therefore, in the literature topographic waves are often referred to as topographic Rossby waves to strengthen this alliance. In Appendix C this interrelationship between these two wave phenomena is worked out in greater detail.

5.3 Convergence

Since the method presented in section 3.2 is an approximation, of which the quality depends on the order N, the convergence of the dispersion curves $\omega(k)$ when increasing the order has to be considered. Yet, the notion "convergence" is only meaningful when it is tested for physically reasonable solutions. Therefore, in infinite channels only branches with a vanishing imaginary part of k will be of interest. To test the quality of convergence up to the Nth mode unit at least the models of order N + 2 must be considered. Therefore, here only the quality of the first mode is discussed. We regard a model as appropriate or accurate for a certain mode, if the disper-

sion curve for that mode is "sufficiently unchanged" by increasing the order of the model. In Figure 15 real branches for the 1st, 2nd and 3rd mode unit are shown using various topography-parameters.

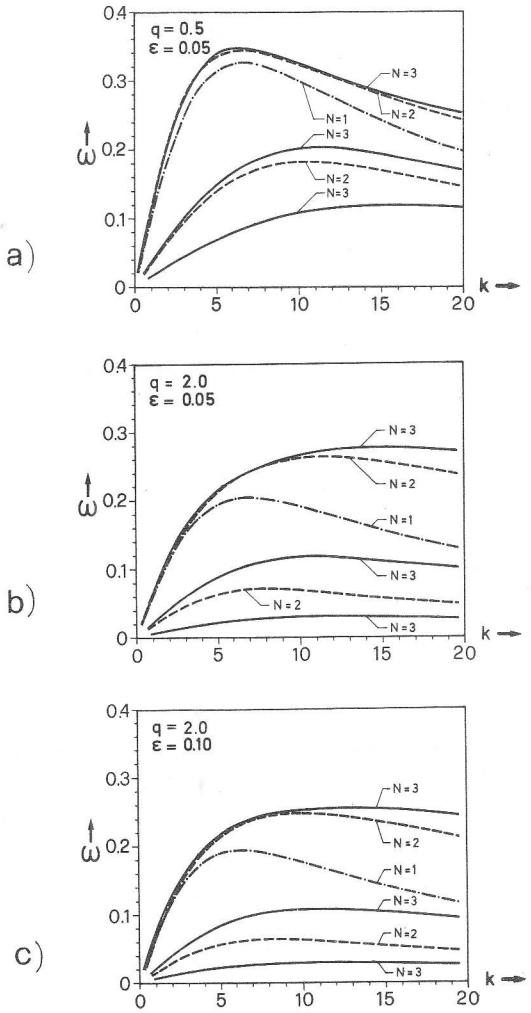

Figure 15

Convergence of the different modes, increasing the order of the model from N = 1 (—·—), N = 2 (— —) to N = 3 (——) for convex (q = 0.5) and concave (q = 2.0) topography and two sidewall parameters.

All three cases show considerable convergence for the first (upper) mode unit. For all ε and q by increasing N the corrections become smaller. However, convergence is not uniform in k. The k-intervall, where convergence seems to be achieved, depends on the topography. Whereas for convex profiles, Figure 15a, reasonable convergence in the third order model is observed in the interval $0 < k < 20$, concave topographies, Figure 15b, show good convergence only for wavenumbers $k < 10$. This suggests, that the more concave the topography is, the higher the order of the model has to be chosen, to obtain satisfactory results. Figure 15c indicates, that the quality of convergence is fairly unaffected by the sidewall parameter ε.

5.4 Topography effects

Topography can appreciably influence the solutions in a channel. Figure 16 shows the influence of the variation of the topography parameter q on the real branch of the dispersion relation in a first and second order model. Basically, the qualitative behaviour is the same for all three orders of the model. Considering waves with a fixed wavelength or wavenumber the frequency is decreasing when proceeding from convex ($q < 1$) to concave ($q > 1$) profiles. This effect could already be ex-

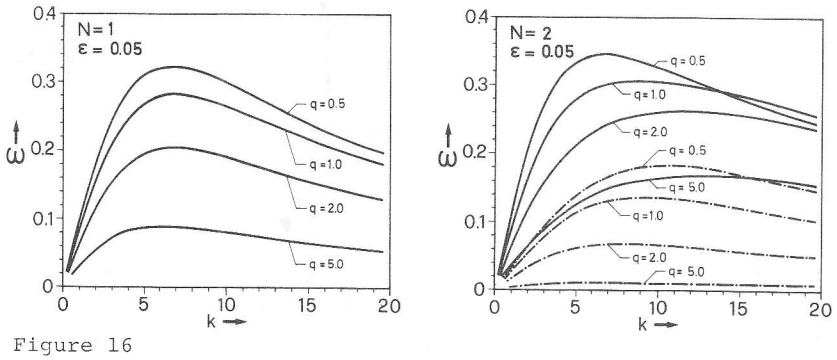

Figure 16

Effect of topography on the dispersion relation in a channel for various profiles, — first mode unit, —·— second mode unit.

pected from the fact, that an extremly concave profile exhibits hardly any topographic variations and therefore, the system can no longer support topographic waves (see Appendix A). On the other hand, given a frequency, the effect of making the topography more concave consists in the fact that longer waves become shorter and shorter waves become longer. However, for N = 2 the behaviour is different when q increases from 0.5 to 1.0 in a domain k > 12. Dispersion curves belonging to different q's may then intersect, a feature that can also be observed for N = 3 when wavenumbers are sufficiently large, see Figure 17.

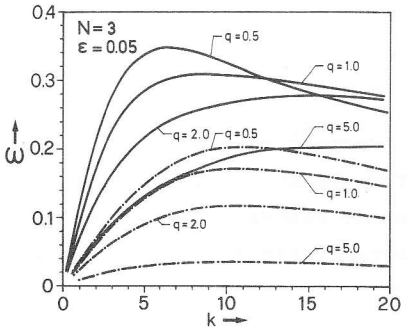

Figure 17

Topography effects in a third order model on the first (——) and second (—·—) mode unit of the dispersion relation.

5.5 Influence of the sidewall

In section 4.1 a sidewall-parameter ε was introduced, which guarantees that all matrix elements (3.23) can be calculated. Figure 18 shows this effect on the dispersion relation of physical solutions in channels of different topographies. Generally an increase of the sidewall relative to the depth of the channel causes a decrease of the frequencies for both types of profiles. This is understandable from the fact that a deep sidewall relative to the total height h_0 (see Figure 7) decreases a possible topography variation. Therefore -by the very same mechanism as described in section 5.4 - smaller frequencies are favoured.

Further, Figure 18 reveals, that for convex topographies

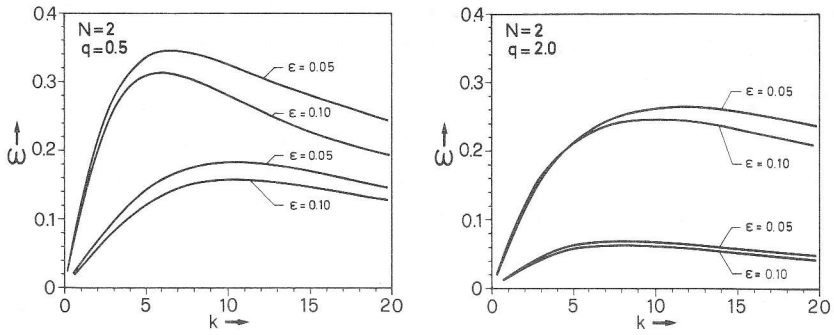

Figure 18

Effect of the sidewall parameter ε on convex ($q = 0.5$) and concave ($q = 2.0$) profiles in a second order model.

($q < 1$) the sidewall effect is more pronounced. This is so, because all convex profiles join horizontally at the sidewall, whereas the more concave the profile is, the steeper it joins at the sidewall. An increase in ε then, cannot appreciably affect the dispersion relation.

5.6 Channel solutions

Solutions in a channel are given by the stream function $\psi(s,n,t)$ in equation (5.13). Since ψ is complex both real and imaginary parts of ψ are solutions. However, $\mathrm{Re}(\psi)$ and $\mathrm{Im}(\psi)$ differ only by a spatial shift along the channel axis, provided the basis functions do not depend on s. Assuming B(s) to be constant as done in section 5.1, the $P_\alpha^{\pm}$'s are independent of s and using the identities

$$\mathrm{Im}(z) \equiv \mathrm{Re}(-i\,z), \quad z \in \mathbb{C},$$

$$-i \equiv e^{-i\frac{\pi}{2}},$$

we obtain from (5.13)

$$\begin{aligned} \mathrm{Im}\left(\psi(s,n,t)\right) &= \mathrm{Re}\left(e^{-i\frac{\pi}{2}}\,\psi(s,n,t)\right) \\ &= \mathrm{Re}\left(\psi(s-\frac{\pi L}{2k_\gamma},n,t)\right). \end{aligned}$$

Therefore, the complete information about the solution ψ is

already obtained when considering Re(ψ) only. In ensuing discussions bird-eye view of the functions Re(ψ) will be shown.

Before discussing the solutions in details, however, a qualitative argument is shown by which the stream function is related to the barotropic velocity field, see Figure 19. To this end recall that it has been demonstrated in section 2.5, that the barotropic part of the velocity field $\underline{u}^{bt}$ is given by

$$\underline{u}^{bt} = \frac{1}{h}(\hat{\underline{z}} \times \nabla\psi). \qquad (5.16)$$

It follows from this, that the deeper the channels are, the weaker the velocities will be. Further, convex stream function surfaces are connected with anti-cyclonic velocity cells (Figure 19), and the steeper the ψ-surfaces are the stronger the velocities in these cells. Therefore, by looking at the stream function the different velocity cells and their rotational sense can readily be deduced by estimating the convexity of the ψ-surface.

Since d_γ in (5.13) is arbitrary, the choices $d_\gamma := \delta_{i\gamma}$, $i = 1,\ldots,4N$ give the solutions to all individual wavenumbers However, by geometrical arguments it is sufficient to look at only one wavenumber in each mode unit.

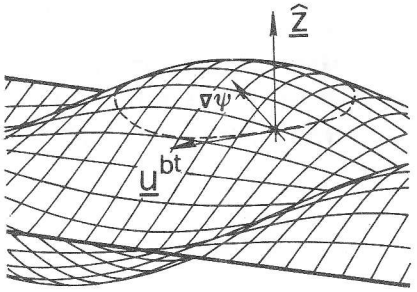

Figure 19

Explaining the anticyclonic barotropic velocity field on a convex stream function surface.

Figure 20 displays a sequence of snapshots of Re(ψ) for a channel solution in a first order model, starting at $t = 0$ with waves which show skew-symmetry with respect to $n = 0$ and proceeding in steps of T/16, where T is the period. Skew-symmetry

of the surface is replaced by symmetry after a quarter period. In between, superpositions of these two aspects can be observed. Looking more closely at the individual wave ridges and their phase motion, it becomes clear that for $n < 0$, the phase progresses in the positive s-direction, while for $n > 0$ the phase progresses in the opposite direction. When the crests of the two domains cross, they merge into a single ridge which then forms the symmetric aspect of the ψ-surface (Figure 20 ff).

It follows that these waves are right bounded in the northern hemisphere, which is a general property of waves governed by the Coriolis force: Kelvin waves, shelf waves, etc., see LeBlond and Mysak (1978).

In terms of the barotropic part of the velocity field the propagation of the stream function crests corresponds to propagating cells in which the barotropic motion is either cyclonic or anticyclonic. Such a time sequence is shown in Figure 20b in which lines of constant ψ are plotted.

In Figures 20b - 25b the n-axis has been stretched by a factor 1.5 to make the transverse structure more visible. The lines of constant ψ were choosen such that all inner most lines correspond to 90 % of the maximal ψ-value in each time step. Therefore, the lines of different time steps cannot be used for amplitude comparison. This disadvantage was made allowance of, to work out the development of the wave structure clearly. The cells rotate anticlockwise. The structure of the cells at $t = 0$ is similar to that of Poincaré wave in a channel (Hutter, 1984b, p. 58). However, Poincaré waves propagate uniformly into one direction and therefore, are distinctly different from topographic waves. With proceeding time the cells in Figure 20b split and merge together; this reflects the mechanism of balance between the symmetric and skew-symmetric aspect. Thus, these cellular domains are not a persistent property, they are rather a feature which exhibits continuous transitions between distinctive cellular patterns.

A second order model extracts the main characteristics of the different mode units introduced earlier. Figures 21 and 22 show channel solutions of the first and second mode unit. The frequencies in the two cases have been chosen such that the wave patterns have about the same wavenumber. The main difference of the two mode units consists in the cross sectional structure of the ψ-surfaces. Considering the wave troughs and crests in the n-direction and counting them, the first mode unit shows a 2-1-2 sequence with respect to time. Channel solutions belonging to the second mode unit have a more structured wave pattern, in that they show a 4-3-4 time sequence. Therefore, each mode unit represents a certain cross sectional wave structure. This is in accord with results from non-approximate wave models (see e.g. Pedlosky, 1979, p. 75 ff), although our method does not a priori imply this connection between mode units and cross sectional structure.

Figure 22b illustrates wave structure of the second mode unit particularly clearly. The 4-3-4 cellular sequence is obvious. Again, the individual cells rotate anticlockwise, and the wave motion is right bounded.

Comparing Figures 20a and 21a also demonstrates the convergence of the solution as the order of the model is increased. The very small effect consists in a smoothening of the ψ-surface towards the channel boundaries.

Figures 23, 24 and 25 illustrate the channel solutions in a third order model. Again each mode unit has its own characteristic cross variation. The phase motion is right bounded and, therefore, opposite in the two channel domains $n < 0$ and $n > 0$, respectively. Comparing Figures 20 and 23 reveal more properties when increasing the order of the model. The wave ridges at $t = 1/4\ T$ in Figures 20a and 23a are flattened on their top. Figures 20b and 23b show at $t = 0$ that the celles are slightly shifted towards the center of the channel which corresponds to a smoothening at the boundaries and a steepening at the center axis.

Figures 20 - 25

Figures 20a - 25a

Time sequence of the stream function surface in steps of 1/16 T. The channel view corresponds to Figure 10 and the coordinates here are chosen $-1/2\ B \leq n \leq 1/2\ B$, $0 \leq s \leq 6\ Lr$ with an aspect ratio $r = 1$. Note the phase motion in the domain $n > 0$ and $n < 0$, respectively.

Figures 20b - 25b

Time sequence of lines of constant ψ relative to 90% of the maximum value of each time step. The cellular structure of cyclonic (+) and anticyclonic (-) vortices is clearly visible.

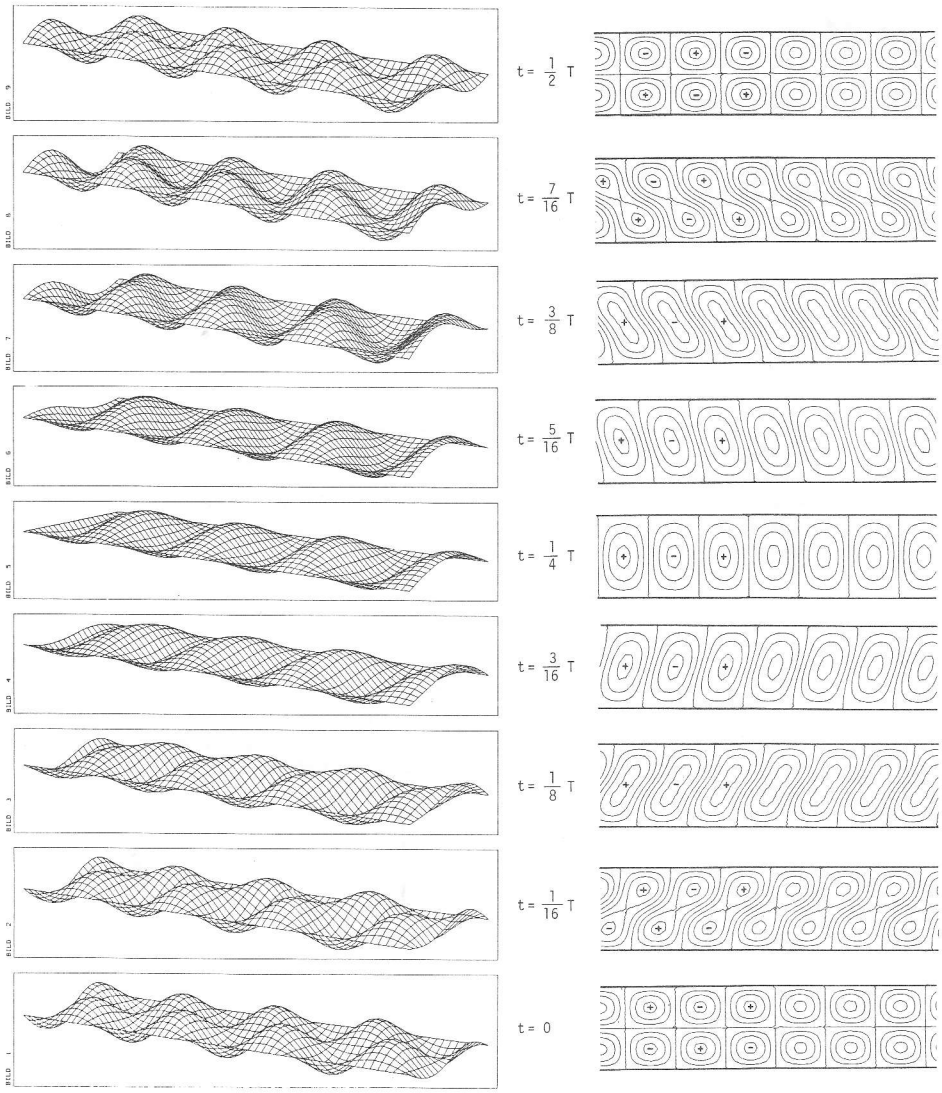

Figure 20 N = 1, ε = 0,05, q = 0,5, ω = 0,287, T = 58,9h, k = 4,01

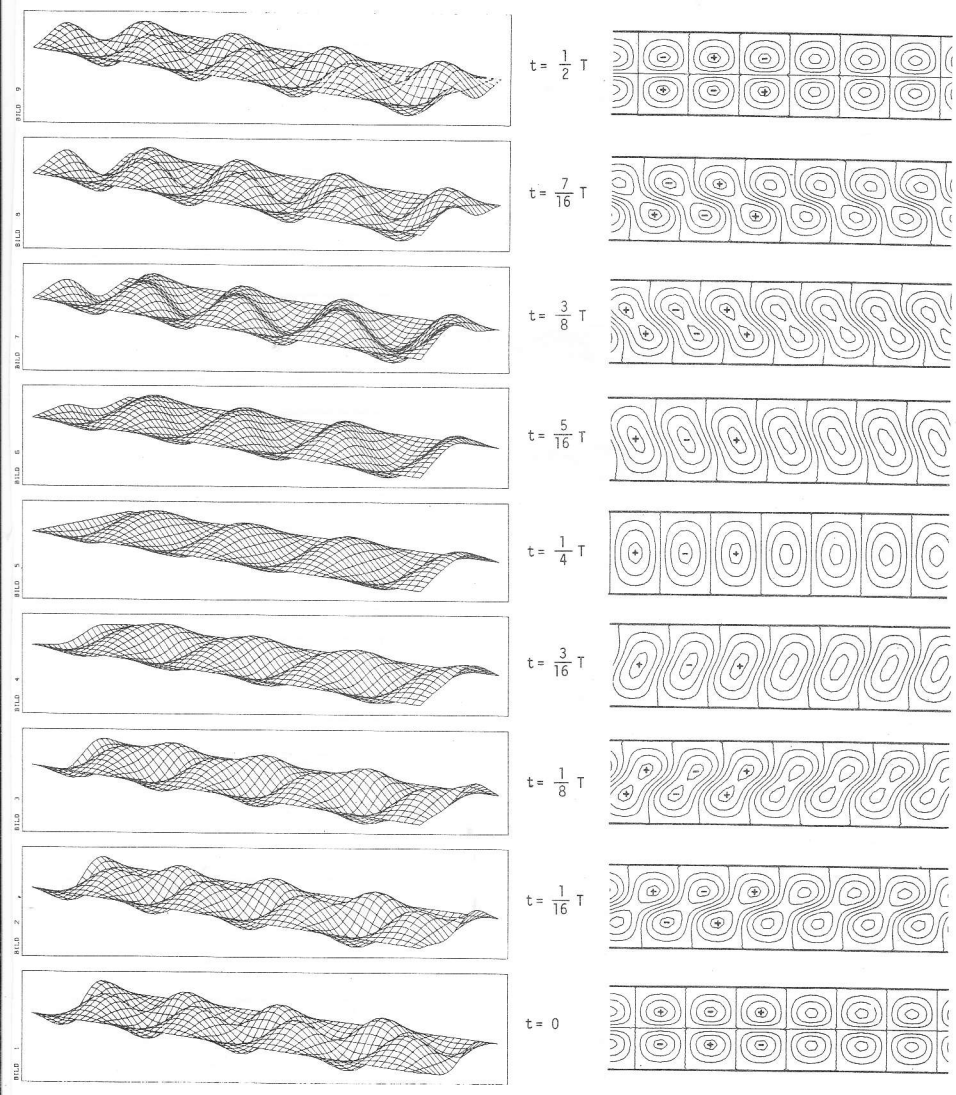

a) b)

Figure 21 N = 2, ε = 0,05, q = 0,5, ω = 0,310, T = 54,5h, k = 4,01

1st Mode Unit

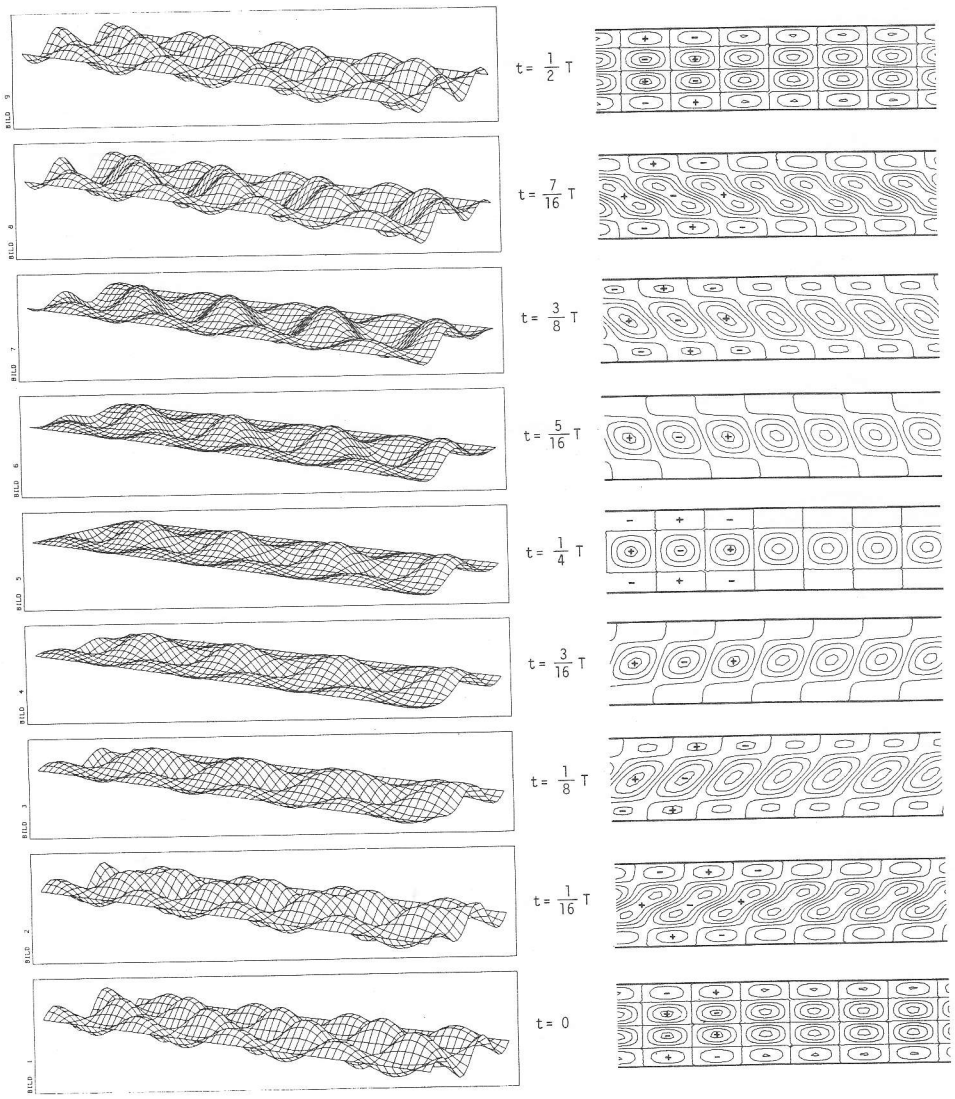

Figure 22 N = 2, ε = 0.05, q = 0.5, ω = 0.120, T = 141h, k = 4.07

2nd Mode Unit

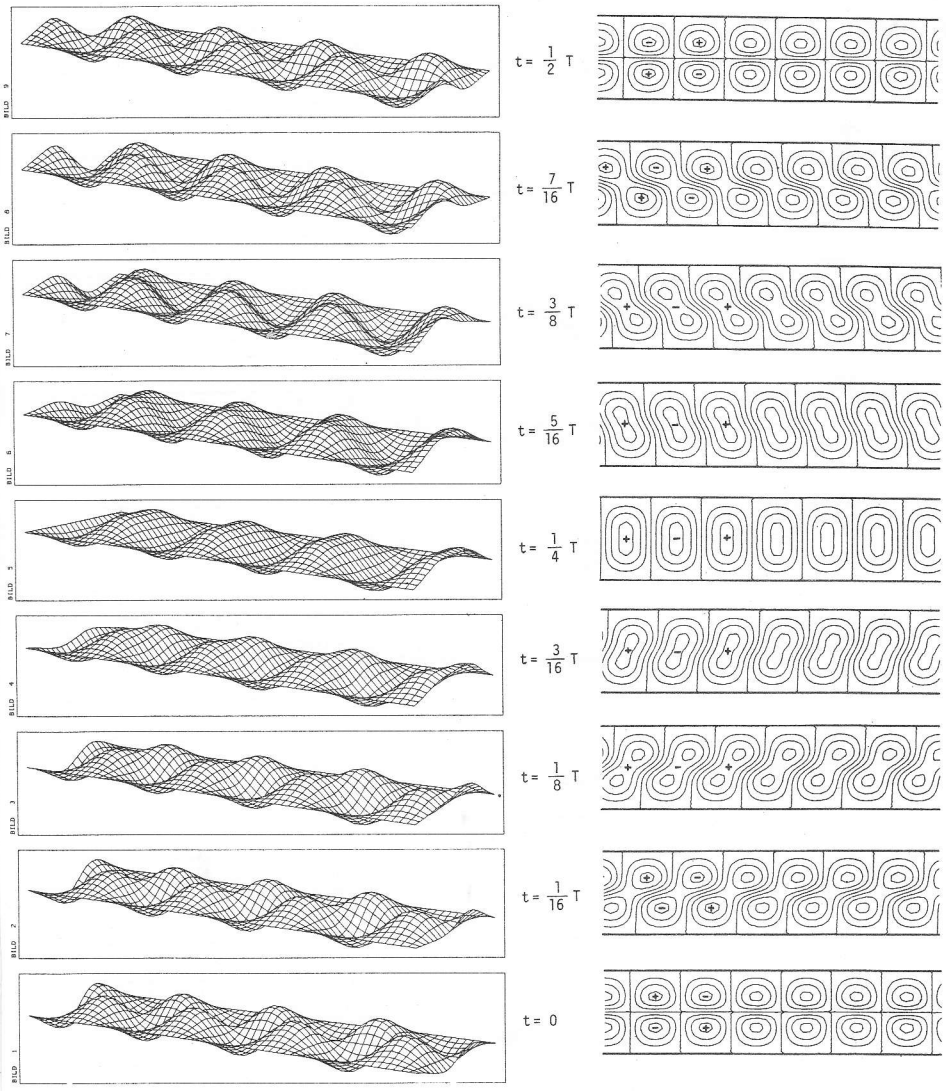

Figure 23 N = 3, ε = 0,05, q = 0,5, ω = 0,314, T = 53,8h, k = 4,00

1st Mode Unit

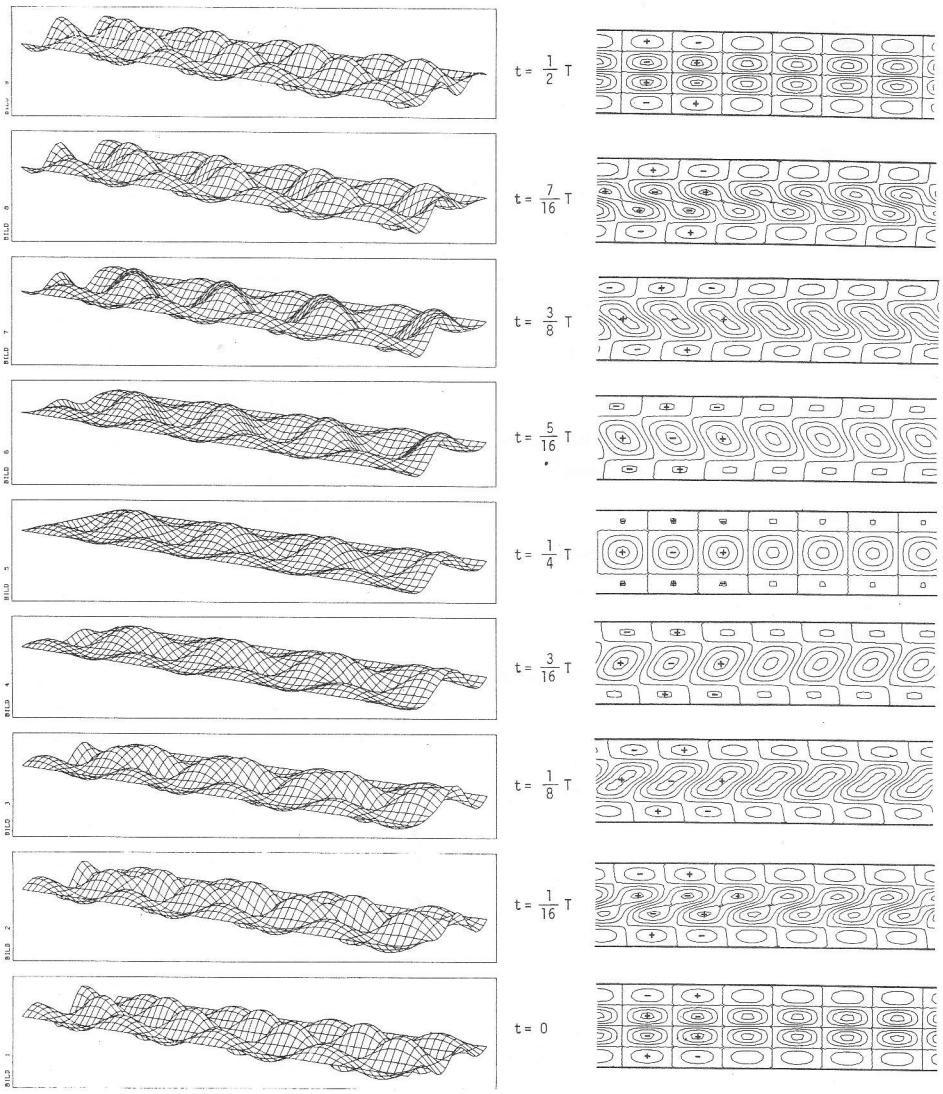

a) b)

Figure 24 N = 3, ε = 0.05, q = 0.5, ω = 0.127, T = 133h, k = 4.00

2nd Mode Unit

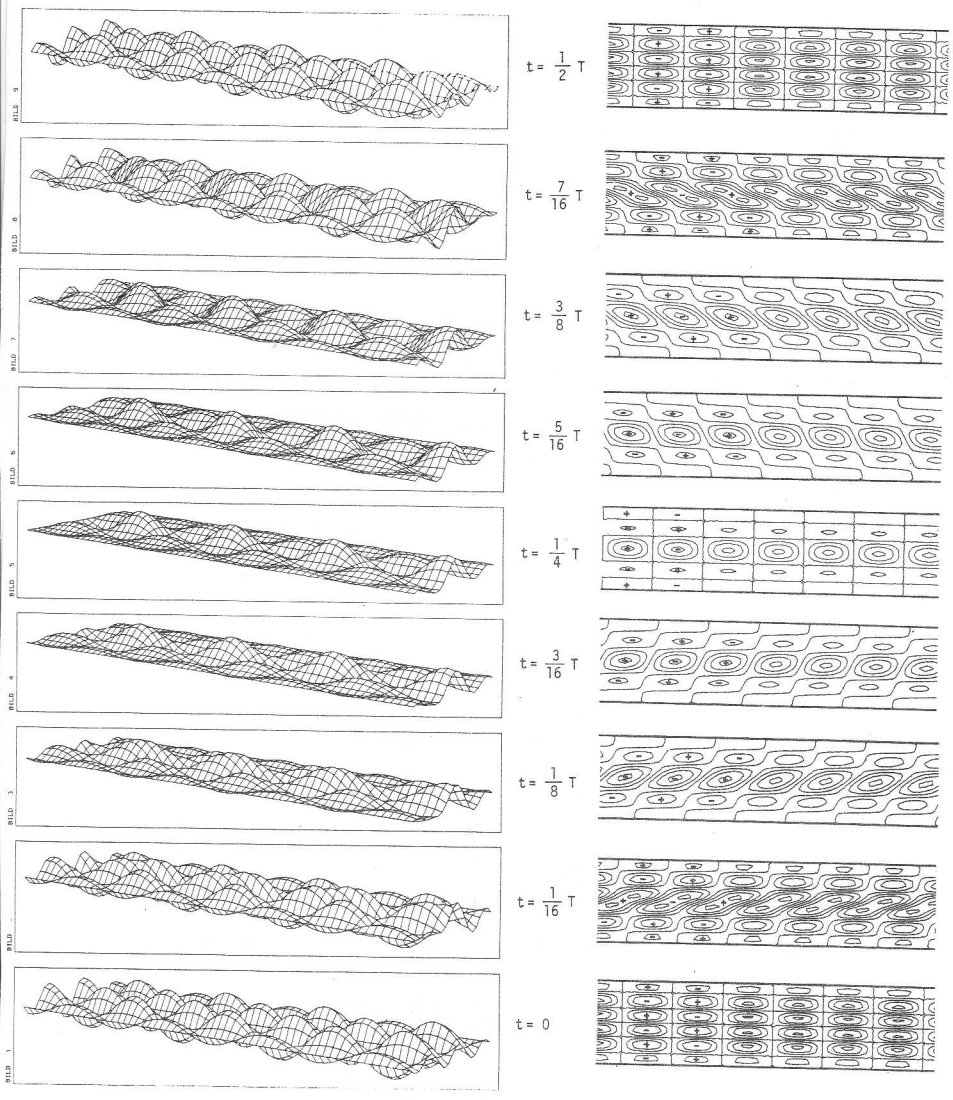

a) b)

Figure 25 N = 3, ε = 0,05, a = 0,5, ω = 0,0573, T = 295h, k = 4,00

3rd Mode Unit

5.7 Comparison with Gratton's channel solutions

Gratton (1983) considered straight channels with various cross topographies. Assuming progressive waves of the form $\phi = \hat{\phi}(n)\, e^{i(\omega t \pm ks)}$, the topographic wave operator could be transformed into an ordinary differential operator on $\hat{\phi}$ with non-constant coefficients depending on the depth function. For roof-shaped and parabolic cross sections the emerging differential equation in $\hat{\phi}$ could be solved and the solutions be expressed in terms of hypergeometric functions (Kummer functions). Without going here into details, Gratton obtains solutions which have a hump close to the right shore (on the northern hemisphere) when looking in the direction of propagation and decay exponentially to zero as the other (left) shore is approached. His formulation yields right bounded waves propagating in both directions along the channel axis, see Figure 26. A linear superposition of two waves propagating in the +s and -s -direction, respectively, would yield qualitatively the same feature as presented in the previous section. This demonstrates that our approximate model yields reasonable results for the topographic wave motion in a channel. More significantly, our method can treat a variety of different topographies without becoming any more complicated. This is a considerable advantage, even though it is bought at the expense of

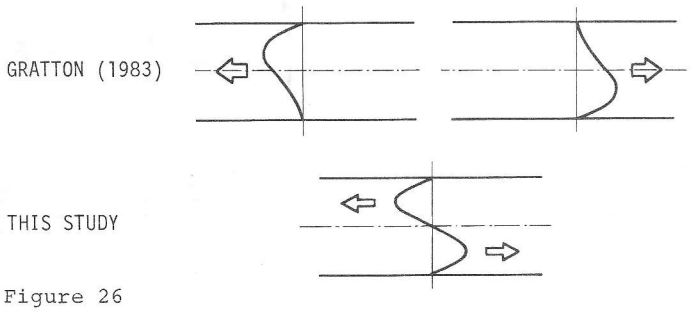

Figure 26

Topographic waves propagating in an infinite channel with cross-topography. Both studies exhibit right bounded waves. Gratton has separate solutions, but this study is a combination of them.

exactness. Indeed, Gratton can only vary cross topographies, must treat bathymetries which do not change along the channel axis and is unable to handle closed channels, i.e. lakes. All these restrictions can be lifted in our approximate integration technique.

6. LAKE MODELS

6.1 From channels to lakes

As there exist 4N independent solutions in a channel for a Nth-order model they may, within the framework of a linear theory, be superposed, such that the resulting solution also fulfils boundary conditions on the s-axis, i.e. $s = 0$ and $s = L$. These must be satisfied for all $\psi_{\pm}^{\alpha}$ in equation (5.12) in order that the combination $\psi(s,n,t)$ obeys the relation

$$\psi(s,n,t) = 0, \quad s = 0,L \tag{6.1}$$

for all times. The critical frequencies, at which the different regimes touch (see Table 5), shall be excluded from consideration. For that case the boundary conditions (6.2) would have to be modified by using the fundamental solutions (5.14). From equation (5.12) 4N conditions are obtained as follows:

$$\begin{aligned}
\psi_{+}^{\alpha}\Big|_{s=0} &= 0 \rightarrow \sum_{\gamma=1}^{4N} c_{\alpha\gamma}\, d_{\gamma} = 0, && \alpha = 1,\ldots,N \\
\psi_{-}^{\alpha-N}\Big|_{s=0} &= 0 \rightarrow \sum_{\gamma=1}^{4N} c_{\alpha\gamma}\, d_{\gamma} = 0, && \alpha = n+1,\ldots,2N \\
\psi_{+}^{\alpha}\Big|_{s=L} &= 0 \rightarrow \sum_{\gamma=1}^{4N} e^{ik\gamma}\, c_{\alpha\gamma}\, d_{\gamma} = 0, && \alpha = 1,\ldots,N \\
\psi_{-}^{\alpha-N}\Big|_{s=L} &= 0 \rightarrow \sum_{\gamma=1}^{4N} e^{ik\gamma}\, c_{\alpha\gamma}\, d_{\gamma} = 0, && \alpha = n+1,\ldots,2N
\end{aligned} \tag{6.2}$$

By defining a $(4N \times 4N)$-matrix $D_{\alpha\gamma}(\omega)$, such that

$$\begin{aligned}
D_{\alpha\gamma} &= c_{\alpha\gamma}, && \alpha = 1,\ldots,2N, \\
D_{\alpha\gamma} &= e^{ik\gamma}\, c_{\alpha-2N,\gamma}, && \alpha = 2N+1,\ldots,4N, \\
& && \gamma = 1,\ldots,4N,
\end{aligned} \tag{6.3}$$

the boundary conditions (6.2) assume the compact form

$$D_{\alpha\gamma}\, d_\gamma = 0, \qquad \alpha,\gamma=1,\ldots,4N\,. \tag{6.4}$$

Non-trivial lake solutions require that

$$\det \underline{D}(\omega) = 0, \tag{6.5}$$

which is the equation determining the eigenfrequency in the lake. Having found an eigenfrequency ω with (6.5) the lake solution can readily be calculated by determining the eigenvector d_γ from (6.4) and evaluating ψ from (5.13). Both, real and imaginary parts of ψ are solutions; however, for simplicity only one of them will be considered. Calculations showed that the eigenfrequency ω could be evaluated from (6.5) with appreciable accuracy. Calculating, in a second step, the eigenvector d_γ by a Gauss algorithm (backward substitution from a left-right decomposition of $\underline{D}$) caused serious difficulties in so far as some of the thus constructed eigenfunctions showed dissatisfaction of the boundary conditions. This is characteristic of numerically stiff systems and occurs particularly in cases, when zeros have to be evaluated which are connected with large derivatives. In these cases the calculation of the zero of a nonlinear function exhibits good and fast convergence although the function value at the root may be far from zero. There was not sufficient time to resolve this problem. Solutions, which do not satisfy the boundary conditions in the above sense are not shown here. However, in cases for which the discrepancies are small, the boundary conditions are artificially enforced by simply setting $\psi \equiv 0$ at the boundaries.

6.2 The spectrum

Obviously, because a boundary value problem is solved, the spectrum is discrete. As it turns out from calculations it is impossible to satisfy the boundary conditions (6.2) unless at least two wavenumbers are real. Therefore, in a first order model with only one mode unit lake solutions have a pure wave-

like structure in the s-direction. However, in higher order models lake solutions can be mixtures of all three types ($k_\gamma \in \mathbb{R}, \tilde{\mathbb{C}}, \mathbb{J}$). The structure of this mixture depends crucially upon both, the topography and the aspect ratio of the basin. It follows from the above that there exists an upper cut-off frequency or lower cut-off period given by the maximum of the real branch of the dispersion curve (compare Figures 12, 13, 14). This cut-off period increases with increasing topography parameter q, which is in accordance with the considerations in Appendix A. The increase occurs for all aspect ratios as can be seen from Tables 10 and 11. Enlarging the aspect ratio, on the other hand, shifts the spectrum to higher periods. Tables 10 and 11 also indicate that the eigenperiods may be grouped into pairs which lie very close together, sometimes with differences of less than an hour. This effect is intensified in the second order model, see Table 11, in that the paired periods differ only in the last digit. Finite difference solutions of topographic waves in enclosed basins further indicate that eigenperiods may cluster in very narrow frequency bands (E. Bäuerle, personal communication).

q	r						
0.5	0.5	57.7	58.8	63.7	64.1	71.5	71.9
	1.0	57.6	58.1	71.5	71.9	89.2	91.0
	2.0	70.3	73.2	109	113	155	158
1.0	0.5	65.9	66.1	72.2	72.7	89.6	90.5
	1.0	65.7	66.3	80.5	80.7	99.3	101
	2.0	79.0	82.4	121	125	170	174
2.0	0.5	99.7	100	124	125	138	140
	1.0	90.7	91.7	111	112	137	140
	2.0	109	114	167	174	234	241
5.0	0.5	209	211	261	265	294	299
	1.0	209	211	260	265	327	339
	2.0	255	272	404	424	575	591

Table 10

Six lowest eigenperiods (in hours) of a first order model with $\varepsilon = 0.05$ for four different values of the topography parameter q and three values of the aspect ratio r. The vertical dashed lines separate pairs of periods which lie close together.

q	r						
	0.5	50.0	50.5	53.5	53.6	62.5	62.7
0.5	1.0	53.7	53.8	62.9	63.3	74.1	74.7
	2.0	63.8	64.6	87.6	88.4	106	108
	0.5	59.8	59.9	63.1	63.2	71.7	71.8
1.0	1.0	57.6	57.6	63.5	63.7	72.2	72.5
	2.0	64.5	64.7	84.1	84.4	108	109
	0.5	68.7	68.7	89.7	89.7	122	122
2.0	1.0	66.5	66.5	71.9	72.0	80.2	80.3
	2.0	72.4	72.5	91.6	91.7	116	117
	0.5	107	107	156	157	422	423
5.0	1.0	111	112	124	124	139	140
	2.0	112	112	140	140	176	178

Table 11

Six lowest eigenperiods (in hours) of a second order model (45° latitude) with $\varepsilon = 0.05$ for four different values of the topography parameter q and three values of the aspect ratio r. The vertical dashed lines separate pairs of periods which lie close together.

The form (Rossby character) of the dispersion relation $\omega(k)$ also implies that modes with higher periods have higher modal structure in the s-direction, because to a given period the two wavenumbers are far apart; so, in a particular solution there is always a contribution of a high wavenumber k. However, it is not possible to arrange the eigenfrequencies in a strict order which would be connectable with the modal structure. This seems to be intrinsic of second class wave motion, since already Ball (1965) has not found such a connection even in an exact, analytical solution, see Figure 8.

6.3 The role of the aspect ratio

In equations (5.9) an aspect ratio parameter $r = \frac{B}{L}$ has been introduced. Up to now we have considered *elongated* lakes with a *cross*-topography and consequently assumed that $r \ll 1$, see Figure 27. In such a situation an expansion procedure corresponded to an approximation in the narrow direction, i.e. along

the n-coordinate, and "exact" integration along the thalweg of the lake. However, in view of the simplifications in section 4.1 (straight lakes of constant width) situations with $r > 1$ can equally be considered. $r > 1$ means that the lake width B exceeds its length L, and these two notions loose their common meaning, see Figure 27. For $r >> 1$ the lake becomes again elongated, but its topography is distinctly different from the small aspect ratio case. Whereas for $r < 1$ the topography (4.3) and the approximation (3.3) vary along the small direction of the lake, $r > 1$ characterizes a lake whose *thalweg* is described by the topography (4.3) and whose motions are approximated in its long direction (Figure 27). The approximation, the weighted integration along the n-direction, is

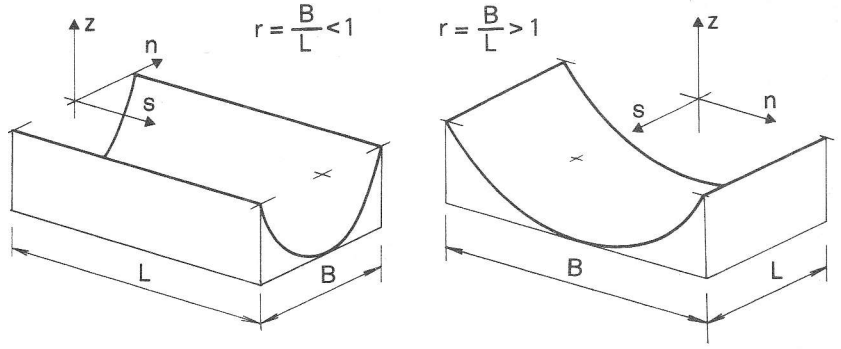

Figure 27
Lake geometry for $r < 1$ and $r > 1$. For $r < 1$ the lake has a cross topography with a constant thalweg-depth, whereas for $r > 1$ there is no cross topography but a variable thalweg-depth.

now performed along the thalweg, i.e. the long side of the lake. Examination of the influence of r, therefore, enables us to answer the question, what would be the important qualities of a lake to sustain topographic waves. The cases $r < 1$ and $r > 1$ then characterize situations for which either the cross- or the thalweg-variation of the lake basin is important.

It was pointed out in section 5.1 that the dispersion rela-

tion depends on the product $r \cdot k$ implying $\omega = \omega(r \cdot k)$. Thus, when plotted as a function of k only, dispersion relations $\omega(k)$ with different aspect ratios emerge from each other by a stretching transformation along the k-axis. Figure 28 illustrates this effect qualitatively. Increasing r means that, for fixed ω, the waves have smaller wavenumbers and, therefore, exhibit within a given distance along the s-direction fewer troughs and fewer crests. This property provides a hint towards an answer of the following questions:

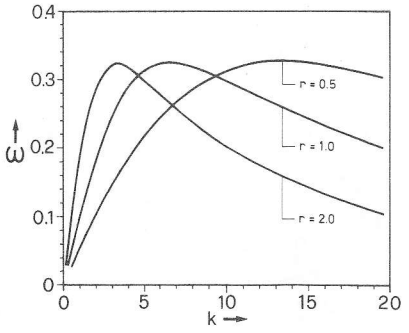

Figure 28

Dispersion relation $\omega(k)$ for different aspect ratios r, retaining the values of the other parameter N, ε, q.

i) What is the domain of the aspect ratio, $r < 1$ or $r > 1$, for which reasonable approximate topographic wave solutions are obtained, which allow a comparison with earlier studies, such as Ball (1965) and Mysak (1984)?

ii) Under which situations must the cases $r < 1$ and $r > 1$ be applied? Can we by any means decide whether a lake favours one over the other?

The answer to the first question has already been sketched above. It follows from the aspect ratio dependence of the dispersion relation that the lower the aspect ratio r is the higher will be the modal structure in the s-direction. This feature can be seen in Figure 29 for the lowest eigenperiod in the first order model. On the left, $r < 1$, the two wavenumbers which correspond to a given ω lie far apart; the stream function is composed of a long wave and a short wave component. The structure of the closed basin mode is therefore rich. This

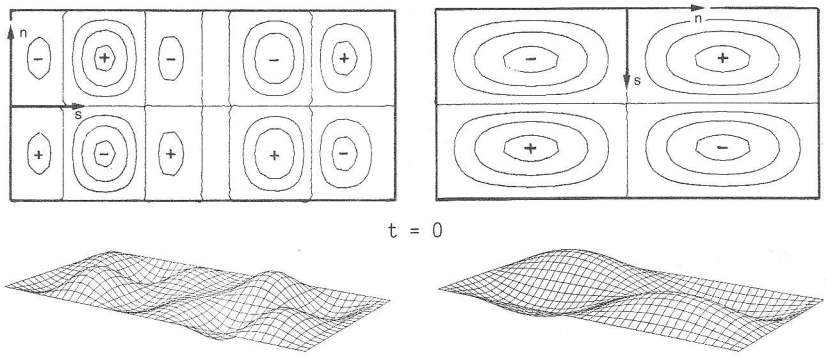

Figure 29
Comparison of the modal structure for an aspect ratio $r < 1$ and $r > 1$, respectively. The parameters are selected $N = 1$, $\varepsilon = 0.05$, $q = 0.5$, time $t = 0$.

fact prevents the occurrence of ground modes*) of topographic waves as presented in Figure 7, section 4.2. On the right $r > 1$, the two wavenumbers are much smaller such that the stream function is composed only of "long" wave components; the modal structure of the basin solution is simple or fundamental. This type of solution, obtained in a first order model, resembles globally the structure of exact, fundamental closed basin solutions, such as those of Ball (1965), see Figure 8, and Mysak (1984).

Now, because it is our aim to use the channel model as a suitable approximation of exact solutions, it seems, at first sight, compelling to conclude that our method can -at least as far as a first order model is concerned - describe topographic wave motion approximately only for lakes with $r > 1$. Solutions of the case $r < 1$, for which the model was motivated, indeed show in a first order model no similiarity with *known* exact solutions. However, since the number of published analytical solutions is rather poor and therefore, does not allow

*) *ground, gravest or fundamental mode: Mode, whose stream function has the least possible structure over the lake domain.*

a general and final comparison with the aim to test our model, it is dangerous to qualify our model at this moment.

In fact, both aspect ratio ranges lead to physically reasonable approximations, but they are distinctly different and describe two limiting aspects of the exact topographic wave operator. Evidently, only the large aspect ratio solution $r > 1$ describes, in a first order model, a global, gravest mode response. To obtain it, the long side of the lake is approximated by the set of basis functions (4.17) and the topography is accounted for by a variable thalweg depth. For this case, the thoughts on the motivation of our method in section 3.2 are inappropriate!

However, no premature inferences should be drawn. For instance, not to consider the case $r < 1$ any longer or stating that fundamental modes cannot occur for small aspect ratios are hasty conclusions. Although, under the above made restrictions, they do not show similarities with the Ball and Mysak solutions it may well be possible that, by making other assumptions on the basis functions and /or the topography, that $r < 1$ would yield reasonable results as well.

6.4 Restrictions of this model

In the previous section it has been explained that for certain aspect ratios our mehtod gives topographic wave motion which is distinctly different from earlier results (Ball, 1965, etc.). We feel that this difference has its origin in the amount of restriction imposed on the differential equation (2.16) by our approximation technique. Evidently, it affects the quality of the approximation. If the restriction is small, which can mean that the order N of the model is large or the basis functions are well chosen, the approximation is expected to describe the physics of the problem satisfactorily. On the other hand, ill chosen basis functions and low order models are prone to unsatisfactory results. Selecting $r < 1$ and taking

a low order model appears to be too big a restriction and, therefore, yields results which do not allow a comparison with earlier studies. It seems, that together with N = 1, the basis functions (4.17) along the narrow side of the lake, as done in section 4.3, are ill chosen. A possible reason of this ill choice may be the fact that smaller aspect ratios r are connected with larger basis function gradients. To make this clear, consider a basis function of the form (4.17)

$$P_\alpha(s,n) = P_\alpha(\frac{2n}{B(s)}) = P_\alpha(\frac{2n}{B}), \tag{6.6}$$

with a constant lake with B. Taking the derivative of (6.6) with respect to n and recalling $r = \frac{B}{L}$ yields

$$\frac{\partial P_\alpha}{\partial n} = \frac{2}{r\,L} P'_\alpha, \tag{6.7}$$

which proves the above statement. Therefore, smoother basis functions seem to represent a weaker restriction on the system.

There is another important qualitative change of our model when r > 1. This is shown in Figure 27. The fact, that for r > 1 the thalweg-depth is variable, gives evidence of the relative importance in a first order model of the cross-sectional topography and the thalweg topography, respectively. It seems, since r > 1 yields results which can be compared with earlier studies, that for low order models (N = 1) the thalweg topography is much more important than the shape of the cross sections. This is in agreement with the fact, that a topographic wave which propagates anticlockwise around the lake (see analytical result in Ball (1965) and Figure 8) must, in an elongated lake, change its direction mainly at the lake ends. This change is made possible by topography gradients and has its origin in the fact that topographic wave motion follows the isobaths of the basin in order to conserve potential vorticity. However, in view of our simplifications of the lake basin, (5.4) with c = 0 and consequently $\frac{\partial h}{\partial s} \equiv 0$, the isobaths do not form continuous closed lines around the lake, see Figure 27. This

serious restriction which affects the very mechanism of topographic wave motion and its removal will be further discussed later on.

To summarize the above considerations, we think that reasonable results with the present restrictions are most likely obtained in a first order model when selecting an aspect ratio domain $r > 1$.

6.5 Topography and sidewall effects

Solutions in channels (section 5) have shown that a change in both, topography and sidewall parameter, does not affect the structure of the waves, but shifts the periods for both increasing q and ε to higher values. Tables 12a and 12b demonstrate that this feature is also observed in lake solutions and that it is qualitatively independent of the choice of the aspect ratio. There are two cases, indicated by a question mark in the tables, which differ from the general behaviour.

a)

r = 0.5	N	q = 0.5	1.0	2.0	5.0
ε = 0.05	1	57.7	65.9	99.7 ?	209
ε = 0.10		65.0	71.4	96.9	223
ε = 0.05	2	50.5	59.8	68.7	107
ε 0.10		56.0	62.9	71.3	n.c.

b)

r = 2.0	N	q = 0.5	1.0	2.0	5.0
ε = 0.05	1	70.3	79.0	109	255
ε = 0.10		81.4	88.0	119	276
ε = 0.05	2	63.8	64.5	72.4	112
ε = 0.10		75.1 ?	73.1	104	n.c.

Table 12
First eigenperiod (in hours) for a lake listed for four topography- and two sidewall-parameters in the first and second order model. Two aspect ratios are considered. n.c. indicates that calculations did not converge and the question mark indicates deviating behaviour.

Examining the lake stream functions reveals no visible differences except in the case N = 2 and r = 2.0, where little wave

intensification in the middle of the lake was observed by increasing q from q = 2.0 to q = 5.0.

6.6 First order lake solutions

In this section lake solutions of a first order model (N = 1) are shown. Figure 30a and 30b display snapshots of the stream function of a lake solution during a semicycle ($\frac{1}{2}$ T) for the small aspect ratio case (r = 0.5). The timestep is $\frac{1}{16}$ T. It is clearly visible that the lake is divided into two similar subcells which in their domain turn anticlockwise, seemingly with no interaction. These quasi-independent subcells consist themselves of smaller cells with cyclonic or anti-cyclonic velocity fields. It is remarkable that s = $\frac{1}{2}$ L is not a center of symmetry, therefore these two subcells are not identical. As worked out in section 6.3 there is a rich modal structure of this topographic wave since r < 1. Thus a comparison with the solutions presented by Ball (1965) is not reasonable.

We turn now to the large aspect ratio case, r > 1, which exhibits wave patterns resembling Ball's analytical solutions. A discussion about the analogies and differences when comparing the solutions will be given in section 6.8. Figures 31-36 show topographic wave motions in a first order model with $\varepsilon = 0.05$, q = 2.0 and r = 2.0 for the six lowest eigenperiods which are listed in Table 10. Figure 31 and 32 show the ground modes for these parameters. As it was expected the modes exhibit a phase propagation typically anticlockwise around the lake. Again, as observed in the infinite channel, the individual cells emerge and split. They are not permanent patterns in the lake but are rather subject to a continuous change. This is reminiscent of topographic wave motion and corresponds to the fact that solutions to a given eigenperiod cannot be arranged into a strict order which would be connectable to its modal structure, as can be done for all separable wave problems (membranes, kettle-drums, hydrogen atom, etc.).

Figures 31-36 demonstrate also how the modal structure de-

Figures 30 - 36

Figures 30a - 36a

Time sequence of the stream function surface in steps of 1/16 T for a first order lake model. The selected parameters are indicated on the individual figures and the lake view and the position of the coordinate system correspond to Figure 27 depending on the aspect ratio.

Figure 30b - 36b

Time sequence of lines of constant ψ relative to 90 % of the maximum value of each time step for a first order lake model.

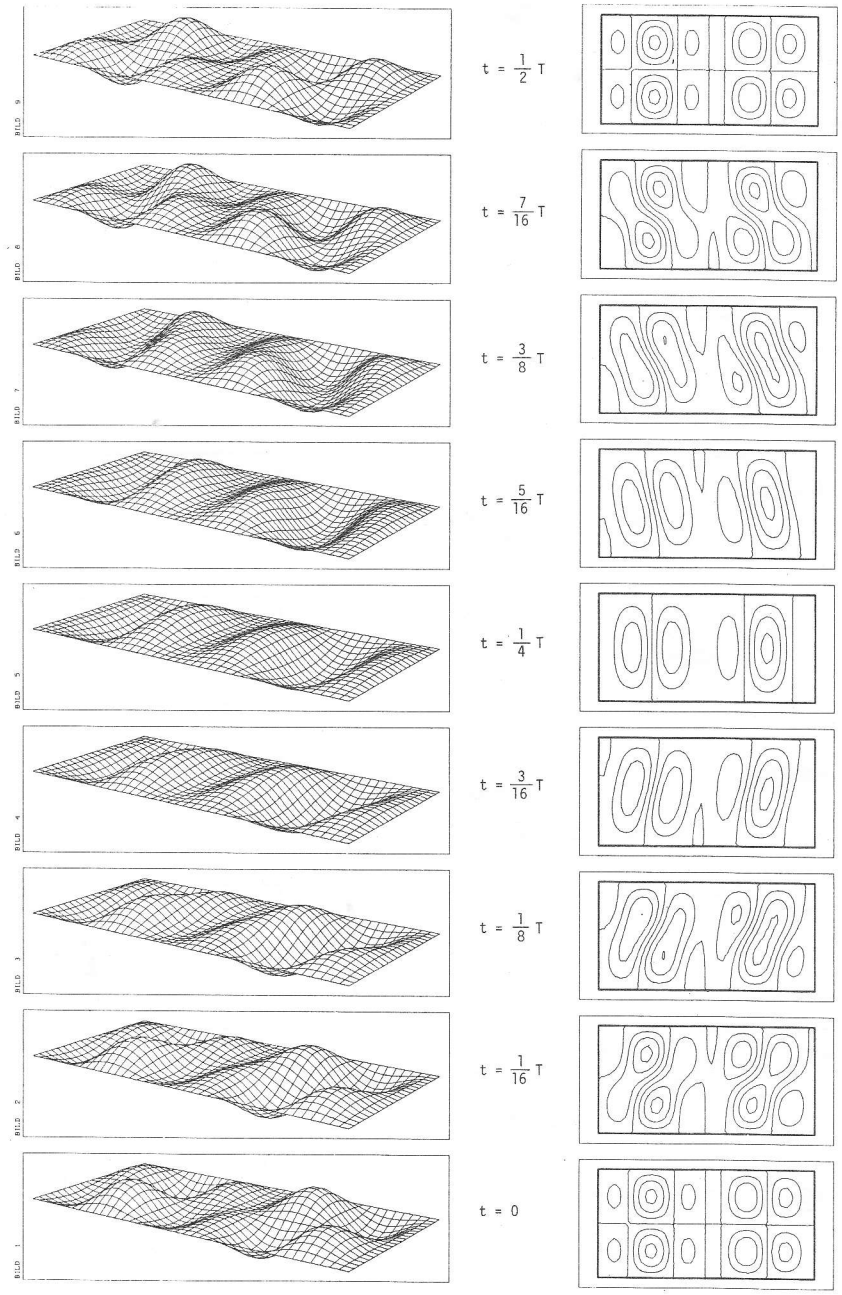

Figure 30 N = 1, r = 0.5, ε = 0.05, q = 0.5, ω = 0.293, T = 57.7 h

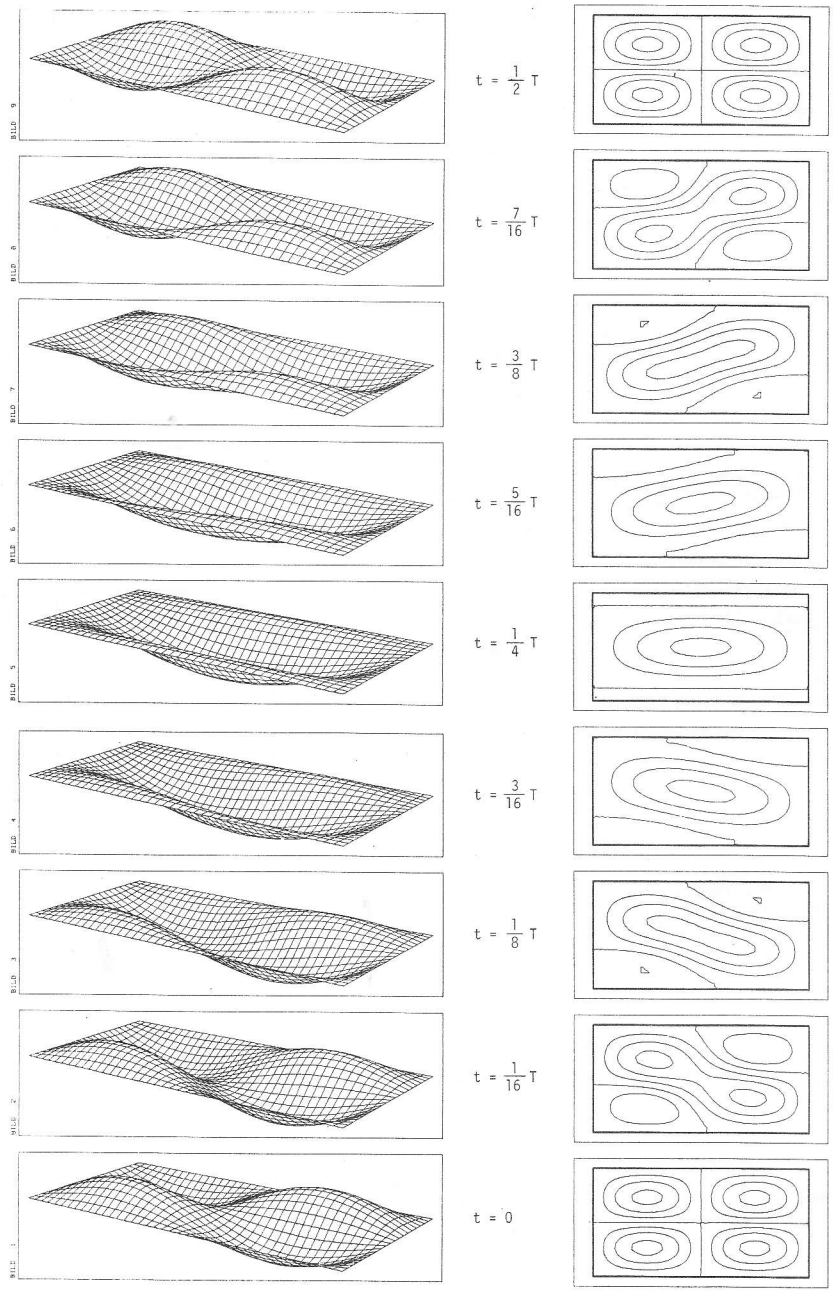

a) b)

Figure 31 N = 1, r = 2.0, ε = 0.05, q = 2.0, ω = 0.155, T = 109h

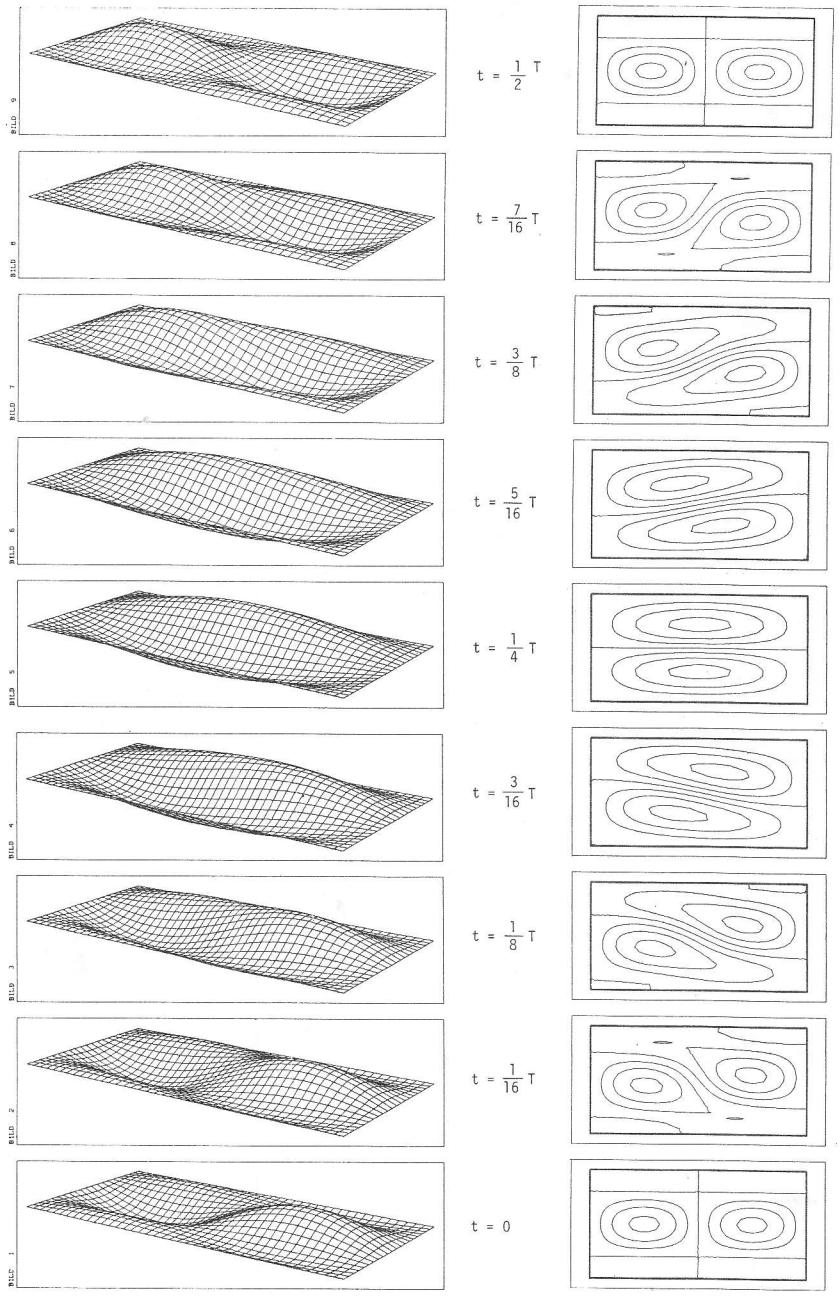

a) b)

Figure 32 N = 1, r = 2.0, ε = 0.05, q = 2.0, ω = 0.148, T = 114h

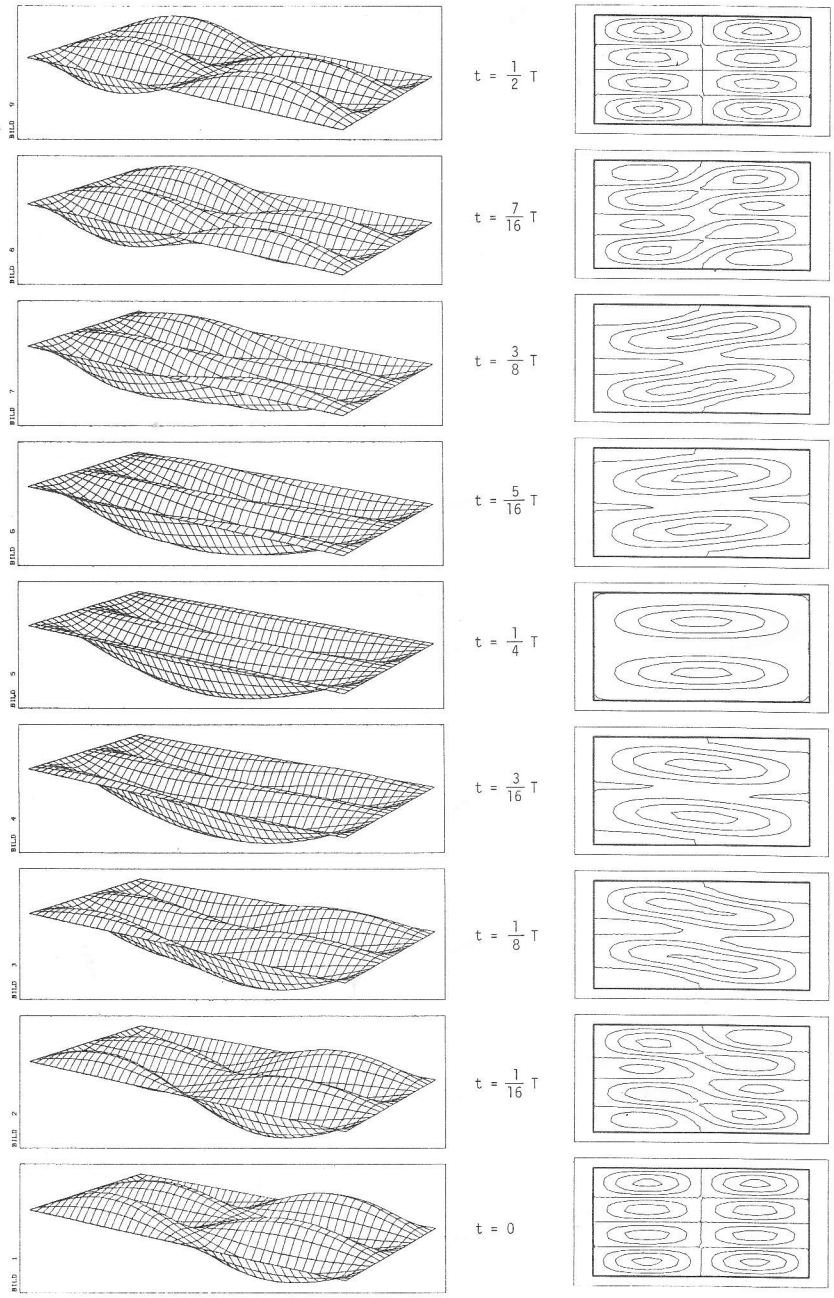

a) b)

Figure 33 N = 1, r = 2,0, ε = 0,05, q = 2,0, ω = 0,101, T = 167 h

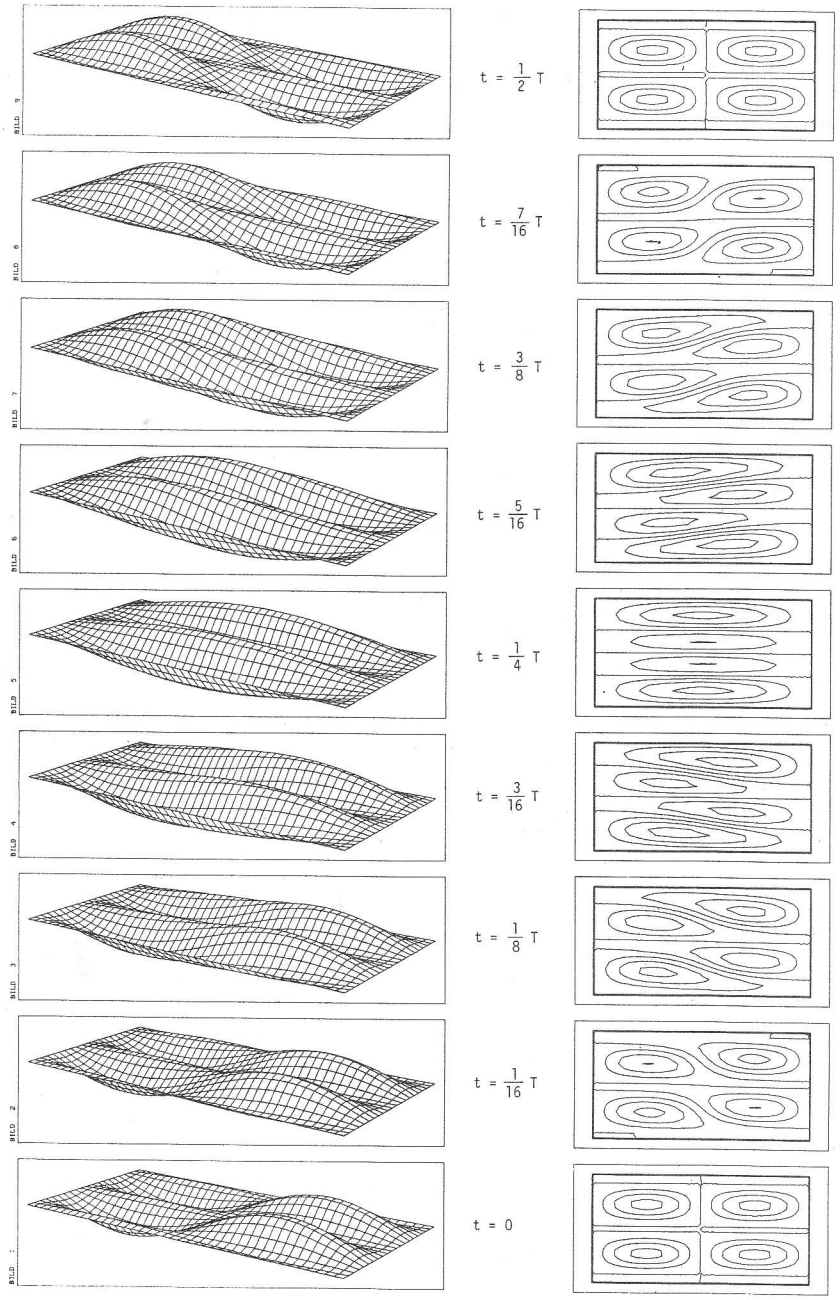

a) b)

Figure 34 N = 1, r = 2,0, ε = 0,05, q = 2,0, ω = 0,0972, T = 174 h

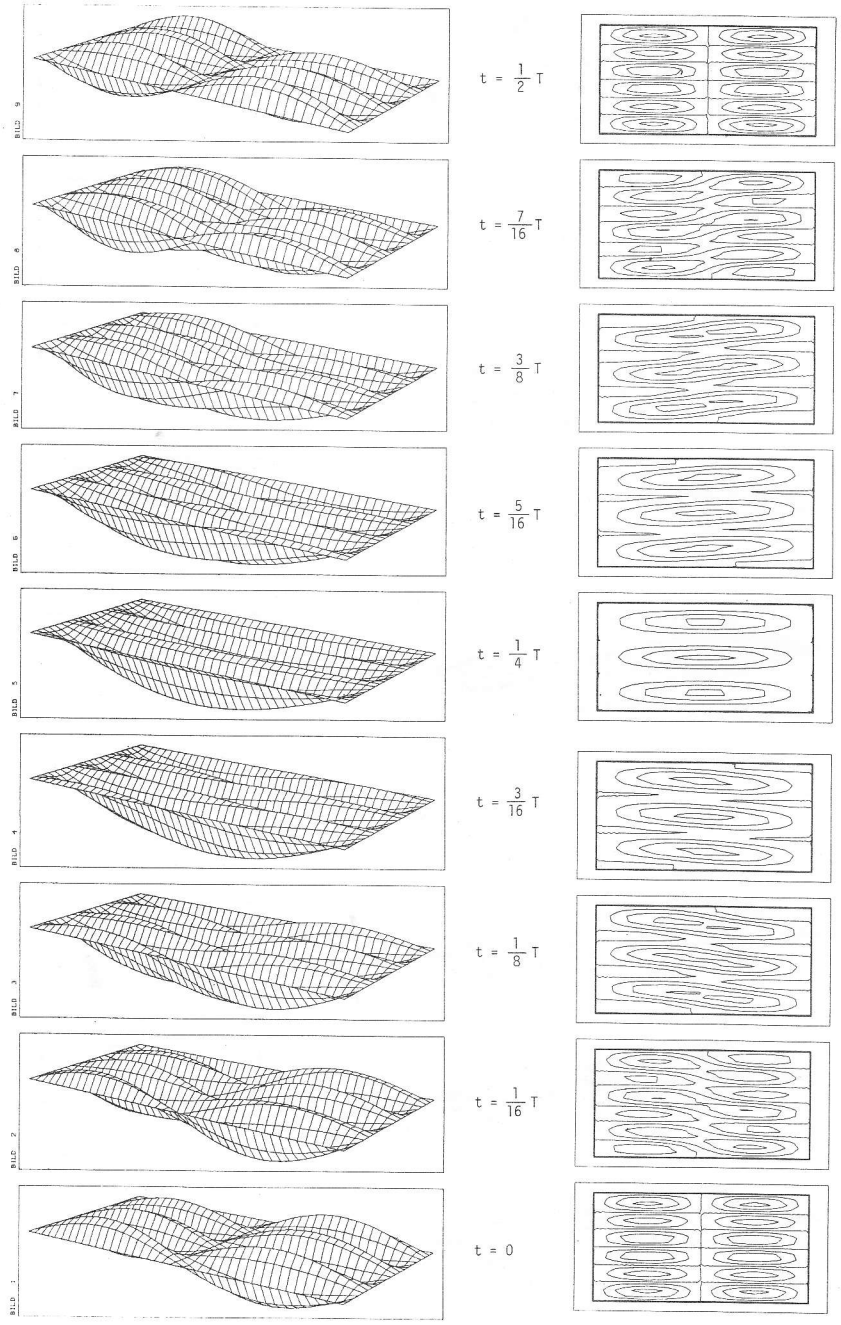

a) b)

Figure 35 N = 1, r = 2.0, ε = 0.05, q = 2.0, ω = 0.0721, T = 234 h

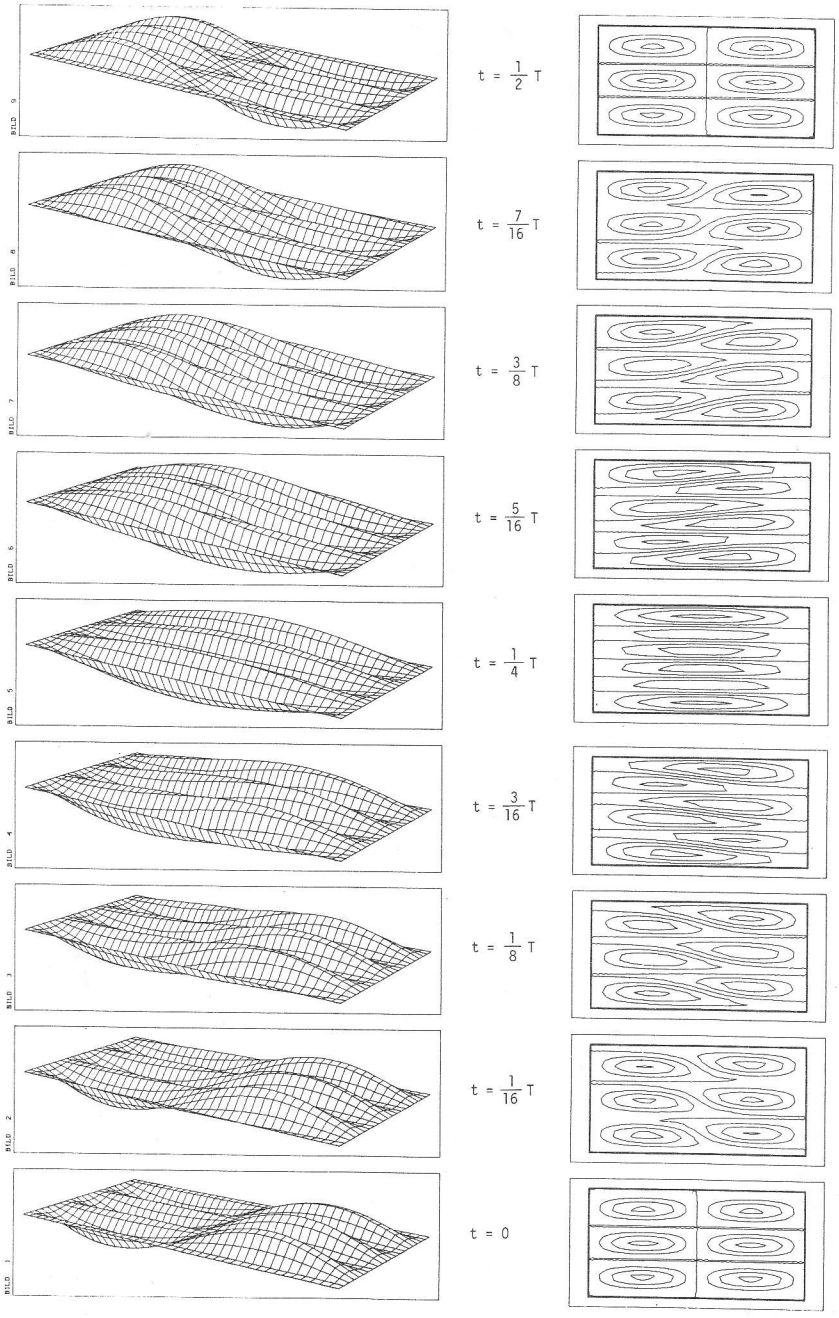

a) b)

Figure 36 N = 1, r = 2.0, ε = 0.05, q = 2.0, ω = 0.0702, T = 241h

velops when increasing the period through the spectrum. The spectrum begins with two eigenperiods (paired), T = 109 h and T = 114 h in Table 10, which have a very simple structure and can therefore be declared as the fundamental modes. The wave with the lowest period T = 109 h, see Figure 31, begins with 4 troughs and crests, transforms after a quarter period (27.3 h) to a structure with only 1 trough to reach, eventually, after half a period (54.5 h) again 4 troughs and crests, however now interchanged. This mode, therefore, shows a 4-1-4 sequence. The next mode in the spectrum with an eigenperiod T_2 = 114 h shows clearly a 2-2-2 sequence, see Figure 32. At this point it is not clear, which of both modes should be declared as the fundamental mode because they have about an equally simple modal structure.

Proceeding in the spectrum, see Figure 33, the next eigenperiod can be found at T = 167 h, cf. Table 10. The modal structure is now described by a 8-2-8 sequence. It is worth noting that the wave motion in the lake can be divided into two subcells separated at $s = \frac{L}{2}$. The subcells do not interact and turn anticlockwise within their domain independently, see Figure 33b. The next eigenperiod T = 174 h is paired with the latter and shows a 4-4-4 sequence which has about the same modal complexity as the previous mode.

Inspection of Figures 31-36 provides an answer to the question, whether there is a rule concerning the modal structure when running through the spectrum. Table 13 answers this question. There is a simple rule which enables us to continue the modal sequence for higher periods, the next pair would be 16-4-16 and 8-8-8. The lower eigenperiod of each pair has a modal structure which is not balanced, i.e. the number of troughs and crests changes appreciably within a period. Consequently, merging and splitting cells can be observed. The second eigenperiod of each pair shows a balanced modal structure, which increases regularly with increasing periods. With respect to the s-direction, (for the definition see Figure 27) the flow

T [h]	Modal sequence	Fig.
109	4-1-4	31
114	2-2-2	32
167	8-2-8	33
174	4-4-4	34
234	12-3-12	35
241	6-6-6	36

Table 13

Modal sequence for the lowest six eigenperiods in a first order model N=1, $\varepsilon = 0.05$, $q = 2.0$, $r = 2.0$. The figures indicate the number of crests and troughs; the first figure gives this number at $t = 0$, the second at $t = 1/4\,T$ and the third at $t = 1/2\,T$. The pairing is not only evident in the period but also in the modal sequence.

in neighbouring cells rotates in the same direction for

$t = \frac{1}{4}\,T$ and the first mode of a pair,

$t = 0, \frac{1}{2}\,T$ and the second mode of a pair,

and in opposite directions for

$t = 0, \frac{1}{2}\,T$ and the first mode of a pair,

$t = \frac{1}{4}\,T$ and the second mode of a pair.

6.7 Second order solutions

This section elaborates on the qualitative changes of the eigenperiods and their associated basin solutions that arise when a second order model is considered. It also casts light on the questions regarding (i) the validity of the above mode assumptions (basis functions, aspect ratio range, topography), (ii) the convergence of the solutions and (iii) the important qualities of a lake to sustain topographic wave motion. For the purpose of comparison with the results in the previous section the same parameters are selected.

First, the low aspect ratio case, $r = 0.5$, shall be considered. Figure 37 shows the solution corresponding to Figure 30 but now for a second order model. As expected for a low aspect ratio case, the structure of the wave pattern is rich. One complex and structured cell, positioned in the middle of the lake

Figures 37 - 43

Figure 37a - 43a

Time sequence of the stream function surface in steps of 1/16 T for a second order lake model. The selected parameters are indicated on the individual figures and the lake view and the position of the coordinate system correspond to Figure 27 depending on the aspect ratio.

Figure 37b - 43b

Time sequence of lines of constant ψ relative to 90 % of the maximum value of each time step for a second order lake model.

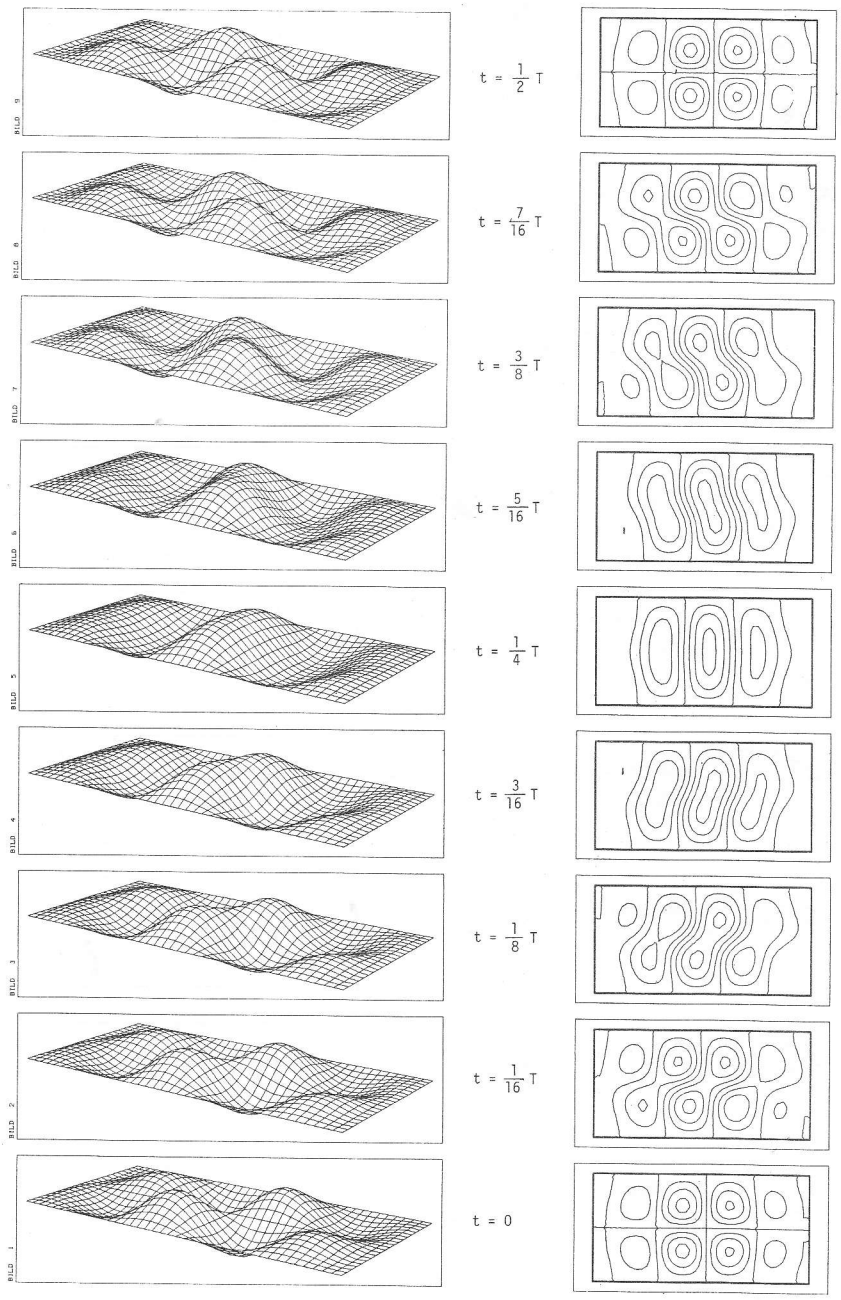

a) b)

Figure 37 N = 2, r = 0,5, ε = 0,05, q = 0,5, ω = 0,335, T = 50,5h

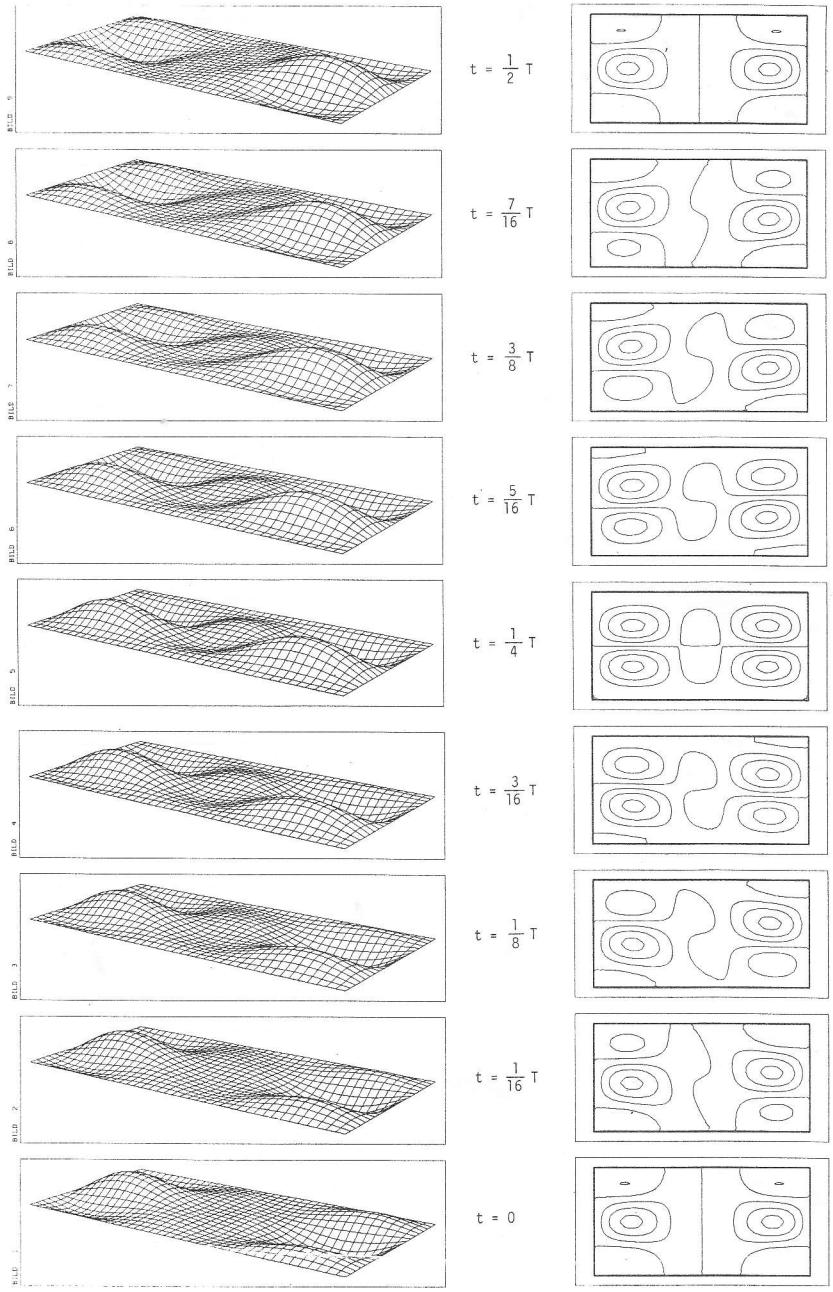

a) b)

Figure 38 N = 2, r = 2.0, ε = 0.05, q = 2.0, ω = 0.234, T = 72.4h

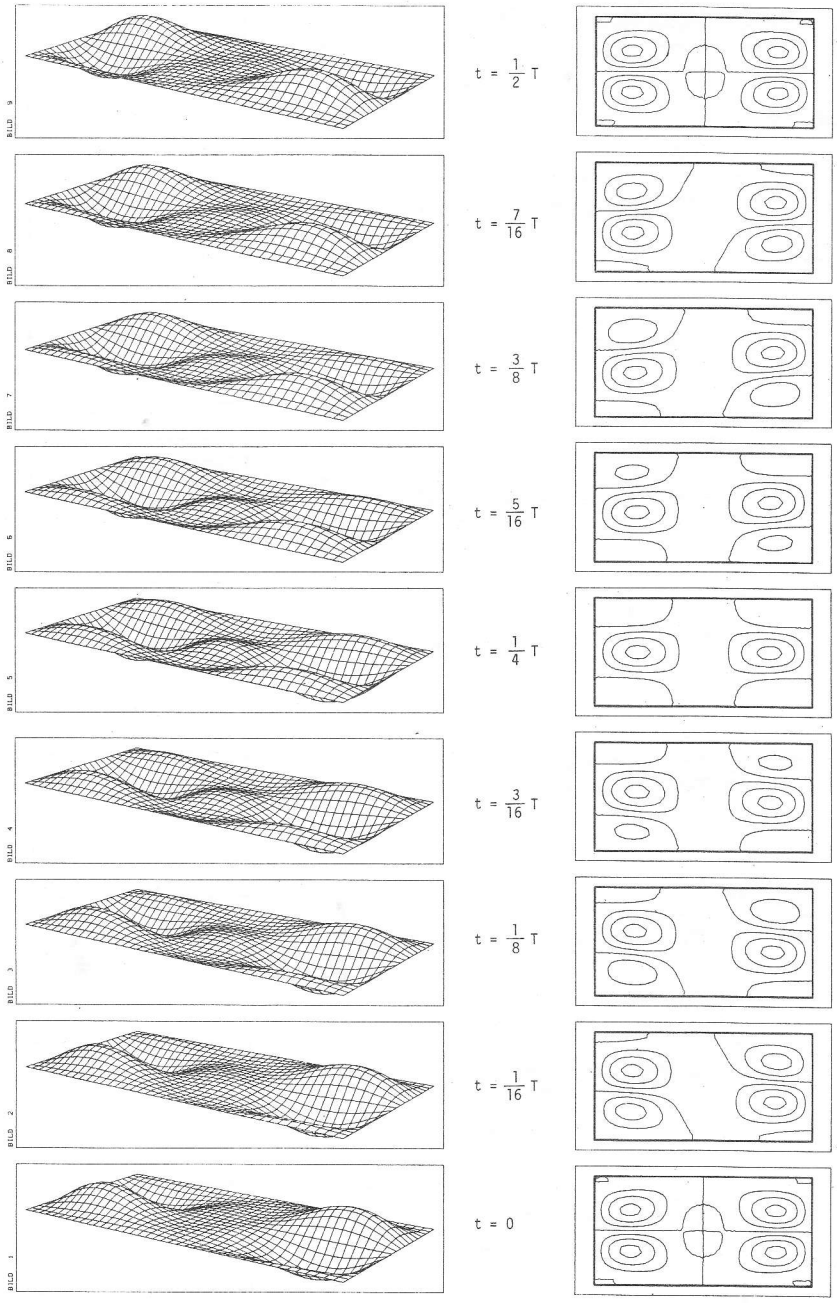

a) b)

Figure 39 N = 2, r = 2.0, ε = 0.05, q = 2.0, ω = 0.233, T = 72.5h

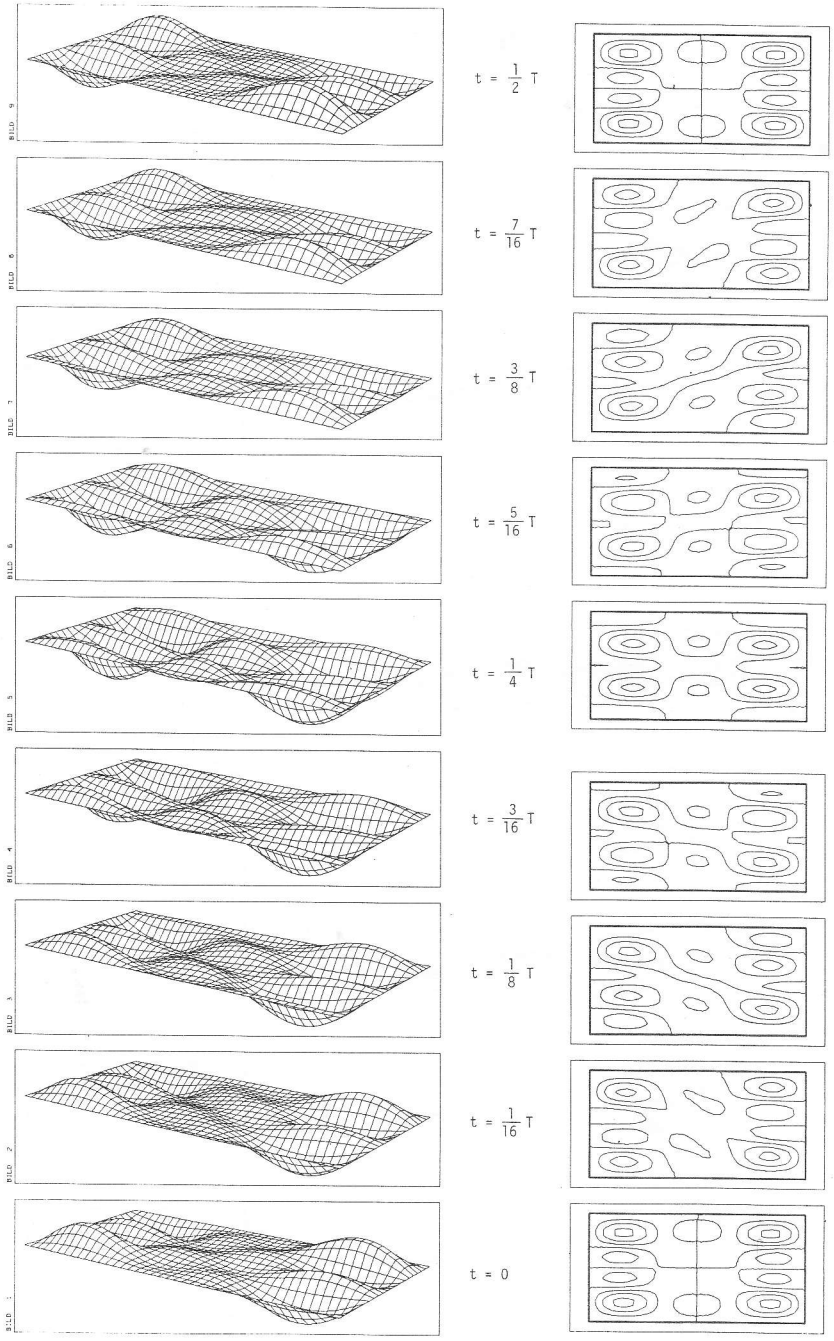

a) b)

Figure 40 N = 2, r = 2,0, ε = 0,05, q = 2,0, ω = 0,185, T = 91,6h

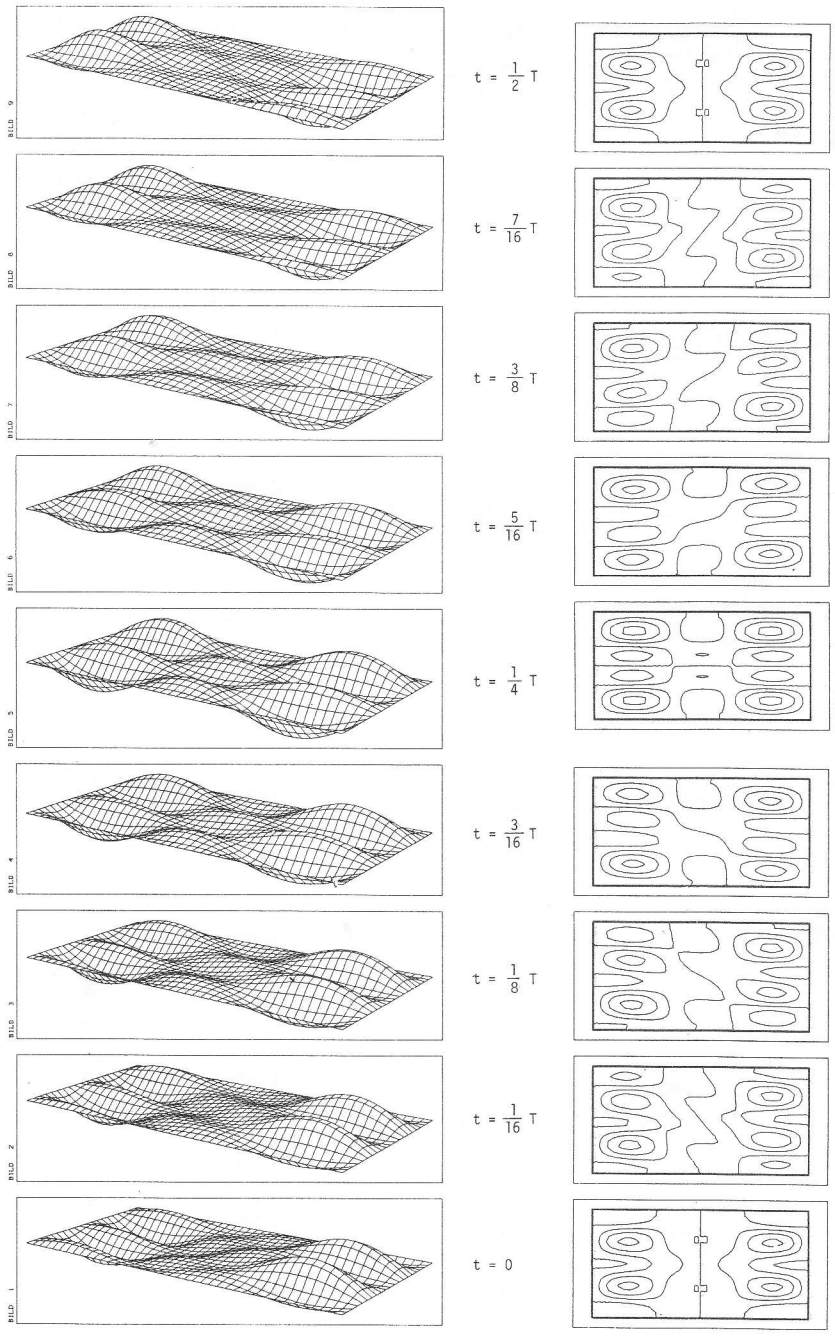

a) b)

Figure 41 N = 2, r = 2,0, ε = 0,05, q = 2,0, ω = 0,184, T = 91,7h

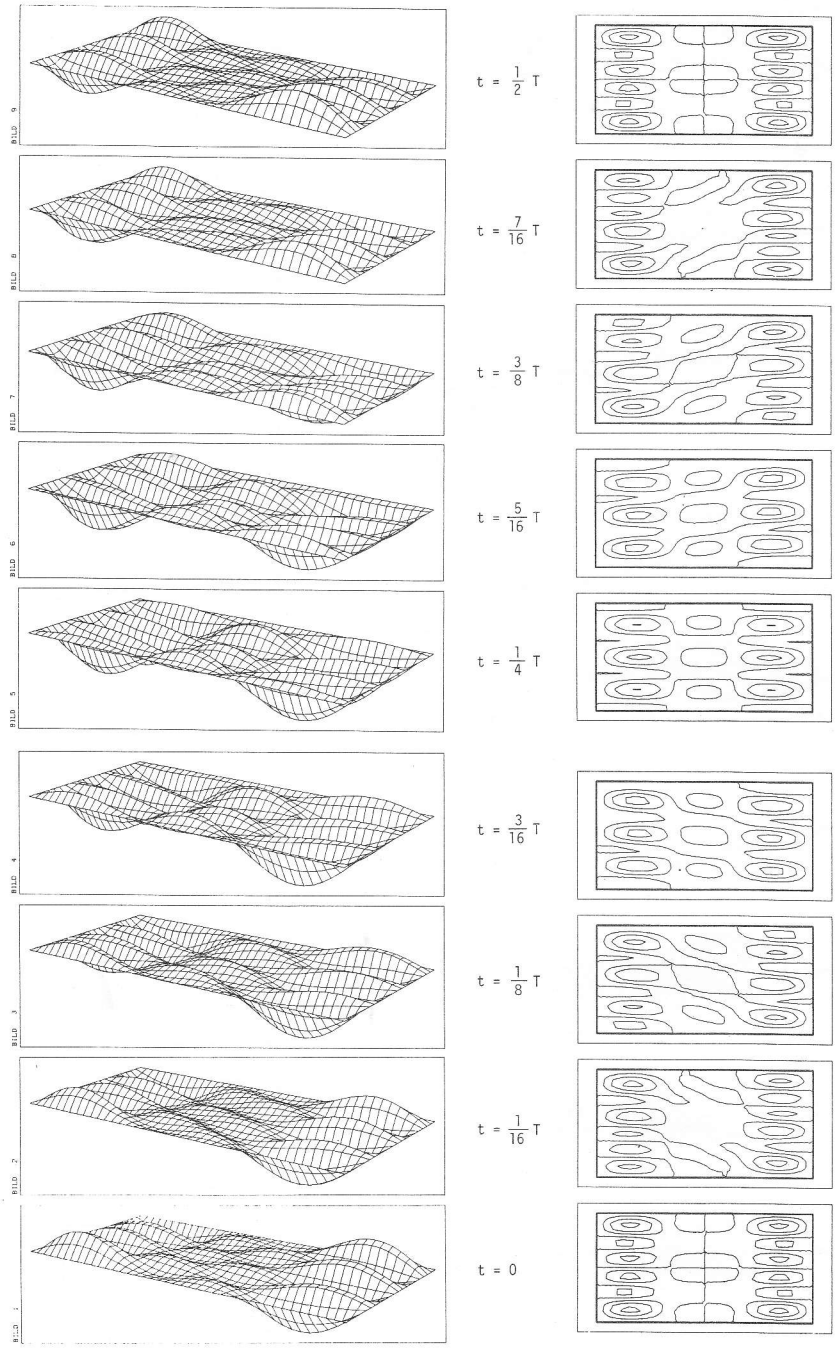

Figure 42 N = 2, r = 2,0, ε = 0,05, q = 2,0, ω = 0,145, T = 116h

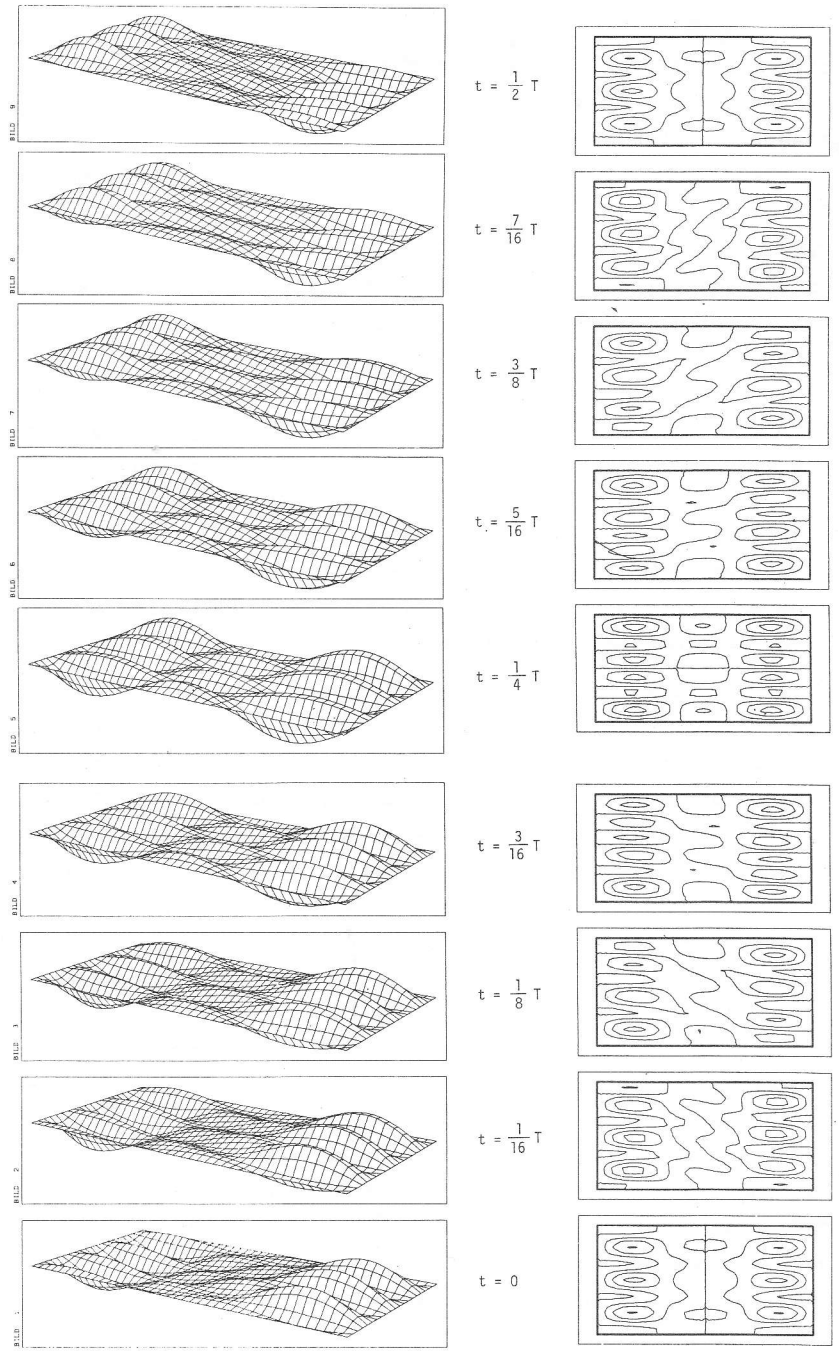

a) b)

Figure 43 N = 2, r = 2,0, ε = 0,05, q = 2,0, ω = 0,144, T = 117h

rotates anticlockwise. The ends of the lake experience little wave motion and are calm. These are the locations where the channel is intersected and no topographic changes occur in the s-direction. Topographic wave motion is therefore expected to be weak.

Comparison of Figure 37 with Figure 30 clearly exhibits the changes that arise when the order of the model is increased for $r < 1$. The graphs of the ψ-surface show that increasing N enhances the wave motion in the center of the lake where the wave activity is concentrated. Simultaneously, stream function amplitudes at the lake ends diminish and larger perturbations move away from the ends of the lake. This suggests that the structures in the middle of the lake in Figure 30a move towards each other to form, eventually, the intensified crests in the center of the lake in Figure 37a. This "centering" seems to be an effect of convergence also because the characteristics of the wave motion is retained.

Turning to Figures 38-43 demonstrates the serious changes which the previously reasonable results of a first order model undergo for the large aspect ratio case $r = 2.0$. Large modifications can be observed when comparing Figure 38 with Figure 31. In a second order model, the pattern which was considered to be intrinsic to topographic waves, i.e. the motion rotating around the lake basin in Figure 31, breaks down. The four pronounced troughs and crests in Figure 31 at $t = 0$ now appear at the lake ends ($n \to \pm \frac{1}{2} B$, for the large aspect ratio case) while the central domain remains calm. This is distinctly different from the low aspect ratio case for which the wave motion seemed to be enhanced in the lake center. This characteristic feature, namely that for $r = 2.0$ the wave motion is torn apart towards the ends of the lake, can be observed for all computed eigenperiods, cf. Figures 38-43, mainly in the contour line pictures. The inner parts of the lake experience for all times and topography parameters q very weak perturbations. The crests and troughs exhibit no counterclockwise rotation around the lake, although an indication of such a ro-

tational sense can still be observed. The crests and troughs at the left end of the lake move still in a right bounded way which can be interpreted as an anticlockwise rotational motion. But because the waves are hindered to propagate *around* the lake they are formed at the long boundary, grow as they move in a right bounded way until they flatten off at the opposite boundary or even in between the two depending on the global modal structure of the lake solution. This process can clearly be observed in Figures 38 and 39.

The higher modes, Figures 40-43, make this modification again evident. The figures (40-43) displaying the ψ-surfaces of the second order model exhibit wave patterns which arise from those of the first order model (33-36) by a "transformation", tearing the waves apart towards the lake's end and leaving the center of the lake without wave perturbations. Apart from this serious effect, which destroys the characteristics of topographic wave motion, the modal structure in the s-direction remains seemingly unaffected.

It has been noticed in section 6.2 that the eigenperiods which lie close to each other move even closer in a second order model, cf. Table 10 and 12. Possibly, this is an effect of convergence such that in the higher order model the former pairs merge to form a single isolated eigenperiod. Inspection of Figures 40b-43b underlines this suggestion. The lake solutions corresponding to paired eigenperiods have globally a similar modal complexity when one of them is regarded to have a time lag of a quarter period relative to the other solution.

Aside from all these phenomenological aspects one is still left with the serious question: Why is it, that this intrinsic feature of topographic wave motion, i.e. a global rotation around the lake, breaks down in a *second* order model?

From a mathematical point of view, a higher order model should be able to describe the physics of a problem more appropriately, because more degrees of freedom are available

and, therefore, the approximate procedure given in equation (3.3), section 3.2, should represent fewer restrictions. This relaxation, by which better results would be expected, seems to be outweighted or rather over compensated by the inaptness of the above made assumptions concerning the basis functions and/or the topography of the basin. From a physical point of view, the breakdown of the global rotation is understandable. The assumption (5.4) with c = 0, which after all is reasonable for infinite channels, is too restrictive; for one of the two mechanisms by which topographic wave motion in lakes is made possible has been seriously affected. What we mean is that isobaths end at the boundaries of the basin, so that a continuous follow-up around the lake is no longer possible.

This defect and the desperating results in Figures 38-43 are, however, not a consequence of the inappropriateness of the *idea* of our method introduced in section 3.2 ff. It is probably rather due to the audacious neglections, which have been made hitherto when modelling the basin topography. A final estimation of the quality of this approximate procedure, i.e. the weighted integration along a selected coordinate, can only be given when more realistic basin topographies are introduced. The fact, that in a first order model reasonable solutions were found is a sign of the possibility that good results can be achieved by the method of Weighted Residuals. A suggestion how the above made assumptions can be refined without incorporating mathematically much more complexity is given in section 7 .

6.8 Comparison with exact solutions

The quality of an approximate method can best be tested when the results are confronted with exact solutions. For this purpose we use the work of Ball (1965), who solved the topographic wave problem for elliptical basins with a paraboloidal topography. Because his work contains only two fundamental modes which are discussed, this comparison is incomplete.

Table 14 lists the periods for the two fundamental modes for various aspect ratios. The topography in our model is parabolic with respect to the n-direction. The eigenperiods of Ball are identical for both r and $\frac{1}{r}$. The large aspect ratio case has been chosen because only in this case our model supplied reasonable results. In agreement with the exact solution, our method brings out periods which are of the same order of

r	Ball solutions		N = 1, ε = 0.05, q = 2.0	
	T_1	T_2	T_1	T_2
1.0	118	84.5	91.7	90.7
2.0	143	97.7	114	109
5.0	282	178	207	200

Table 14
The two eogenperiods in hours, calculated from the non-dimensional frequencies by the scaling $2\pi/f$ = 16.9 h, of the two fundamental modes, see Figure 8 for different aspect ratios. The aspect ratio is meant to be the ratio of the major and the minor axis of Ball's elliptic lake. Those cases are compared which yield qualitatively similar wave solutions.

magnitude and exhibit the same aspect ratio dependence, i.e. increasing periods with increasing aspect ratios. For T_1 our model yields values which are about 25 % too small and for T_2 the values exceed the true periods by about 10 %. This is due to the "pairing" of the eigenfrequencies which draws the approximate values into the gap between the eigenperiods of the two exact fundamental modes. It is likely that this pairing will be cancelled when refined approximations, see section 7, are used.

Figure 44 displays a comparison of the first eigenmode of our model with the corresponding Ball solution. The wave pattern starts with 4 troughs and crests in both solutions. After ⅛ T two diagonal cells have merged, however, in Ball's solution it is the cyclonic cell contrary to our model where the anticyclonic cell intensifies. After a quarter period the exact solution still exhibits three cells, whereas the anti-

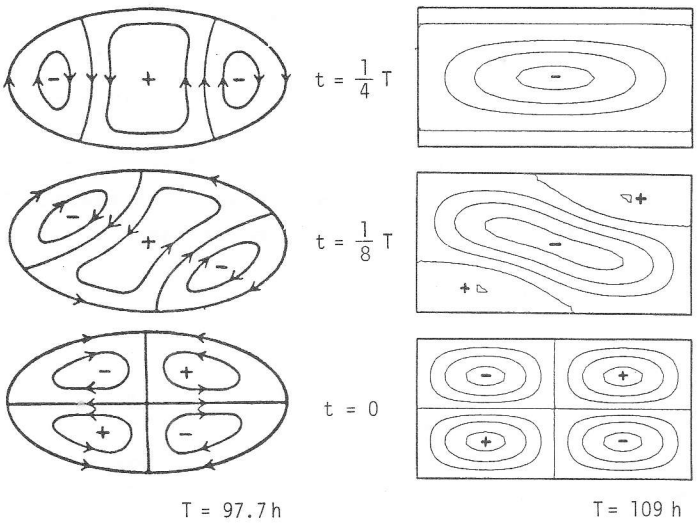

Figure 44
Comparison of the solution of the first eigenperiod in a first order model (identical to Figure 31b) with the "quadratic" mode of Ball.

cyclonic cell in the approximate model continues to increase until the small cyclonic cells die away. The exact solution can be characterized by a clear 4-3-4 modal sequence which is different from the 4-1-4 sequence obtained by our method. The reason for this lies in the order of the selected model. A three cell structure with respect to n as observed in Ball's solution is only possible when selecting $N \geq 2$, cf. P_2^+ in Figure 9.

Figure 45 displays Ball's exact "linear" solution and our corresponding approximate solution. If a time lag of 1/4 T of the approximate solution is taken into account the two solutions exhibit the same wave pattern with good agreement.

These comparisons show that, roughly, our simple model exhibits wave structures which can be well compared with exact solutions. However, there are several pronounced differences such as the intensification of opposite cells or the observed time lag. We tried to make other assumptions about the time

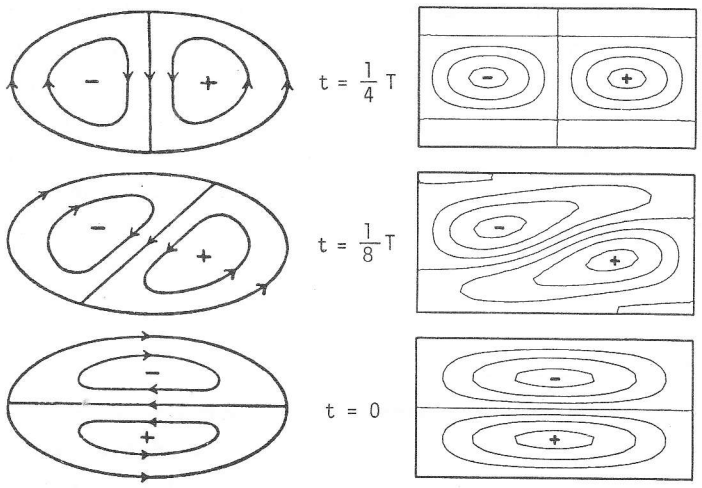

Figure 45

Comparison of the solution of the second eigenperiod in a first order model (identical to Figure 32b) with the "linear" mode of Ball.

dependence introduced in equation (5.1) or taking the imaginary part of (5.13) insted of the real but the approximate solutions maintained the presented structure (Figures 44, 45). We are convinced that all the demonstrated discrepancies between this model and the exact solutions will be considerably diminished when the refinements suggested in the following sections are adopted.

7. MODEL IMPROVEMENTS

The previous sections revealed that our model describes topographic waves satisfactorily in channels, and in lakes provided that aspect ratios are large *and* a *first* order model is taken. However, contrary to the anticipation that the results improve when increasing the order of the model, the results loose their similarity with known exact solutions for both aspect ratio domains $r < 1$ and $r > 1$. The fact, that a first

order model describes -under the assumptions made hitherto the physics of the problem more appropriate than a second order model, suggests the conclusion that the constancy of the topography with respect to s, seems to represent too big a restriction on the physics when taking a *higher* order model, $N \geq 2$. A higher order model, which *per se* describes the problem more accurately, requires refined assumptions, i.e. a better choice of the basis functions (4.17) and/or a more realistic basin topography.

7.1 Other basis functions

From a mathematical standpoint, the approximate procedure introduced in section 3.2 with equation (3.3) makes sense only when the set $\{P_\alpha(s,n)\}$ forms a *complete* set of functions in a given interval $[B^-(s), B^+(s)]$ with respect to n. On the other hand, physical boundary conditions require that the selected set fulfils (3.9). Possible sets have to satisfy these two conditions. Abramowitz and Stegun (1972) give a variety of sets of functions, e.g. Legendre functions, orthogonal polynomials etc., but few of them fulfil boundary conditions of the form (3.9).

The choice, which has been made by taking the set of the trigonometric functions is certainly the simplest and handiest one. A selection of a set of basis functions is a *mathematical* affair and does not much influence the physical response of the system. Taking another set does not mean a change let alone an improvement from a *physical* point of view. Thus, we think that this problem plays a minor role within the framework of this model.

7.2 Refined basin topography

The solutions obtained hitherto suggest that the assumptions on the basin topography made in section 5.1 were too restrictive. Indeed, since the variation of the topography is one of the driving mechanisms of topographic wave motion, cf. Appendix B, any model describing these processes is certainly

expected to be very sensitive to assumptions or rather neglections in the bathymetry, more precisely h(s,n) may need to show variations in both directions. It seems, that (4.3) was generally a good representation of the cross topography of an elongated lake. Through the parameter q a variety of lake cross sections can easily be approximated. However, the simple assumption about the topography in the s-direction, $h_0(s)$ = constant was certainly not adequate *for a lake*. In channels, $h_0(s)$ = constant is a common and reasonable assumption which was made also by Gratton (1983) in his work. In lakes and *closed* basins, however, this assumption, as the results make clear, is a restriction which destroys the characteristics of topographic wave motion. Analytical calculations, Ball (1965) etc., showed that the fundamental modes follow the isobaths of the basin and travel around the lake. Assuming $h_0(s)$ = constant, $\frac{\partial h_0}{\partial s} = 0$ discontinues the isobaths at s = 0, and s = L such that a continuous follow-up around the lake is no longer possible. In a first order model this defect is not felt because fundamental modes are enforced. Evidently, in a second or higher order model a mechanism which would facilitate a turning of the waves at the lake ends is required but absent in the $h_0(s)$ = constant case.

This defect is easily lifted by dropping the assumption $\frac{\partial h_0}{\partial s} = 0$ and allowing variable topographies along the s-direction. However, an arbitrary choice of $h_0(s)$, such as e.g. a polynomial, turns the operator $\underline{\tilde{M}}$ in equation (5.3) into a differential operator, which has coefficients depending on the variable s. Solving the emerging system of differential equations then amounts to solving a standard two point boundary value problem. A possibility to keep the coefficients of $\underline{\tilde{M}}$ constant is sketched in equation (5.4). When selecting for the three subdomains $h_0(s) \sim e^{-\frac{c}{L}s}$ the basin shape is shown in Figure 11. Adopting such a profile recovers an operator $\underline{\tilde{M}}$ with constant coefficients, but equally produces isobaths which form closed lines (however rectangles) around the lake. Because of this less restrictive assumption calculations become mo-

re complicated, but the compact matrix formalism is still useful. As done in section 5.1 and 6.1, we briefly demonstrate the emerging formalism.

In Figure 11 a continuous basin profile is chosen as follows

$$\begin{aligned} h_0^{I}(s) &= \varepsilon h\left(1+\frac{1}{\varepsilon}\right)^{\frac{s}{s_1}}, && 0 \le s \le s_1, \\ h_0^{II}(s) &= h(1+\varepsilon), && s_1 \le s \le s_2, \\ h_0^{III}(s) &= \varepsilon h\left(1+\frac{1}{\varepsilon}\right)^{\frac{L-s}{L-s_2}}, && s_2 \le s \le L. \end{aligned} \tag{7.1}$$

The constant c, introduced in (5.4) then reads for the different basin domains I, II, III

$$\begin{aligned} c^{I} &= -\frac{L}{s_1}\ln\left(1+\frac{1}{\varepsilon}\right), \\ c^{II} &= 0, \qquad c^{III} = \frac{L}{L-s_2}\ln\left(1+\frac{1}{\varepsilon}\right). \end{aligned} \tag{7.2}$$

The matrix elements $C_{\beta\alpha}$ in (5.9) now contain further components because terms proportional to $\frac{\partial h_0}{\partial s}$ must not be neglected. With the aid of (5.3) the matrix elements become

$$\begin{aligned} C_{\beta\alpha} &= \omega\Big((rk)^2\, K^{00++}_{\beta\alpha} + K^{22++}_{\beta\alpha} \\ &\quad - i(rk)(rc)\, K^{00++}_{\beta\alpha}\Big), && \alpha,\beta = 1,\ldots,N \\ C_{\beta\alpha} &= i\,(rk)\,(K^{20-+}_{\beta,\alpha-N} - K^{02-+}_{\beta,\alpha-N}) \\ &\quad + (rc)\, K^{20-+}_{\beta,\alpha-N}, && \begin{matrix}\beta = 1,\ldots,N \\ \alpha = N+1,\ldots,2N\end{matrix} \\ C_{\beta\alpha} &= -\,i(rk)(K^{20+-}_{\beta-N,\alpha} + K^{02+-}_{\beta-N,\alpha}) \\ &\quad - (rc)\, K^{20+-}_{\beta-N,\alpha}, && \begin{matrix}\alpha = 1,\ldots,N \\ \beta = N+1,\ldots,2N\end{matrix} \\ C_{\beta\alpha} &= \omega\Big((rk)^2\, K^{00--}_{\beta-N,\alpha-N} + K^{22--}_{\beta-N,\alpha-N} \\ &\quad - i(rk)(rc)\, K^{00--}_{\beta-N,\alpha-N}\Big), && \alpha,\beta = N+1,\ldots,2N \end{aligned} \tag{7.3}$$

which is identical to (5.9) when selcting c = 0. The dispersion relation is obtained from

$$\det \underline{C}(\omega,k,c) = 0, \qquad (7.4)$$

which now, additionally, depends on c. The five points which are discussed on p. 61 must now be revised under the aspect of $c \neq 0$.

ad 1) The dispersion relation depends on both rk and rc.

ad 2) The coefficients of the emerging polynomial are no longer real, however, there are still 4N roots for a given ω.

ad 3) Cancelled.

ad 4) Cancelled.

ad 5) Still holds.

Equation (7.4) implies that the dispersion relation depends on c, i.e. on the lake domain with respect to the s-direction. Therefore, the set

$$\{k_\gamma\},\ k_\gamma \in \mathbb{C}, \qquad \gamma = 1,\ldots,4N,$$

equally, depends on the selected domain. Henceforth, this will be indicated by a Roman superscript I, II, III. The solutions can now readily be constructed following the procedure given in section 5.1 for the three lake domains:

$$\begin{aligned}
\psi^{I}(s,n,t) &= \sin\omega t\left[\sum_{\alpha=1}^{N} P_\alpha^+(s,n)\cdot\sum_{\gamma=1}^{4N} e^{i\frac{k_\gamma^I}{L}s}\, c_{\alpha\gamma}^I\, d_\gamma^I\right] \\
&\quad +\cos\omega t\left[\sum_{\alpha=N+1}^{2N} P_{\alpha-N}^-(s,n)\cdot\sum_{\gamma=1}^{4N} e^{i\frac{k_\gamma^I}{L}s}\, c_{\alpha\gamma}^I\, d_\gamma^I\right], \qquad 0 \le s \le s_1 \\
\psi^{II}(s,n,t) &= \sin\omega t\left[\sum_{\alpha=1}^{N} P_\alpha^+(s,n)\cdot\sum_{\gamma=1}^{4N} e^{i\frac{k_\gamma^{II}}{L}s}\, c_{\alpha\gamma}^{II}\, d_\gamma^{II}\right] \\
&\quad +\cos\omega t\left[\sum_{\alpha=N+1}^{2N} P_{\alpha-N}^-(s,n)\cdot\sum_{\gamma=1}^{4N} e^{i\frac{k_\gamma^{II}}{L}s}\, c_{\alpha\gamma}^{II}\, d_\gamma^{II}\right], \qquad s_1 \le s \le s_2 \qquad (7.5) \\
\psi^{III}(s,n,t) &= \sin\omega t\left[\sum_{\alpha=1}^{N} P_\alpha^+(s,n)\cdot\sum_{\gamma=1}^{4N} e^{i\frac{k_\gamma^{III}}{L}s}\, c_{\alpha\gamma}^{III}\, d_\gamma^{III}\right] \\
&\quad +\cos\omega t\left[\sum_{\alpha=N+1}^{2N} P_{\alpha-N}^-(s,n)\cdot\sum_{\gamma=1}^{4N} e^{i\frac{k_\gamma^{III}}{L}s}\, c_{\alpha\gamma}^{III}\, d_\gamma^{III}\right]. \qquad s_2 \le s \le L
\end{aligned}$$

The three vectors $\underline{d}^{I}$, $\underline{d}^{II}$, $\underline{d}^{III}$ must now be chosen such that ψ^{I}, ψ^{II}, ψ^{III} is a lake solution, which satisfies the boundary conditions at $s=0$ and $s=L$. Because the lake is subdivided into three domains matching conditions at $s=s_1$ and $s=s_2$ must be fulfilled. The matching conditions are that ψ must be smooth, i.e. continuous and differentiable at the matching points. The conditions then read, cf. section 6.1,

$$
\begin{aligned}
&\psi^{I\alpha}\Big|_0 = 0 \qquad \rightarrow \sum c^{I}_{\alpha\gamma}\, d^{I}_{\gamma} = 0,\\
&\psi^{I\alpha}\Big|_{s_1} = \psi^{II\alpha}\Big|_{s_2} \qquad \rightarrow \sum e^{i\frac{k^{I}_{\gamma}}{L}s_1}\, c^{I}_{\alpha\gamma}\, d^{I}_{\gamma}\\
&\qquad - \sum e^{i\frac{k^{I}_{\gamma}}{L}s_1}\, c^{II}_{\alpha\gamma}\, d^{II}_{\gamma} = 0,\\
&\frac{\partial\psi^{I\alpha}}{\partial s}\Big|_{s_1} = \frac{\partial\psi^{II\alpha}}{\partial s}\Big|_{s_2} \rightarrow \sum i\frac{k^{I}_{\gamma}}{L}\, e^{i\frac{k^{I}_{\gamma}}{L}s_1}\, c^{I}_{\alpha\gamma}\, d^{I}_{\gamma}\\
&\qquad - \sum i\frac{k^{II}_{\gamma}}{L}\, e^{i\frac{k^{II}_{\gamma}}{L}s_1}\, c^{II}_{\alpha\gamma}\, d^{II}_{\gamma} = 0,\\
&\psi^{II\alpha}\Big|_{s_2} = \psi^{III\alpha}\Big|_{s_2} \qquad \rightarrow \sum e^{i\frac{k^{II}_{\gamma}}{L}s_2}\, c^{II}_{\alpha\gamma}\, d^{II}_{\gamma}\\
&\qquad - \sum e^{i\frac{k^{III}_{\gamma}}{L}s_2}\, c^{III}_{\alpha\gamma}\, d^{III}_{\gamma} = 0,\\
&\frac{\partial\psi^{II\alpha}}{\partial s}\Big|_{s_2} = \frac{\partial\psi^{III\alpha}}{\partial s}\Big|_{s_2} \rightarrow \sum i\frac{k^{II}_{\gamma}}{L}\, e^{i\frac{k^{II}_{\gamma}}{L}s_2}\, c^{II}_{\alpha\gamma}\, d^{II}_{\gamma}\\
&\qquad - \sum i\frac{k^{III}_{\gamma}}{L}\, e^{i\frac{k^{III}_{\gamma}}{L}s_2}\, c^{III}_{\alpha\gamma}\, d^{III}_{\gamma} = 0,\\
&\psi^{III\alpha}\Big|_{L} = 0 \qquad \rightarrow \sum e^{ik^{III}_{\gamma}}\, c^{III}_{\alpha\gamma}\, d^{III}_{\gamma} = 0,
\end{aligned}
\tag{7.6}
$$

where $\alpha=1,\ldots,2N$ and summation is meant over $\gamma=1,\ldots,4N$. The

system (7.6) can be written in matrix form

$$E_{\alpha\gamma}\, e_{\gamma} = 0, \qquad \alpha,\gamma = 1,\ldots,12N, \tag{7.7}$$

where $\underline{E}$ is a $(12N \times 12N)$-Matrix which depends on ω and the lake topography parameters q, ε, s_1, s_2 and acts on the vector $\underline{e} = (\underline{d}^{I}, \underline{d}^{II}, \underline{d}^{III})$. A non-trivial eigenvector $\underline{e}$ of (7.7) requires

$$\det \underline{E}(\omega) = 0, \tag{7.8}$$

which is the equation yielding the eigenfrequencies of the given lake. Although, from a numerical point of view calculations become more complex, a vast variety of realistic basin topographies can now be considered. This is shown in Figure 46.

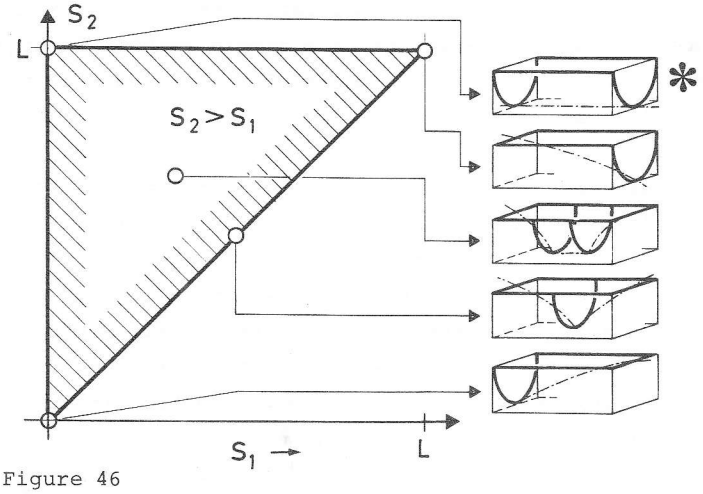

Figure 46

Variety of basin topographies in the parameter space (s_1, s_2) which can be treated after the refinement of the topography assumptions. Up to section 6, in this work only solutions to topographies marked with * were calculated.

A possible continuation of this work will certainly adopt this procedure; it allows the modelling of various basin topographies without having to abandon the compact matrix formulation. It is expected that realistic eigenperiods and solutions are obtained which can be compared with exact solutions for

both aspect ratio ranges. If these results are reasonable this model has made a fair step towards an understanding of topographic wave motion.

8. CONCLUDING REMARKS

8.1 Channel models

The calculations and solutions of topographic waves showed that the Method of Weighted Residuals is a strong tool in solving an inherent two-dimensional boundary value problem. After having established the matrix formalism and determined the matrix elements for a given topography the solution of the differential equation transforms to a simple problem of Linear Algebra. For such problems good and efficient computer software exists which is a further argument for the application of our method.

Although this matrix procedure is approximate and computational efficiency was not evident ab initio satisfactory results are already obtained for models of very low order. Convergence, discussed in section 5.3 is convincing, the reliability and stability of the solutions are clearly exhibited. Furthermore, the method allows examination of a large variety of channel topographies which was not possible hitherto. Gratton (1983) who investigated channels with an analytical method using separation of variables only considered two qualitatively different cross topographies, viz. a weakly linear and quadratic profile. This is a serious restriction on possible configurations that could be treated. By contrast, our method allows for almost *any* transverse topography, i.e. also more complicated cross profiles for instance shoulders or islands etc., could be considered. This only modifies the matrix elements and does not complicate calculations once those are determined. Presently, only Finite Difference techniques are able to cope with the generality of application, which our method offers. These, however, require much more and more

difficult computer work than the method of Weigthed Residuals.

Moreover, Gratton's study is limited to straight channels and is, therefore, not able to investigate the effect of curvature on the topographic wave motion. Channels with a *constant* curvature could however also easily be analyzed with our model, since this again only modifies the matrix elements.

All this demonstrates, that our approximate method opens many possibilities in the investigation of topographic wave motion under a variety of aspects.

8.2 Lake models

The application of the method to lakes brought out clearly, that the quality of the results depends crucially upon the assumptions about the basin topography. Bathymetries, which are unrealistic in that they do not have continuous isobaths, show reasonable solutions in a first order model with special aspect ratios. Overly simplified topographies do not pay. A possible way out of this difficulty is shown in the previous section where topographies varying in both horizontal dimensions are incorporated without a qualitative increase of complexity. As long as the refined method is not tested, however, a final qualification of our model for lake application cannot be given. First order models show reasonable results which can be associated with exact solutions of e.g. Ball (1965).

Our channel method occupies a place between the exact analytical models, such as Lamb (1932), Ball (1965) and Mysak (1983, 1984) on the one hand, and the Finite Difference Methods on the other hand (E. Bäuerle, work under progress). Although our method offers greater flexibility to model the lake basin as the exact models do, it does not require as much computer work as do the FD-calculations. In that sense the method of Weighted Residuals represents an economic way of solving the topographic wave problem.

It is also possible to study boundary effects, such as noses, bays etc.; but in these cases a compact matrix formalism does no longer suffice. The coefficients of the system of differential equations (5.2) then depend on the variable s and a transformation of the form (5.7) into an algebraic system can not be performed. Therefore, a coupled two-point boundary value problem with variable coefficients emerges from (5.2) which has to be solved by iterative numerical methods.

8.3 Computational peculiarities

The evaluation of the eigenfrequencies of a given lake could be done with good accuracy by using equation (6.5). The determinant of $\underline{D}$ depends strongly upon the frequency and a slight change of ω effects large variations of det $\underline{D}$. Adopting the Regula Falsi, the zero, i.e. the eigenfrequency, can therefore be calculated with high accuracy. On the other hand, it is often very difficult to determine the associated eigenvector, the kernel vector $\underline{d}$ because, by the above argument, the numerical system is very stiff, cf. section 6.1. Inaccuracies of the eigenvector $\underline{d}$ turn up with dissatisfactions of the boundary conditions at $s = 0$ and $s = L$. A thorough study of numerical methods could certainly lift this problem.

REFERENCES

Abramowitz, M., Stegun, I.A. 1972. Handbook of Mathematical Functions. Dover Publications, New York.

Ball, F.K. 1965. Second-Class Motions of a Shallow Liquid. J. Fluid Mech., Vol. 23, p. 545 ff.

Bäuerle, E. 1984. Internal free Oscillations in Lake of Geneva. Annales Geophysica (submitted).

Courant, R., Hilbert, D. 1967. Methoden der Mathematischen Physik I und II. Heidelberger Taschenbücher 30, 31. Springer Verlag.

Csanady, G.T. 1976. Topographic waves in Lake Ontario. J. Phys. Oceanogr., Vol. 6., p. 93-103.

Finlayson, B.A. 1972. The Method of Weighted Residuals and Variational Principles. Academic Press, New York.

Graf, W. 1983. Hydrodynamics of the Lake of Geneva. Schweiz. Z. Hydrol., 45/1, 1983.

Gratton, Y. 1983. Low-frequency Vorticity Waves over strong Topography. Ph. D. Thesis, University of British Columbia.

Hamblin, P.F. 1972. Some free oscillations of a rotating natural basin. Ph.D. Thesis, University of Washington.

Holton, J.R. 1979. An Introduction to Dynamical Meteorology, 2nd ed. International Geophysics Series, Vol. 23, p. 165 ff.

Hutter, K. 1983. Strömungsdynamische Untersuchungen im Zürich- und im Luganersee. Schweiz. Z. Hydrol., 45/1, 1983.

Hutter, K. 1984a. Fundamental Equations and Approximations. Hydrodynamics of Lakes, ed by K. Hutter, CISM 286. Springer Verlag.

Hutter, K. 1984b. Linear Gravity Waves. Hydrodynamics of Lakes, ed. by K. Hutter, CISM 286. Springer Verlag.

Hutter, K. 1984c. Mathematische Vorhersage von barotropen und baroklinen Prozessen im Zürich- und Luganersee. Vierteljahresschrift der Natf. Ges., Zürich, 129/1, p. 51 ff.

Lamb, H. 1932. Hydrodynamics. Dover Publications, §§ 193.

LeBlond, P.H., Mysak, L.A. 1978. Waves in the Ocean. Elsevier Oceanography Series, Vol. 20.

Mysak, L.A. 1983. Elliptical Topographic Waves. Geophys. Astrophys. Fluid Dyn. (submitted).

Mysak, L.A. 1984. Topographic Waves in Lakes. Hydrodynamics of Lakes, ed. by K. Hutter, CISM 286. Springer Verlag.

Mysak, L.A., Salvadè, G., Hutter, K., Scheiwiller, T. 1983. Lake of Lugano and topographic waves. Nature, Vol. 306, pp. 46-48.

Mysak, L.A., Salvadè, G., Hutter, K., Scheiwiller, T. 1984. Topographic waves in an elliptical basin, with application to the Lake of Lugano. Phil Trans. R. Soc., London (in press).

Pearson, C.E. 1974. Handbook of Applied Mathematics. VNR Company, p. 139 ff.

Pedlosky, J. 1979. Geophysical Fluid Dynamics. Springer Verlag.

Poincaré, H. 1910. Leçons de méchanique céleste. Gauthier-Villars, Paris.

Simons, T.J. 1975. Verification of numerical models of Lake Ontario: II Stratified circulation and temperature changes. J. Phys. Oceanogr., Vol. 5, p. 98-110.

Saylor, J.H., Huang, C.K., Reid, R.O. 1980. Vortex Modes in Southern Lake Michigan. J. Phys. Oceanogr., Vol. 10, p. 1814 ff.

APPENDIX

Appendix A : Necessary conditions for topographic wave motion

Appendix B : Symmetric wave motion

Appendix C : Topographic waves and Rossby waves

Appendix D : A mechanical analogy for topographic wave motion

Appendix E : Numerical calculation of the matrix elements up to fourth order

APPENDIX A: Necessary conditions for topographic wave motion

Topographic wave motion requires two necessary conditions, which must be fulfilled:

1. The system, in which topographic waves are sustained, must be in rotation. Therefore the Coriolis parameter f must differ from 0, $f \neq 0$.

2. The basin must have a gradient of topography, $\nabla H \neq 0$. To prove this statement we start from the homogeneous part of equation (2.6) and the boundary condition (2.20)

$$\begin{aligned} \nabla\cdot(H^{-1}\nabla\frac{\partial}{\partial t}\psi) + f(\nabla\psi\times\nabla H^{-1})\cdot\underline{\hat{z}} &= 0, \quad \text{in } \mathcal{D} \\ \psi &= 0, \quad \text{on } \partial\mathcal{D}. \end{aligned} \tag{A.1}$$

Unless both conditions above are fulfilled, (A.1) reduces to

$$\begin{aligned} \nabla^2\frac{\partial}{\partial t}\psi &= 0, \quad \text{in } \mathcal{D} \\ \psi &= 0, \quad \text{on } \partial\mathcal{D}. \end{aligned} \tag{A.2}$$

Assuming a harmonic time dependence of the form $\exp(i\omega t)$ with $\omega \neq 0$, (A.2) reduces to the potential problem

$$\begin{aligned} \nabla^2\tilde{\psi} &= 0, \quad \text{in } \mathcal{D} \\ \tilde{\psi} &= 0, \quad \text{on } \partial\mathcal{D} \end{aligned}$$

which, invoking the Maximum Principle, admits only the trivial solution $\tilde{\psi} = 0$ in $\mathcal{D}$. Therefore, if either $f = 0$ or $\nabla H = 0$, the stream function is trivial and there is no wave motion governed by equation (A.1) in the system.

APPENDIX B: Symmetric wave motion

In this appendix a proof will be given, that the governing equations (2.16) do not allow solutions that retain their symmetry for all times. Starting from (4.16) and using the boundary condition (2.20) yields (+ subscript is dropped)

$$\begin{aligned} i\omega\, \nabla\cdot(h^{-1}\,\nabla\psi) &= 0, \quad \text{on } \mathcal{D} \\ \hat{\underline{z}}\cdot(\nabla\psi\times\nabla h^{-1}) &= 0, \quad \text{on } \mathcal{D} \\ \psi &= 0, \quad \text{on } \partial\mathcal{D} \end{aligned} \tag{B.1}$$

where no quantity depends on the vertical coordinate z. It is claimed, that for $\omega \neq 0$, equations (B.1) permit only the trivial solution. To this end, consider the vector identity

$$\hat{\underline{z}}\cdot(\nabla\psi\times\nabla h^{-1}) = -\,\hat{\underline{z}}\cdot\nabla\times h^{-1}\nabla\psi, \tag{B.2}$$

which implies the existence of a scalar field $\phi(x,y)$ such that

$$\underline{u} = \nabla\phi. \tag{B.3}$$

With the definition

$$\underline{u} := h^{-1}\nabla\psi, \tag{B.4}$$

then, the system (B.1) reduces to the compact form

$$i\omega\,\nabla^2\phi = 0. \quad \text{in } \mathcal{D} \tag{B.5}$$

Along the boundary we have from (B.4)

$$\underline{u}\cdot\hat{\underline{\ell}} = h^{-1}\,\nabla\psi\cdot\hat{\underline{\ell}} = h^{-1}\,\frac{\partial\psi}{\partial\ell}, \tag{B.6}$$

where $\hat{\underline{\ell}}$ is the unit vector tangential to the boundary. $(B.1)_3$ states, that ψ does not change on $\partial\mathcal{D}$, and therefore, provided $h \neq 0$ on $\partial\mathcal{D}$

$$\underline{u}\cdot\hat{\underline{\ell}} = 0, \quad \text{on } \partial\mathcal{D}, \tag{B.7}$$

Accordingly, by (B.3), it follows that

$$0 = \nabla\phi\cdot\hat{\underline{\ell}} = \frac{\partial\phi}{\partial\ell}, \quad \text{on } \partial\mathcal{D}, \tag{B.8}$$

which implies, that ϕ is a constant along $\partial\mathcal{D}$. Thus (B.1) takes on the form

$$\begin{aligned} i\omega\nabla^2\phi &= 0, \quad \text{in } \mathcal{D} \\ \phi &= \phi_0, \quad \text{on } \partial\mathcal{D} \end{aligned} \tag{B.9}$$

which, by $\tilde{\phi} := \phi - \phi_0$, transforms to the boundary value problem

$$\begin{aligned} i\omega \nabla^2 \tilde{\phi} &= 0, \quad \text{in } \mathcal{D} \\ \tilde{\phi} &= 0. \quad \text{on } \partial\mathcal{D} \end{aligned} \tag{B.10}$$

Invoking the Maximum Principle, this implies straightforwardly

$$\tilde{\phi} \equiv 0, \quad \text{in } \mathcal{D} \tag{B.11}$$

if $\omega \neq 0$. Therefore, the stream function ψ can only be a constant within the domain, which is the trivial solution for (B.1). Allowing non-trivial stream functions ψ, on the other hand, implies $\omega = 0$, which shows, that this would not be a solution representing a wave. Thus, any wave solution of (2.16) or (3.21) must necessarily be a composition of symmetric and skew-symmetric parts.

APPENDIX C: Topographic waves and Rossby waves

In order to work out the interrelationship between atmospheric Rossby waves (Pedlosky, 1979, p. 108ff) and topographic waves in channels and lakes, we start from

$$\nabla \cdot \frac{\nabla \frac{\partial}{\partial t} \psi}{H} + \hat{\underline{z}} \cdot (\nabla \psi \times \nabla \frac{f}{H}) = 0, \tag{C.1}$$

which is the nonscaled more general form of the homogeneous part of (2.16), see Hutter (1984a, p. 28).

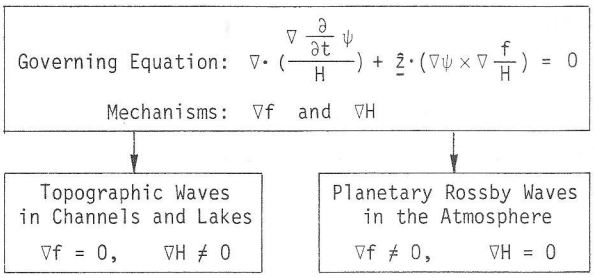

Figure C1
The different wave phenomena that are governed by equation (C.1).

At mid-latitude, calculations are performed on a β-plane. This means that spherical effects are accounted for with a linear increase of the Coriolis parameter f to the north. Selecting a coordinate system, whose x-axis points to the east and y-axis to the north, then

$$\nabla f = (0, \frac{\partial f}{\partial y}, 0) = (0, \beta, 0). \qquad (C.2)$$

(C.1) is the equation which yields the topographic waves when assuming $\nabla f = 0$ and $\nabla H \neq 0$. On the other hand let ψ have a wave like structure

$$\psi = e^{i(\omega t - kx - \ell y)}, \qquad (C.3)$$

and assume an atmosphere with constant depth H (no orography), then (C.1) yields the well-known dispersion relation

$$\omega = - \frac{\beta k}{k^2 + \ell^2}. \qquad (C.4)$$

This is the dispersion relation of planetary Rossby waves in an aptmosphere at rest (Pedlosky, 1979, p. 109). Therefore, we have demonstrated the alliance between those two wave phenomena. In an atmosphere with strong orography, e.g. in the Alps, it might be likely to observe waves which have both, topographic and Rossby wave character.

APPENDIX D: A mechanical analogy for topographic wave motion

The mechanism of topographic or second class wave motion is the conservation of angular momentum, when a fluid column changes its position in a basin with topography. To understand this, consider the simple model sketched in Figure D1. The water column is assumed to be a rigid body rotating around its vertical axis with an angular velocity which in the two respective positions is Ω_1 and Ω_2.

The angular velocity which column 1 will take on when it is transported to position 2 can be calculated when the conserva-

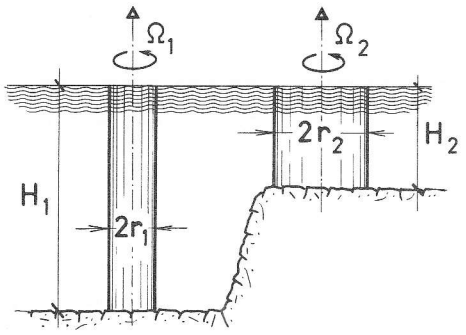

Figure D1

A mechanical analogy of the mechanism of topographic wave motion.

tion laws of mass and angular momentum are applied. Balance of mass in the columns requires

$$r_1^2 H_1 = r_2^2 H_2, \tag{D.1}$$

and conservation of angular momentum yields

$$\frac{1}{2} m_1 r_1^2 \Omega_1 = \frac{1}{2} m_2 r_2^2 \Omega_2. \tag{D.2}$$

Equations (D.1) and (D.2) are satisfied provided the quantity $\frac{\Omega}{H}$ following the fluid motion remains constant:

$$\frac{\Omega}{H} = \text{constant}. \tag{D.3}$$

Because the vertical component of the absolute vorticity of rigid body motion is twice the *total* angular velocity, (D.3), on a rotating earth, is identical to

$$\frac{\omega_z + f}{H} = \text{constant}, \tag{D.4}$$

where ω_z is the vertical component of relative vorticity and f the Coriolis parameter. This quantity must therefore be conserved when one follows the fluid motion, implying that (D.4) takes on the well-known form

$$\frac{d}{dt}\left(\frac{\omega_z + f}{H}\right) = 0, \tag{D.5}$$

which is the conservation law of barotropic potential vorticity. The operator $\frac{d}{dt}$ is the convective derivative operator

$$\frac{d}{dt} = \frac{\partial}{\partial t} + \underline{u} \cdot \nabla,$$

in which $\underline{u}$ is the fluid velocity.

Equation (D.5) can be transformed into an equation for the barotropic or mass transport stream function ψ given by

$$\psi_y = -Hu,$$
$$\psi_x = Hv.$$

These last equations satisfy the continuity equation under the rigid lid assumption. In terms of ψ the vertical component of the relative vorticity reads

$$\omega_z = \frac{\partial v}{\partial x} - \frac{\partial u}{\partial y} = \nabla \cdot \frac{1}{H} \nabla \psi .$$

In a two-dimensional barotropic model (D.5) then becomes

$$\frac{1}{H} \frac{\partial}{\partial t} \nabla \cdot \frac{1}{H} \nabla \psi - \frac{1}{H} \frac{\partial \psi}{\partial y} \frac{\partial}{\partial x} \left(\frac{f}{H}\right) + \frac{1}{H} \frac{\partial \psi}{\partial x} \frac{\partial}{\partial y} \left(\frac{f}{H}\right) = 0, \qquad (D.6)$$

here, non-linear terms have been ignored and f and H have been assumed to be time-independent. Equation (D.6) can be written in the compact vector form

$$\frac{\partial}{\partial t} \left(\nabla \cdot \frac{1}{H} \nabla \psi\right) + \hat{\underline{z}} \cdot \left(\nabla \psi \times \nabla \frac{f}{H}\right) = 0, \qquad (D.7)$$

which describes both planetary Rossby waves and topographic waves in lake basins, see Appendix C. Equation (D.7) is a special case of equation (2.6) containing the rigid lid assumption and no wind forcing, from which we started our study. Therefore, it is demonstrated that the fundamental mechanism of second class wave motion consists in the conservation of angular momentum.

APPENDIX E: Numerical calculation of the matrix elements up to fourth order

In this Appendix the constant part of the matrix elements (4.31) $M^{ij\cdot\cdot}_{\beta\alpha}$, i.e. $K^{ij\cdot\cdot}_{\beta\alpha}$ in section 5.1, are listed up to the fourth order, thus $\alpha, \beta = 1,\ldots,4$. They are calculated on a computer using the IMSL-library with a relative accuracy of 10^{-6}.

$\varepsilon = 0{,}05 \qquad q = 0{,}5$

$$K^{00++} = \begin{bmatrix} .11059E+01 & -.55575E+00 & .14451E+00 & -.13062E+00 \\ -.55575E+00 & .18062E+01 & -.83089E+00 & .32483E+00 \\ .14451E+00 & -.83089E+00 & .19865E+01 & -.93633E+00 \\ -.13062E+00 & .32483E+00 & -.93633E+00 & .20648E+01 \end{bmatrix}$$

$$K^{00--} = \begin{bmatrix} .16617E+01 & -.70026E+00 & .27514E+00 & -.18032E+00 \\ -.70026E+00 & .19368E+01 & -.88058E+00 & .38058E+00 \\ .27514E+00 & -.88058E+00 & .20422E+01 & -.95891E+00 \\ -.18032E+00 & .38058E+00 & -.95891E+00 & .20946E+01 \end{bmatrix}$$

$$K^{10++} = \begin{bmatrix} .11047E+01 & .26152E-01 & -.82213E+00 & .81687E+00 \\ -.22008E+01 & .27948E+01 & .14492E+01 & -.26762E+01 \\ .20276E+01 & -.57589E+01 & .35686E+01 & .32763E+01 \\ -.17465E+01 & .54292E+01 & -.87072E+01 & .39995E+01 \end{bmatrix}$$

$$K^{10--} = \begin{bmatrix} .21921E+01 & .69257E+00 & -.16867E+01 & .17431E+01 \\ -.40727E+01 & .32596E+01 & .23462E+01 & -.36746E+01 \\ .38219E+01 & -.72738E+01 & .38202E+01 & .42671E+01 \\ -.32906E+01 & .69309E+01 & -.10057E+02 & .41518E+01 \end{bmatrix}$$

$$K^{01++} = \begin{bmatrix} .11047E+01 & -.22008E+01 & .20276E+01 & -.17465E+01 \\ .26152E-01 & .27948E+01 & -.57589E+01 & .54292E+01 \\ -.82213E+00 & .14492E+01 & .35686E+01 & -.87072E+01 \\ .81687E+00 & -.26762E+01 & .32763E+01 & .39995E+01 \end{bmatrix}$$

$$K^{01--} = \begin{bmatrix} .21921E+01 & -.40727E+01 & .38219E+01 & -.32906E+01 \\ .69257E+00 & .32596E+01 & -.72738E+01 & .69309E+01 \\ -.16867E+01 & .23462E+01 & .38202E+01 & -.10057E+02 \\ .17431E+01 & -.36746E+01 & .42671E+01 & .41518E+01 \end{bmatrix}$$

$$K^{20+-} = \begin{bmatrix} -.55809E+01 & -.17377E+01 & .49178E+01 & -.40035E+01 \\ .50016E+01 & -.13792E+02 & -.57558E+01 & .10211E+02 \\ -.40181E+01 & .13289E+02 & -.20611E+02 & -.10441E+02 \\ .34462E+01 & -.10629E+02 & .20447E+02 & -.26847E+02 \end{bmatrix}$$

$$K^{20-+} = \begin{bmatrix} -.30646E+00 & -.29299E+01 & .15065E+01 & -.25667E+01 \\ .95968E+01 & .33213E+01 & -.78264E+01 & .58102E+01 \\ -.95011E+01 & .17106E+02 & .78331E+01 & -.13158E+02 \\ .73945E+01 & -.17101E+02 & .23617E+02 & .12738E+02 \end{bmatrix}$$

$$K^{02+-} = \begin{bmatrix} -.30646E+00 & .96968E+01 & -.95011E+01 & .73945E+01 \\ -.29299E+01 & .33213E+01 & .17106E+02 & -.17101E+02 \\ .15065E+01 & -.78264E+01 & .78331E+01 & .23617E+02 \\ -.25667E+01 & .58102E+01 & -.13158E+02 & .12738E+02 \end{bmatrix}$$

$$K^{02-+} = \begin{bmatrix} -.55809E+01 & .50016E+01 & -.40181E+01 & .34462E+01 \\ -.17377E+01 & -.13792E+02 & .13289E+02 & -.10629E+02 \\ .49178E+01 & -.57558E+01 & -.20611E+02 & .20447E+02 \\ -.40035E+01 & .10211E+02 & -.10441E+02 & -.26847E+02 \end{bmatrix}$$

$$K^{11++} = \begin{bmatrix} .56452E+01 & -.12418E+02 & .13433E+02 & -.13054E+02 \\ -.12418E+02 & .37731E+02 & -.49766E+02 & .46232E+02 \\ .13433E+02 & -.49766E+02 & .92681E+02 & -.10501E+03 \\ -.13054E+02 & .46232E+02 & -.10501E+03 & .17094E+03 \end{bmatrix}$$

$$K^{11--} = \begin{bmatrix} .18875E+02 & -.28904E+02 & .28697E+02 & -.26800E+02 \\ -.28904E+02 & .62353E+02 & -.75069E+02 & .66369E+02 \\ .28697E+02 & -.75069E+02 & .12887E+03 & -.13964E+03 \\ -.26800E+02 & .66369E+02 & -.13964E+03 & .21899E+03 \end{bmatrix}$$

$$K^{22++} = \begin{bmatrix} .32447E+02 & -.48142E+02 & .45680E+02 & -.44944E+02 \\ -.48142E+02 & .22982E+03 & -.19998E+03 & .15448E+03 \\ .45680E+02 & -.19998E+03 & .59391E+03 & -.43019E+03 \\ -.44944E+02 & .15448E+03 & -.43019E+03 & .11262E+04 \end{bmatrix}$$

$$K^{22--} = \begin{bmatrix} .10785E+03 & -.11697E+03 & .94163E+02 & -.94882E+02 \\ -.11697E+03 & .38795E+03 & -.30819E+03 & .21780E+03 \\ .94163E+02 & -.30819E+03 & .83542E+03 & -.57928E+03 \\ -.94882E+02 & .21780E+03 & -.57928E+03 & .14521E+04 \end{bmatrix}$$

$$K^{12+-} = \begin{bmatrix} -.22123E+02 & .56981E+02 & -.57120E+02 & .51648E+02 \\ .25712E+02 & -.10537E+03 & .16645E+03 & -.13920E+03 \\ -.24884E+02 & .94567E+02 & -.24121E+03 & .32911E+03 \\ .23785E+02 & -.81763E+02 & .19068E+03 & -.43088E+03 \end{bmatrix}$$

$$K^{12-+} = \begin{bmatrix} -.22123E+02 & .25712E+02 & -.24884E+02 & .23785E+02 \\ .56981E+02 & -.10537E+03 & .94567E+02 & -.81763E+02 \\ -.57120E+02 & .16645E+03 & -.24121E+03 & .19068E+03 \\ .51648E+02 & -.13920E+03 & .32911E+03 & -.43088E+03 \end{bmatrix}$$

$\varepsilon = 0.05 \qquad q = 1.0$

$$K^{00++} = \begin{bmatrix} .74550E+00 & -.30487E+00 & .11361E+00 & -.86321E-01 \\ -.30487E+00 & .11640E+01 & -.50480E+00 & .24861E+00 \\ .11361E+00 & -.50480E+00 & .12990E+01 & -.59488E+00 \\ -.86321E-01 & .24861E+00 & -.59488E+00 & .13670E+01 \end{bmatrix}$$

$$K^{00--} = \begin{bmatrix} .10504E+01 & -.41848E+00 & .19993E+00 & -.13500E+00 \\ -.41848E+00 & .12503E+01 & -.55347E+00 & .29001E+00 \\ .19993E+00 & -.55347E+00 & .13404E+01 & -.62149E+00 \\ -.13500E+00 & .29001E+00 & -.62149E+00 & .13909E+01 \end{bmatrix}$$

$$K^{10++} = \begin{bmatrix} .70922E+00 & -.95967E-02 & -.35640E+00 & .40323E+00 \\ -.14216E+01 & .19234E+01 & .62843E+00 & -.12690E+01 \\ .13535E+01 & -.38782E+01 & .26556E+01 & .15495E+01 \\ -.12247E+01 & .37306E+01 & -.59853E+01 & .31494E+01 \end{bmatrix}$$

$$K^{10--} = \begin{bmatrix} .14248E+01 & .27233E+00 & -.77331E+00 & .88008E+00 \\ -.27007E+01 & .23341E+01 & .10685E+01 & -.17965E+01 \\ .25919E+01 & -.49614E+01 & .29271E+01 & .20744E+01 \\ -.23445E+01 & .48011E+01 & -.69548E+01 & .33409E+01 \end{bmatrix}$$

$$K^{01++} = \begin{bmatrix} .70922E+00 & -.14216E+01 & .13535E+01 & -.12247E+01 \\ -.95967E-02 & .19234E+01 & -.38782E+01 & .37306E+01 \\ -.35640E+00 & .62843E+00 & .26556E+01 & -.59853E+01 \\ .40323E+00 & -.12690E+01 & .15495E+01 & .31494E+01 \end{bmatrix}$$

$$K^{01--} = \begin{bmatrix} .14248E+01 & -.27007E+01 & .25919E+01 & -.23445E+01 \\ .27233E+00 & .23341E+01 & -.49614E+01 & .48011E+01 \\ -.77331E+00 & .10685E+01 & .29271E+01 & -.69548E+01 \\ .88008E+00 & -.17965E+01 & .20744E+01 & .33409E+01 \end{bmatrix}$$

$$K^{20+-} = \begin{bmatrix} -.35706E+01 & -.10327E+01 & .22932E+01 & -.20788E+01 \\ .32264E+01 & -.93358E+01 & -.32060E+01 & .49767E+01 \\ -.27677E+01 & .87881E+01 & -.14298E+02 & -.58646E+01 \\ .24707E+01 & -.75462E+01 & .13664E+02 & -.18834E+02 \end{bmatrix}$$

$$K^{20-+} = \begin{bmatrix} .56402E-01 & -.12641E+01 & .85571E+00 & -.12349E+01 \\ .65091E+01 & .19474E+01 & -.36780E+01 & .31595E+01 \\ -.61675E+01 & .11830E+02 & .44350E+01 & -.64768E+01 \\ .52267E+01 & -.11326E+02 & .16566E+02 & .72655E+01 \end{bmatrix}$$

$$K^{02+-} = \begin{bmatrix} .56402E-01 & .65091E+01 & -.61675E+01 & .52267E+01 \\ -.12641E+01 & .19474E+01 & .11830E+02 & -.11326E+02 \\ .85571E+00 & -.36780E+01 & .44350E+01 & .16566E+02 \\ -.12349E+01 & .31595E+01 & -.64768E+01 & .72655E+01 \end{bmatrix}$$

$$K^{02-+} = \begin{bmatrix} -.35706E+01 & .32264E+01 & -.27677E+01 & .24707E+01 \\ -.10327E+01 & -.93358E+01 & .87881E+01 & -.75462E+01 \\ .22932E+01 & -.32060E+01 & -.14298E+02 & .13664E+02 \\ -.20788E+01 & .49767E+01 & -.58646E+01 & -.18834E+02 \end{bmatrix}$$

$$K^{11++} = \begin{bmatrix} .40918E+01 & -.94403E+01 & .11153E+02 & -.11807E+02 \\ -.94403E+01 & .28581E+02 & -.39043E+02 & .39504E+02 \\ .11153E+02 & -.39043E+02 & .70655E+02 & -.82524E+02 \\ -.11807E+02 & .39504E+02 & -.82524E+02 & .12966E+03 \end{bmatrix}$$

$$K^{11--} = \begin{bmatrix} .14050E+02 & -.22479E+02 & .24283E+02 & -.24709E+02 \\ -.22479E+02 & .47498E+02 & -.59051E+02 & .56912E+02 \\ .24283E+02 & -.59051E+02 & .98049E+02 & -.10946E+03 \\ -.24709E+02 & .56912E+02 & -.10946E+03 & .16551E+03 \end{bmatrix}$$

$$K^{22++} = \begin{bmatrix} .22690E+02 & -.36972E+02 & .40968E+02 & -.43543E+02 \\ -.36972E+02 & .16704E+03 & -.15526E+03 & .14409E+03 \\ .40968E+02 & -.15526E+03 & .43070E+03 & -.33115E+03 \\ -.43543E+02 & .14409E+03 & -.33115E+03 & .81128E+03 \end{bmatrix}$$

$$K^{22--} = \begin{bmatrix} .78726E+02 & -.89620E+02 & .88100E+02 & -.91840E+02 \\ -.89620E+02 & .28333E+03 & -.23688E+03 & .20648E+03 \\ .88100E+02 & -.23688E+03 & .60549E+03 & -.44155E+03 \\ -.91840E+02 & .20648E+03 & -.44155E+03 & .10445E+04 \end{bmatrix}$$

$$K^{12+-} = \begin{bmatrix} -.16124E+02 & .42665E+02 & -.46708E+02 & .47357E+02 \\ .20690E+02 & -.79308E+02 & .12544E+03 & -.11490E+03 \\ -.22317E+02 & .78009E+02 & -.18125E+03 & .24650E+03 \\ .23047E+02 & -.75655E+02 & .15723E+03 & -.32138E+03 \end{bmatrix}$$

$$K^{12-+} = \begin{bmatrix} -.16124E+02 & .20690E+02 & -.22317E+02 & .23047E+02 \\ .42665E+02 & -.79308E+02 & .78009E+02 & -.75655E+02 \\ -.46708E+02 & .12544E+03 & -.18125E+03 & .15723E+03 \\ .47357E+02 & -.11490E+03 & .24650E+03 & -.32138E+03 \end{bmatrix}$$

$\varepsilon = 0{,}05 \qquad q = 2{,}0$

$$K^{00++} = \begin{bmatrix} .57045E+00 & -.14127E+00 & .76439E-01 & -.49958E-01 \\ -.14127E+00 & .78816E+00 & -.26767E+00 & .16220E+00 \\ .76439E-01 & -.26767E+00 & .87392E+00 & -.33059E+00 \\ -.49958E-01 & .16220E+00 & -.33059E+00 & .92236E+00 \end{bmatrix}$$

$$K^{00--} = \begin{bmatrix} .71172E+00 & -.21771E+00 & .12640E+00 & -.85759E-01 \\ -.21771E+00 & .83812E+00 & -.30347E+00 & .18932E+00 \\ .12640E+00 & -.30347E+00 & .90104E+00 & -.35191E+00 \\ -.85759E-01 & .18932E+00 & -.35191E+00 & .93960E+00 \end{bmatrix}$$

$$K^{10++} = \begin{bmatrix} .46508E+00 & .74064E-01 & -.15149E+00 & .19250E+00 \\ -.90548E+00 & .12303E+01 & .41243E+00 & -.57411E+00 \\ .85049E+00 & -.25430E+01 & .17919E+01 & .89627E+00 \\ -.79269E+00 & .23963E+01 & -.40106E+01 & .22270E+01 \end{bmatrix}$$

$$K^{10--} = \begin{bmatrix} .88079E+00 & .21994E+00 & -.34679E+00 & .41375E+00 \\ -.17504E+01 & .15304E+01 & .64023E+00 & -.82680E+00 \\ .16460E+01 & -.32938E+01 & .20223E+01 & .11756E+01 \\ -.15369E+01 & .31098E+01 & -.46993E+01 & .24101E+01 \end{bmatrix}$$

$$K^{01++} = \begin{bmatrix} .46508E+00 & -.90548E+00 & .85049E+00 & -.79269E+00 \\ .74064E-01 & .12303E+01 & -.25430E+01 & .23963E+01 \\ -.15149E+00 & .41243E+00 & .17919E+01 & -.40106E+01 \\ .19250E+00 & -.57411E+00 & .89627E+00 & .22270E+01 \end{bmatrix}$$

$$K^{01--} = \begin{bmatrix} .88079E+00 & -.17504E+01 & .16460E+01 & -.15369E+01 \\ .21994E+00 & .15304E+01 & -.32938E+01 & .31098E+01 \\ -.34679E+00 & .64023E+00 & .20223E+01 & -.46993E+01 \\ .41375E+00 & -.82680E+00 & .11756E+01 & .24101E+01 \end{bmatrix}$$

$$K^{20+-} = \begin{bmatrix} -.23529E+01 & -.11459E+01 & .10217E+01 & -.10463E+01 \\ .19709E+01 & -.64457E+01 & -.26572E+01 & .22675E+01 \\ -.17666E+01 & .54644E+01 & -.10145E+02 & -.44194E+01 \\ .16171E+01 & -.49410E+01 & .86079E+01 & -.13603E+02 \end{bmatrix}$$

$$K^{20-+} = \begin{bmatrix} .52307E+00 & -.48178E+00 & .50338E+00 & -.52456E+00 \\ .44649E+01 & .18635E+01 & -.16195E+01 & .16279E+01 \\ -.37741E+01 & .83320E+01 & .35128E+01 & -.29585E+01 \\ .34021E+01 & -.70698E+01 & .11899E+02 & .53688E+01 \end{bmatrix}$$

$$K^{02+-} = \begin{bmatrix} .52307E+00 & .44649E+01 & -.37741E+01 & .34021E+01 \\ -.48178E+00 & .18635E+01 & .83320E+01 & -.70698E+01 \\ .50338E+00 & -.16195E+01 & .35128E+01 & .11899E+02 \\ -.52456E+00 & .16279E+01 & -.29585E+01 & .53688E+01 \end{bmatrix}$$

$$K^{02-+} = \begin{bmatrix} -.23529E+01 & .19709E+01 & -.17666E+01 & .16171E+01 \\ -.11459E+01 & -.64457E+01 & .54644E+01 & -.49410E+01 \\ .10217E+01 & -.26572E+01 & -.10145E+02 & .86079E+01 \\ -.10463E+01 & .22675E+01 & -.44194E+01 & -.13603E+02 \end{bmatrix}$$

$$K^{11++} = \begin{bmatrix} .28590E+01 & -.67465E+01 & .84240E+01 & -.95013E+01 \\ -.67465E+01 & .20655E+02 & -.28820E+02 & .30715E+02 \\ .84240E+01 & -.28820E+02 & .51820E+02 & -.61542E+02 \\ -.95013E+01 & .30715E+02 & -.61542E+02 & .95418E+02 \end{bmatrix}$$

$$K^{11--} = \begin{bmatrix} .99721E+01 & -.16406E+02 & .18664E+02 & -.20233E+02 \\ -.16406E+02 & .34649E+02 & -.43887E+02 & .44555E+02 \\ .18664E+02 & -.43887E+02 & .72092E+02 & -.81749E+02 \\ -.20233E+02 & .44555E+02 & -.81749E+02 & .12177E+03 \end{bmatrix}$$

$$K^{22++} = \begin{bmatrix} .15591E+02 & -.25701E+02 & .32091E+02 & -.36195E+02 \\ -.25701E+02 & .12098E+03 & -.10979E+03 & .11701E+03 \\ .32091E+02 & -.10979E+03 & .31491E+03 & -.23445E+03 \\ -.36195E+02 & .11701E+03 & -.23445E+03 & .59379E+03 \end{bmatrix}$$

$$K^{22--} = \begin{bmatrix} .56788E+02 & -.62500E+02 & .71102E+02 & -.77079E+02 \\ -.62500E+02 & .20719E+03 & -.16719E+03 & .16973E+03 \\ .71102E+02 & -.16719E+03 & .44383E+03 & -.31142E+03 \\ -.77079E+02 & .16973E+03 & -.31142E+03 & .76468E+03 \end{bmatrix}$$

$$K^{12+-} = \begin{bmatrix} -.11222E+02 & .30526E+02 & -.34717E+02 & .38281E+02 \\ .15136E+02 & -.57303E+02 & .91226E+02 & -.86801E+02 \\ -.17690E+02 & .58638E+02 & -.13211E+03 & .17984E+03 \\ .19376E+02 & -.61841E+02 & .11913E+03 & -.23436E+03 \end{bmatrix}$$

$$K^{12-+} = \begin{bmatrix} -.11222E+02 & .15136E+02 & -.17690E+02 & .19376E+02 \\ .30526E+02 & -.57303E+02 & .58638E+02 & -.61841E+02 \\ -.34717E+02 & .91226E+02 & -.13211E+03 & .11913E+03 \\ .38281E+02 & -.86801E+02 & .17984E+03 & -.23436E+03 \end{bmatrix}$$

$\varepsilon = 0.05 \qquad q = 5.0$

$$K^{00++} = \begin{bmatrix} .49221E+00 & -.34287E-01 & .31620E-01 & -.23091E-01 \\ -.34287E-01 & .55812E+00 & -.88997E-01 & .72086E-01 \\ .31620E-01 & -.88997E-01 & .59858E+00 & -.12018E+00 \\ -.23091E-01 & .72086E-01 & -.12018E+00 & .62371E+00 \end{bmatrix}$$

$$K^{00--} = \begin{bmatrix} .52650E+00 & -.65907E-01 & .54711E-01 & -.40466E-01 \\ -.65907E-01 & .58121E+00 & -.10637E+00 & .85897E-01 \\ .54711E-01 & -.10637E+00 & .61239E+00 & -.13150E+00 \\ -.40466E-01 & .85897E-01 & -.13150E+00 & .63320E+00 \end{bmatrix}$$

$$K^{10++} = \begin{bmatrix} .30724E+00 & .21946E+00 & -.93620E-01 & .87608E-01 \\ -.54132E+00 & .64607E+00 & .52197E+00 & -.28842E+00 \\ .44944E+00 & -.15302E+01 & .96439E+00 & .85882E+00 \\ -.41820E+00 & .12809E+01 & -.24589E+01 & .12411E+01 \end{bmatrix}$$

$$K^{10--} = \begin{bmatrix} .46816E+00 & .36751E+00 & -.18744E+00 & .17983E+00 \\ -.10452E+01 & .81137E+00 & .68615E+00 & -.39628E+00 \\ .87385E+00 & -.20005E+01 & .11073E+01 & .10395E+01 \\ -.81647E+00 & .16745E+01 & -.29072E+01 & .13669E+01 \end{bmatrix}$$

$$K^{01++} = \begin{bmatrix} .30724E+00 & -.54132E+00 & .44944E+00 & -.41820E+00 \\ .21946E+00 & .64607E+00 & -.15302E+01 & .12809E+01 \\ -.93620E-01 & .52197E+00 & .96439E+00 & -.24589E+01 \\ .87608E-01 & -.28842E+00 & .85882E+00 & .12411E+01 \end{bmatrix}$$

$$K^{01--} = \begin{bmatrix} .46816E+00 & -.10452E+01 & .87385E+00 & -.81647E+00 \\ .36751E+00 & .81137E+00 & -.20005E+01 & .16745E+01 \\ -.18744E+00 & .68615E+00 & .11073E+01 & -.29072E+01 \\ .17983E+00 & -.39628E+00 & .10395E+01 & .13669E+01 \end{bmatrix}$$

$$K^{20+-} = \begin{bmatrix} -.15860E+01 & -.16911E+01 & .51842E+00 & -.46015E+00 \\ .10223E+01 & -.44468E+01 & -.31471E+01 & .10721E+01 \\ -.91858E+00 & .28696E+01 & -.71640E+01 & -.46832E+01 \\ .85285E+00 & -.26073E+01 & .45847E+01 & -.97959E+01 \end{bmatrix}$$

$$K^{20-+} = \begin{bmatrix} .99581E+00 & -.26317E+00 & .22736E+00 & -.22274E+00 \\ .30403E+01 & .24063E+01 & -.78916E+00 & .69893E+00 \\ -.19688E+01 & .58177E+01 & .39064E+01 & -.13690E+01 \\ .17815E+01 & -.37396E+01 & .84890E+01 & .54757E+01 \end{bmatrix}$$

$$K^{02+-} = \begin{bmatrix} .99581E+00 & .30403E+01 & -.19688E+01 & .17815E+01 \\ -.26317E+00 & .24063E+01 & .58177E+01 & -.37396E+01 \\ .22736E+00 & -.78916E+00 & .39064E+01 & .84890E+01 \\ -.22274E+00 & .69893E+00 & -.13690E+01 & .54757E+01 \end{bmatrix}$$

$$K^{02-+} = \begin{bmatrix} -.15860E+01 & .10223E+01 & -.91858E+00 & .85285E+00 \\ -.16911E+01 & -.44468E+01 & .28696E+01 & -.26073E+01 \\ .51842E+00 & -.31471E+01 & -.71640E+01 & .45847E+01 \\ -.46015E+00 & .10721E+01 & -.46832E+01 & -.97959E+01 \end{bmatrix}$$

$$K^{11++} = \begin{bmatrix} .17555E+01 & -.40539E+01 & .51584E+01 & -.61631E+01 \\ -.40539E+01 & .12923E+02 & -.18001E+02 & .19429E+02 \\ .51584E+01 & -.18001E+02 & .33234E+02 & -.39166E+02 \\ -.61631E+01 & .19429E+02 & -.39166E+02 & .61972E+02 \end{bmatrix}$$

$$K^{11--} = \begin{bmatrix} .61041E+01 & -.10089E+02 & .11647E+02 & -.13360E+02 \\ -.10089E+02 & .21997E+02 & -.27712E+02 & .28466E+02 \\ .11647E+02 & -.27712E+02 & .46575E+02 & -.52321E+02 \\ -.13360E+02 & .28466E+02 & -.52321E+02 & .79392E+02 \end{bmatrix}$$

$$K^{22++} = \begin{bmatrix} .97925E+01 & -.13789E+02 & .19729E+02 & -.23840E+02 \\ -.13789E+02 & .82278E+02 & -.60843E+02 & .74473E+02 \\ .19729E+02 & -.60843E+02 & .21857E+03 & -.13119E+03 \\ -.23840E+02 & .74473E+02 & -.13119E+03 & .41624E+03 \end{bmatrix}$$

$$K^{22--} = \begin{bmatrix} .37816E+02 & -.34273E+02 & .44614E+02 & -.51748E+02 \\ -.34273E+02 & .14263E+03 & -.93234E+02 & .10912E+03 \\ .44614E+02 & -.93234E+02 & .30983E+03 & -.17456E+03 \\ -.51748E+02 & .10912E+03 & -.17456E+03 & .53766E+03 \end{bmatrix}$$

$$K^{12+-} = \begin{bmatrix} -.67366E+01 & .18971E+02 & -.20728E+02 & .24700E+02 \\ .88524E+01 & -.36258E+02 & .58390E+02 & -.52987E+02 \\ -.11198E+02 & .35474E+02 & -.85233E+02 & .11668E+03 \\ .12992E+02 & -.40462E+02 & .73177E+02 & -.15266E+03 \end{bmatrix}$$

$$K^{12-+} = \begin{bmatrix} -.67366E+01 & .88524E+01 & -.11198E+02 & .12992E+02 \\ .18971E+02 & -.36258E+02 & .35474E+02 & -.40462E+02 \\ -.20728E+02 & .58390E+02 & -.85233E+02 & .73177E+02 \\ .24700E+02 & -.52987E+02 & .11668E+03 & -.15266E+03 \end{bmatrix}$$

$\varepsilon = 0.10 \qquad q = 0.5$

$$K^{00++} = \begin{bmatrix} .97276E+00 & -.41687E+00 & .72211E-01 & -.77907E-01 \\ -.41687E+00 & .14618E+01 & -.56699E+00 & .16692E+00 \\ .72211E-01 & -.56699E+00 & .15566E+01 & -.61355E+00 \\ -.77907E-01 & .16692E+00 & -.61355E+00 & .15914E+01 \end{bmatrix}$$

$$K^{00--} = \begin{bmatrix} .13896E+01 & -.48908E+00 & .15012E+00 & -.94711E-01 \\ -.48908E+00 & .15397E+01 & -.58379E+00 & .19668E+00 \\ .15012E+00 & -.58379E+00 & .15863E+01 & -.61860E+00 \\ -.94711E-01 & .19668E+00 & -.61860E+00 & .16064E+01 \end{bmatrix}$$

$$K^{10++} = \begin{bmatrix} .86629E+00 & .25770E+00 & -.83396E+00 & .71888E+00 \\ -.16467E+01 & .18408E+01 & .17769E+01 & -.24548E+01 \\ .13940E+01 & -.41316E+01 & .21485E+01 & .34557E+01 \\ -.11245E+01 & .36303E+01 & -.61946E+01 & .22846E+01 \end{bmatrix}$$

$$K^{10--} = \begin{bmatrix} .15608E+01 & .10108E+01 & -.16169E+01 & .14712E+01 \\ -.29598E+01 & .20436E+01 & .26195E+01 & -.32622E+01 \\ .25826E+01 & -.51840E+01 & .22357E+01 & .43194E+01 \\ -.20866E+01 & .46121E+01 & -.71559E+01 & .23298E+01 \end{bmatrix}$$

$$K^{01++} = \begin{bmatrix} .86629E+00 & -.16467E+01 & .13940E+01 & -.11245E+01 \\ .25770E+00 & .18408E+01 & -.41316E+01 & .36303E+01 \\ -.83396E+00 & .17769E+01 & .21485E+01 & -.61946E+01 \\ .71888E+00 & -.24548E+01 & .34557E+01 & .22846E+01 \end{bmatrix}$$

$$K^{01--} = \begin{bmatrix} .15608E+01 & -.29598E+01 & .25826E+01 & -.20866E+01 \\ .10108E+01 & .20436E+01 & -.51840E+01 & .46121E+01 \\ -.16169E+01 & .26195E+01 & .22357E+01 & -.71559E+01 \\ .14712E+01 & -.32622E+01 & .43194E+01 & .23298E+01 \end{bmatrix}$$

$$K^{20+-} = \begin{bmatrix} -.44281E+01 & -.25931E+01 & .46690E+01 & -.33745E+01 \\ .35638E+01 & -.10483E+02 & -.67322E+01 & .91376E+01 \\ -.26300E+01 & .92451E+01 & -.15614E+02 & -.11146E+02 \\ .21479E+01 & -.67752E+01 & .14179E+02 & -.20461E+02 \end{bmatrix}$$

$$K^{20-+} = \begin{bmatrix} .29937E+00 & -.28587E+01 & .13148E+01 & -.21035E+01 \\ .74269E+01 & .43340E+01 & -.71805E+01 & .47257E+01 \\ -.66893E+01 & .12926E+02 & .87304E+01 & -.11541E+02 \\ .47341E+01 & -.11892E+02 & .17913E+02 & .13238E+02 \end{bmatrix}$$

$$K^{02+-} = \begin{bmatrix} .29037E+00 & .74269E+01 & -.66893E+01 & .47341E+01 \\ -.28587E+01 & .43340E+01 & .12926E+02 & -.11892E+02 \\ .13148E+01 & -.71805E+01 & .87304E+01 & .17913E+02 \\ -.21035E+01 & .47257E+01 & -.11541E+02 & .13238E+02 \end{bmatrix}$$

$$K^{02-+} = \begin{bmatrix} -.44281E+01 & .35638E+01 & -.26300E+01 & .21479E+01 \\ -.25931E+01 & -.10483E+02 & .92451E+01 & -.67752E+01 \\ .46690E+01 & -.67322E+01 & -.15614E+02 & .14179E+02 \\ -.33745E+01 & .91376E+01 & -.11146E+02 & -.20461E+02 \end{bmatrix}$$

$$K^{11++} = \begin{bmatrix} .37365E+01 & -.75931E+01 & .72018E+01 & -.62952E+01 \\ -.75931E+01 & .23812E+02 & -.29850E+02 & .24294E+02 \\ .72018E+01 & -.29850E+02 & .59057E+02 & -.63701E+02 \\ -.62952E+01 & .24294E+02 & -.63701E+02 & .11043E+03 \end{bmatrix}$$

$$K^{11--} = \begin{bmatrix} .12034E+02 & -.17347E+02 & .15143E+02 & -.12708E+02 \\ -.17347E+02 & .39478E+02 & -.45238E+02 & .34942E+02 \\ .15143E+02 & -.45238E+02 & .82706E+02 & -.85265E+02 \\ -.12708E+02 & .34942E+02 & -.85265E+02 & .14230E+03 \end{bmatrix}$$

$$K^{22++} = \begin{bmatrix} .22726E+02 & -.27032E+02 & .20919E+02 & -.18915E+02 \\ -.27032E+02 & .16109E+03 & -.11294E+03 & .68229E+02 \\ .20919E+02 & -.11294E+03 & .42410E+03 & -.24744E+03 \\ -.18915E+02 & .68229E+02 & -.24744E+03 & .81441E+03 \end{bmatrix}$$

$$K^{22--} = \begin{bmatrix} .74446E+02 & -.66385E+02 & .40978E+02 & -.40581E+02 \\ -.66385E+02 & .27408E+03 & -.17672E+03 & .94569E+02 \\ .40978E+02 & -.17672E+03 & .60013E+03 & -.33695E+03 \\ -.40581E+02 & .94569E+02 & -.33695E+03 & .10542E+04 \end{bmatrix}$$

$$K^{12+-} = \begin{bmatrix} -.14356E+02 & .36372E+02 & -.30890E+02 & .24069E+02 \\ .14056E+02 & -.67645E+02 & .10767E+03 & -.75543E+02 \\ -.11837E+02 & .51037E+02 & -.15738E+03 & .21628E+03 \\ .10354E+02 & -.37963E+02 & .10406E+03 & -.28500E+03 \end{bmatrix}$$

$$K^{12-+} = \begin{bmatrix} -.14356E+02 & .14056E+02 & -.11837E+02 & .10354E+02 \\ .36372E+02 & -.67645E+02 & .51037E+02 & -.37963E+02 \\ -.30890E+02 & .10767E+03 & -.15738E+03 & .10406E+03 \\ .24069E+02 & -.75543E+02 & .21628E+03 & -.28500E+03 \end{bmatrix}$$

$\varepsilon = 0.10 \qquad a = 1.0$

$$K^{00++} = \begin{bmatrix} .68511E+00 & -.24856E+00 & .77697E-01 & -.58078E-01 \\ -.24856E+00 & .10114E+01 & -.38434E+00 & .16361E+00 \\ .77697E-01 & -.38434E+00 & .10973E+01 & -.43653E+00 \\ -.58078E-01 & .16361E+00 & -.43653E+00 & .11349E+01 \end{bmatrix}$$

$$K^{00--} = \begin{bmatrix} .93368E+00 & -.32626E+00 & .13577E+00 & -.85915E-01 \\ -.32626E+00 & .10694E+01 & -.41218E+00 & .18797E+00 \\ .13577E+00 & -.41218E+00 & .11216E+01 & -.44981E+00 \\ -.85915E-01 & .18797E+00 & -.44981E+00 & .11477E+01 \end{bmatrix}$$

$$K^{10++} = \begin{bmatrix} .59672E+00 & .12385E+00 & -.42832E+00 & .43054E+00 \\ -.11522E+01 & .14093E+01 & .94227E+00 & -.13859E+01 \\ .10252E+01 & -.30150E+01 & .17873E+01 & .19495E+01 \\ -.87804E+00 & .27387E+01 & -.45747E+01 & .19995E+01 \end{bmatrix}$$

$$K^{10--} = \begin{bmatrix} .11109E+01 & .50779E+00 & -.88302E+00 & .89854E+00 \\ -.21330E+01 & .16331E+01 & .14356E+01 & -.18977E+01 \\ .19274E+01 & -.38167E+01 & .19093E+01 & .24886E+01 \\ -.16545E+01 & .34946E+01 & -.52942E+01 & .20737E+01 \end{bmatrix}$$

$$K^{01++} = \begin{bmatrix} .59672E+00 & -.11522E+01 & .10252E+01 & -.87804E+00 \\ .12385E+00 & .14093E+01 & -.30150E+01 & .27387E+01 \\ -.42832E+00 & .94227E+00 & .17873E+01 & -.45747E+01 \\ .43054E+00 & -.13859E+01 & .19495E+01 & .19995E+01 \end{bmatrix}$$

$$K^{01--} = \begin{bmatrix} .11109E+01 & -.21330E+01 & .19274E+01 & -.16545E+01 \\ .50779E+00 & .16331E+01 & -.38167E+01 & .34946E+01 \\ -.88302E+00 & .14356E+01 & .19093E+01 & -.52942E+01 \\ .89854E+00 & -.18977E+01 & .24886E+01 & .20737E+01 \end{bmatrix}$$

$$K^{20+-} = \begin{bmatrix} -.30347E+01 & -.15419E+01 & .24862E+01 & -.21005E+01 \\ .25208E+01 & -.76125E+01 & -.40703E+01 & .51346E+01 \\ -.20235E+01 & .66621E+01 & -.11506E+02 & -.69132E+01 \\ .17234E+01 & -.53617E+01 & .10236E+02 & -.15113E+02 \end{bmatrix}$$

$$K^{20-+} = \begin{bmatrix} .33810E+00 & -.13797E+01 & .91385E+00 & -.11821E+01 \\ .53796E+01 & .26652E+01 & -.38700E+01 & .31086E+01 \\ -.47369E+01 & .95589E+01 & .54153E+01 & -.65484E+01 \\ .37515E+01 & -.85287E+01 & .13297E+02 & .83577E+01 \end{bmatrix}$$

$$K^{02+-} = \begin{bmatrix} .33810E+00 & .53796E+01 & -.47369E+01 & .37515E+01 \\ -.13797E+01 & .26652E+01 & .95589E+01 & -.85287E+01 \\ .91385E+00 & -.38700E+01 & .54153E+01 & .13297E+02 \\ -.11821E+01 & .31086E+01 & -.65484E+01 & .83577E+01 \end{bmatrix}$$

$$K^{02-+} = \begin{bmatrix} -.30347E+01 & .25208E+01 & -.20235E+01 & .17234E+01 \\ -.15419E+01 & -.76125E+01 & .66621E+01 & -.53617E+01 \\ .24862E+01 & -.40703E+01 & -.11506E+02 & .10236E+02 \\ -.21005E+01 & .51346E+01 & -.69132E+01 & -.15113E+02 \end{bmatrix}$$

$$K^{11++} = \begin{bmatrix} .28897E+01 & -.62282E+01 & .66211E+01 & -.64320E+01 \\ -.62282E+01 & .19241E+02 & -.25061E+02 & .22795E+02 \\ .66211E+01 & -.25061E+02 & .47478E+02 & -.53021E+02 \\ -.64320E+01 & .22795E+02 & -.53021E+02 & .87790E+02 \end{bmatrix}$$

$$K^{11--} = \begin{bmatrix} .95904E+01 & -.14531E+02 & .14143E+02 & -.13212E+02 \\ -.14531E+02 & .31876E+02 & -.37862E+02 & .32729E+02 \\ .14143E+02 & -.37862E+02 & .66110E+02 & -.70566E+02 \\ -.13212E+02 & .32729E+02 & -.70566E+02 & .11256E+03 \end{bmatrix}$$

$$K^{22++} = \begin{bmatrix} .16904E+02 & -.23068E+02 & .22347E+02 & -.21906E+02 \\ -.23068E+02 & .12316E+03 & -.95242E+02 & .76051E+02 \\ .22347E+02 & -.95242E+02 & .32091E+03 & -.20420E+03 \\ -.21906E+02 & .76051E+02 & -.20420E+03 & .61078E+03 \end{bmatrix}$$

$$K^{22--} = \begin{bmatrix} .57805E+02 & -.55381E+02 & .46755E+02 & -.45674E+02 \\ -.55381E+02 & .20978E+03 & -.14579E+03 & .10819E+03 \\ .46755E+02 & -.14579E+03 & .45346E+03 & -.27375E+03 \\ -.45674E+02 & .10819E+03 & -.27375E+03 & .78972E+03 \end{bmatrix}$$

$$K^{12+-} = \begin{bmatrix} -.11219E+02 & .29140E+02 & -.27887E+02 & .25399E+02 \\ .12571E+02 & -.54029E+02 & .85619E+02 & -.67977E+02 \\ -.12214E+02 & .46210E+02 & -.12425E+03 & .16978E+03 \\ .11680E+02 & -.40193E+02 & .93141E+02 & -.22245E+03 \end{bmatrix}$$

$$K^{12-+} = \begin{bmatrix} -.11219E+02 & .12571E+02 & -.12214E+02 & .11680E+02 \\ .29140E+02 & -.54029E+02 & .46210E+02 & -.40193E+02 \\ -.27887E+02 & .85619E+02 & -.12425E+03 & .93141E+02 \\ .25399E+02 & -.67977E+02 & .16978E+03 & -.22245E+03 \end{bmatrix}$$

$\varepsilon = 0.10 \qquad q = 2.0$

$$K^{00++} = \begin{bmatrix} .53720E+00 & -.12116E+00 & .61186E-01 & -.37686E-01 \\ -.12116E+00 & .71954E+00 & -.22003E+00 & .12449E+00 \\ .61186E-01 & -.22003E+00 & .78285E+00 & -.26415E+00 \\ -.37686E-01 & .12449E+00 & -.26415E+00 & .81529E+00 \end{bmatrix}$$

$$K^{00--} = \begin{bmatrix} .65836E+00 & -.18234E+00 & .98872E-01 & -.63306E-01 \\ -.18234E+00 & .75723E+00 & -.24565E+00 & .14300E+00 \\ .98872E-01 & -.24565E+00 & .80135E+00 & -.27808E+00 \\ -.63306E-01 & .14300E+00 & -.27808E+00 & .82610E+00 \end{bmatrix}$$

$$K^{10++} = \begin{bmatrix} .41337E+00 & .13243E+00 & -.20296E+00 & .23284E+00 \\ -.78259E+00 & .98590E+00 & .58999E+00 & -.70850E+00 \\ .69786E+00 & -.21262E+01 & .13400E+01 & .11774E+01 \\ -.62400E+00 & .19117E+01 & -.32927E+01 & .15808E+01 \end{bmatrix}$$

$$K^{10--} = \begin{bmatrix} .73845E+00 & .33894E+00 & -.44313E+00 & .48498E+00 \\ -.14840E+01 & .11815E+01 & .87215E+00 & -.99243E+00 \\ .13292E+01 & -.27255E+01 & .14710E+01 & .15003E+01 \\ -.11933E+01 & .24576E+01 & -.38352E+01 & .16739E+01 \end{bmatrix}$$

$$K^{01++} = \begin{bmatrix} .41337E+00 & -.78259E+00 & .69786E+00 & -.62400E+00 \\ .13243E+00 & .98590E+00 & -.21262E+01 & .19117E+01 \\ -.20296E+00 & .58999E+00 & .13400E+01 & -.32927E+01 \\ .23284E+00 & -.70850E+00 & .11774E+01 & .15808E+01 \end{bmatrix}$$

$$K^{01--} = \begin{bmatrix} .73845E+00 & -.14840E+01 & .13292E+01 & -.11933E+01 \\ .33894E+00 & .11815E+01 & -.27255E+01 & .24576E+01 \\ -.44313E+00 & .87215E+00 & .14710E+01 & -.38352E+01 \\ .48498E+00 & -.99243E+00 & .15003E+01 & .16739E+01 \end{bmatrix}$$

$$K^{20+-} = \begin{bmatrix} -.21073E+01 & -.13553E+01 & .11998E+01 & -.11788E+01 \\ .16555E+01 & -.56019E+01 & -.31009E+01 & .25827E+01 \\ -.14155E+01 & .44612E+01 & -.86915E+01 & -.50652E+01 \\ .12471E+01 & -.38596E+01 & .69183E+01 & -.11571E+02 \end{bmatrix}$$

$$K^{20-+} = \begin{bmatrix} .61631E+00 & -.57449E+00 & .57801E+00 & -.57657E+00 \\ .39273E+01 & .21924E+01 & -.18722E+01 & .18026E+01 \\ -.31183E+01 & .71809E+01 & .40626E+01 & -.33236E+01 \\ .26869E+01 & -.57206E+01 & .10131E+02 & .60998E+01 \end{bmatrix}$$

$$K^{02+-} = \begin{bmatrix} .61631E+00 & .39273E+01 & -.31183E+01 & .26869E+01 \\ -.57449E+00 & .21924E+01 & .71809E+01 & -.57206E+01 \\ .57801E+00 & -.18722E+01 & .40626E+01 & .10151E+02 \\ -.57657E+00 & .18026E+01 & -.33236E+01 & .60998E+01 \end{bmatrix}$$

$$K^{02-+} = \begin{bmatrix} -.21073E+01 & .16555E+01 & -.14155E+01 & .12471E+01 \\ -.13553E+01 & -.56019E+01 & .44612E+01 & -.38596E+01 \\ .11998E+01 & -.31009E+01 & -.86915E+01 & .69183E+01 \\ -.11788E+01 & .25827E+01 & -.50652E+01 & -.11571E+02 \end{bmatrix}$$

$$K^{11++} = \begin{bmatrix} .21438E+01 & -.47717E+01 & .54784E+01 & -.57913E+01 \\ -.47717E+01 & .14840E+02 & -.19833E+02 & .19401E+02 \\ .54784E+01 & -.19833E+02 & .36926E+02 & -.42086E+02 \\ -.57913E+01 & .19401E+02 & -.42086E+02 & .68061E+02 \end{bmatrix}$$

$$K^{11--} = \begin{bmatrix} .72597E+01 & -.11396E+02 & .11921E+02 & -.12125E+02 \\ -.11396E+02 & .24745E+02 & -.30064E+02 & .27956E+02 \\ .11921E+02 & -.30064E+02 & .51365E+02 & -.55903E+02 \\ -.12125E+02 & .27956E+02 & -.55903E+02 & .87017E+02 \end{bmatrix}$$

$$K^{22++} = \begin{bmatrix} .12282E+02 & -.17352E+02 & .19921E+02 & -.21059E+02 \\ -.17352E+02 & .94338E+02 & -.72121E+02 & .70549E+02 \\ .19921E+02 & -.72121E+02 & .24643E+03 & -.15304E+03 \\ -.21059E+02 & .70549E+02 & -.15304E+03 & .46732E+03 \end{bmatrix}$$

$$K^{22--} = \begin{bmatrix} .44344E+02 & -.41440E+02 & .43348E+02 & -.44089E+02 \\ -.41440E+02 & .16176E+03 & -.10933E+03 & .10166E+03 \\ .43348E+02 & -.10933E+03 & .34828E+03 & -.20328E+03 \\ -.44089E+02 & .10166E+03 & -.20328E+03 & .60354E+03 \end{bmatrix}$$

$$K^{12+-} = \begin{bmatrix} -.83145E+01 & .22272E+02 & -.22610E+02 & .23164E+02 \\ .10040E+02 & -.41555E+02 & .66035E+02 & -.55632E+02 \\ -.10895E+02 & .37797E+02 & -.95663E+02 & .13043E+03 \\ .11244E+02 & -.36998E+02 & .76142E+02 & -.17034E+03 \end{bmatrix}$$

$$K^{12-+} = \begin{bmatrix} -.83145E+01 & .10040E+02 & -.10895E+02 & .11244E+02 \\ .22272E+02 & -.41555E+02 & .37797E+02 & -.36998E+02 \\ -.22610E+02 & .66035E+02 & -.95663E+02 & .76142E+02 \\ .23164E+02 & -.55632E+02 & .13043E+03 & -.17034E+03 \end{bmatrix}$$

$\varepsilon = 0.10 \qquad q = 5.0$

$$K^{00++} = \begin{bmatrix} .46882E+00 & -.30352E-01 & .27551E-01 & -.19602E-01 \\ -.30352E-01 & .52672E+00 & -.77506E-01 & .61498E-01 \\ .27551E-01 & -.77506E-01 & .56067E+00 & -.10296E+00 \\ -.19602E-01 & .61498E-01 & -.10296E+00 & .58066E+00 \end{bmatrix}$$

$$K^{00--} = \begin{bmatrix} .49917E+00 & -.57903E-01 & .47154E-01 & -.33946E-01 \\ -.57903E-01 & .54632E+00 & -.91850E-01 & .72609E-01 \\ .47154E-01 & -.91850E-01 & .57178E+00 & -.11184E+00 \\ -.33946E-01 & .72609E-01 & -.11184E+00 & .58794E+00 \end{bmatrix}$$

$$K^{10++} = \begin{bmatrix} .28598E+00 & .22736E+00 & -.11113E+00 & .10601E+00 \\ -.49617E+00 & .56389E+00 & .56580E+00 & -.34538E+00 \\ .39813E+00 & -.13764E+01 & .80425E+00 & .94512E+00 \\ -.36078E+00 & .11131E+01 & -.21847E+01 & .99752E+00 \end{bmatrix}$$

$$K^{10--} = \begin{bmatrix} .42038E+00 & .39206E+00 & -.22423E+00 & .21690E+00 \\ -.94788E+00 & .69127E+00 & .75077E+00 & -.47383E+00 \\ .76602E+00 & -.17873E+01 & .90577E+00 & .11478E+01 \\ -.69763E+00 & .14446E+01 & -.25709E+01 & .10809E+01 \end{bmatrix}$$

$$K^{01++} = \begin{bmatrix} .28598E+00 & -.49617E+00 & .39815E+00 & -.36078E+00 \\ .22736E+00 & .56389E+00 & -.13764E+01 & .11131E+01 \\ -.11113E+00 & .56580E+00 & .80425E+00 & -.21847E+01 \\ .10601E+00 & -.34538E+00 & .94512E+00 & .99752E+00 \end{bmatrix}$$

$$K^{01--} = \begin{bmatrix} .42038E+00 & -.94788E+00 & .76602E+00 & -.69763E+00 \\ .39206E+00 & .69127E+00 & -.17873E+01 & .14446E+01 \\ -.22423E+00 & .75077E+00 & .90577E+00 & -.25709E+01 \\ .21690E+00 & -.47383E+00 & .11478E+01 & .10809E+01 \end{bmatrix}$$

$$K^{20+-} = \begin{bmatrix} -.14819E+01 & -.16901E+01 & .58325E+00 & -.52740E+00 \\ .91855E+00 & -.40958E+01 & -.31936E+01 & .12141E+01 \\ -.80190E+00 & .25296E+01 & -.65424E+01 & -.47881E+01 \\ .72656E+00 & -.22353E+01 & .39896E+01 & -.88947E+01 \end{bmatrix}$$

$$K^{20-+} = \begin{bmatrix} .98023E+00 & -.29307E+00 & .26029E+00 & -.25569E+00 \\ .28173E+01 & .24271E+01 & -.89166E+00 & .80141E+00 \\ -.17503E+01 & .53333E+01 & .39813E+01 & -.15512E+01 \\ .15399E+01 & -.32735E+01 & .77282E+01 & .56110E+01 \end{bmatrix}$$

$$K^{02+-} = \begin{bmatrix} .98023E+00 & .28173E+01 & -.17503E+01 & .15399E+01 \\ -.29307E+00 & .24271E+01 & .53333E+01 & -.32735E+01 \\ .26029E+00 & -.89166E+00 & .39813E+01 & .77282E+01 \\ -.25569E+00 & .80141E+00 & -.15512E+01 & .56110E+01 \end{bmatrix}$$

$$K^{02-+} = \begin{bmatrix} -.14819E+01 & .91855E+00 & -.80190E+00 & .72656E+00 \\ -.16901E+01 & -.40958E+01 & .25296E+01 & -.22353E+01 \\ .58325E+00 & -.31936E+01 & -.65424E+01 & .39896E+01 \\ -.52740E+00 & .12141E+01 & -.47881E+01 & -.88947E+01 \end{bmatrix}$$

$$K^{11++} = \begin{bmatrix} .14136E+01 & -.30995E+01 & .36847E+01 & -.42186E+01 \\ -.30995E+01 & .10056E+02 & -.13483E+02 & .13552E+02 \\ .36847E+01 & -.13483E+02 & .25643E+02 & -.29089E+02 \\ -.42186E+01 & .13552E+02 & -.29089E+02 & .47681E+02 \end{bmatrix}$$

$$K^{11--} = \begin{bmatrix} .47937E+01 & -.76166E+01 & .82050E+01 & -.90275E+01 \\ -.76166E+01 & .17026E+02 & -.20651E+02 & .19711E+02 \\ .82050E+01 & -.20651E+02 & .35870E+02 & -.38776E+02 \\ -.90275E+01 & .19711E+02 & -.38776E+02 & .61062E+02 \end{bmatrix}$$

$$K^{22++} = \begin{bmatrix} .82379E+01 & -.99339E+01 & .13699E+02 & -.15921E+02 \\ -.99339E+01 & .68998E+02 & -.42689E+02 & .50501E+02 \\ .13699E+02 & -.42689E+02 & .18328E+03 & -.90814E+02 \\ -.15921E+02 & .50501E+02 & -.90814E+02 & .34957E+03 \end{bmatrix}$$

$$K^{22--} = \begin{bmatrix} .31753E+02 & -.24315E+02 & .30556E+02 & -.34126E+02 \\ -.24315E+02 & .11957E+03 & -.64904E+02 & .73444E+02 \\ .30556E+02 & -.64904E+02 & .25998E+03 & -.12034E+03 \\ -.34126E+02 & .73444E+02 & -.12034E+03 & .45198E+03 \end{bmatrix}$$

$$K^{12+-} = \begin{bmatrix} -.53637E+01 & .14973E+02 & -.14746E+02 & .16824E+02 \\ .63884E+01 & -.28476E+02 & .45729E+02 & -.37052E+02 \\ -.77297E+01 & .24984E+02 & -.66653E+02 & .91186E+02 \\ .86333E+01 & -.27288E+02 & .50905E+02 & -.11929E+03 \end{bmatrix}$$

$$K^{12-+} = \begin{bmatrix} -.53637E+01 & .63884E+01 & -.77297E+01 & .86333E+01 \\ .14973E+02 & -.28476E+02 & .24984E+02 & -.27288E+02 \\ -.14746E+02 & .45729E+02 & -.66653E+02 & .50905E+02 \\ .16824E+02 & -.37052E+02 & .91186E+02 & -.11929E+03 \end{bmatrix}$$

ACKNOWLEDGEMENT

The completion of this work was made possible by Prof. D. Vischer's generosity in providing a fruitful atmosphere and an efficient infrastructure.

The substantial aid we received from F. Langenegger, C. Bucher and I. Wiederkehr is gratefully thanked.